

Amalie Hjellestad Hella

Modeling and Control of a Foiling Trimaran Sailboat

Master's thesis in Marine Technology

Supervisor: Thomas Sauder

Co-supervisor: Astrid H. Brodtkorb

June 2021

NTNU
Norwegian University of Science and Technology
Faculty of Engineering
Department of Marine Technology

Amalie Hjellevstad Hella

Modeling and Control of a Foiling Trimaran Sailboat

Master's thesis in Marine Technology
Supervisor: Thomas Sauder
Co-supervisor: Astrid H. Brodtkorb
June 2021

Norwegian University of Science and Technology
Faculty of Engineering
Department of Marine Technology





MASTER OF TECHNOLOGY THESIS DEFINITION (30 SP)

Name of the candidate:	Hella, Amalie Hjellevstad
Field of study:	Marine cybernetics
Thesis title (Norwegian):	Modellering og kontroll av en foilende trimaran seilbåt
Thesis title (English):	Modeling and control of a foiling trimaran sailboat

Background

Foils on racing sailboats have been used more in recent years. This can be seen in for example America's Cup as well as in the Olympics with the foiling Nacra17. When flying, the speed of the boat increases due to the reduced hydrodynamic resistance compared to "Archimedean" non-foiling conditions. In offshore racing, a foiling sailboat can, in addition to increase speed, have better performance in waves, but the stability of the boat needs to be good to avoid sudden water entries and violent reduction of speed.

The Ultim class gathers 32m-long trimarans that are designed for offshore double or singlehanded racing in rough conditions. Today, the foils are controlled manually using hydraulic rams and manually-operated winches. It is interesting to see whether these foils can be controlled automatically (and how) to achieve better stability in waves, which leads to more flying time, increased average speeds, and can also mean better safety for the sailors.

A sailboat is subjected to aerodynamical forces on sail and rig, and hydrodynamical forces on the hull and foils. For the boat to be stable, these needs to be in balance. The Ultim trimaran have six foils that can potentially be controlled. These needs to be modelled to understand how the foils interact and what the effects of changing them have on the hull and performance of the boat. In addition, the control structure needs to be modelled to prepare for control of the foils.

Using common modeling tools in marine hydrodynamics and cybernetics, previous master theses and published papers, a model of a generic Ultim type of boat and a control system will be devised.

Scope of Work

- 1) Perform a background and literature review to provide information and relevant references on history of foiling vessels, control of high speed/foiling boats, control of sailboats. Write a list with abbreviations and definitions of terms and symbols, relevant to the literature study and project report.
- 2) Develop a mathematical model of the physical system. Include details about the boat, the foils and the assumptions that are made.
- 3) Model of the system in Matlab, and perform an analysis of the boat at equilibrium. Study the various loads applied to the boat, their order of magnitude, and study the action of each foil on the boat.
- 4) Model the system in Simulink for dynamic simulations and present the result. This includes all relevant components of a control system.
- 5) Propose various alternatives to control attitude and heading of the boat, i.e. different ways to allocate the control force to the actuators/foils
- 6) Define test cases that can be used to compare the result from the different controllers (change of set points, disturbances, etc...). Analyze and compare the performance for the various controllers.
- 7) Present the work performed in the project thesis in a structured manner, and conclude on the achievements, lessons learned, and possible improvements to the model and controllers.

Specifications

Every week throughout the project period, the candidate shall send a status email to the supervisor and co-advisors, providing two brief bulleted lists: 1) work done recent week, and 2) work planned to be done next week.

The scope of work may prove to be larger than initially anticipated. By the approval from the supervisor, described topics may be deleted or reduced in extent without consequences with regard to grading.

The candidate shall present personal contribution to the resolution of problems within the scope of work. Theories and conclusions should be based on mathematical derivations and logic reasoning identifying the steps in the deduction.


The report shall be organized in a logical structure to give a clear exposition of background, problem/research statement, design/method, analysis, and results. The text should be brief and to the point, with a clear language. Rigorous mathematical deductions and illustrating figures are preferred over lengthy textual descriptions. The report shall have font size 11 pts., and it is not expected to be longer than 70 A4-pages, 100 B5-pages, from introduction to conclusion, unless otherwise agreed. It shall be written in English (preferably US) and contain the elements: Title page, abstract, preface (incl. description of help, resources, and internal and external factors that have affected the project process), acknowledgement, project definition, list of symbols and acronyms, table of contents, introduction (project background/motivation, objectives, scope and delimitations, and contributions), technical background and literature review, problem formulation, method, results and analysis, conclusions with recommendations for further work, references, and optional appendices. Figures, tables, and equations shall be numerated. The original contribution of the candidate and material taken from other sources shall be clearly identified. Work from other sources shall be properly acknowledged using quotations and a Harvard citation style (e.g. natbib Latex package). The work is expected to be conducted in an honest and ethical manner, without any sort of plagiarism and misconduct, which is taken very seriously by the university and will result in consequences. NTNU can use the results freely in research and teaching by proper referencing, unless otherwise agreed.

The thesis shall be submitted with an electronic copy to the main supervisor and department according to NTNU administrative procedures. The final revised version of this thesis definition shall be included after the title page. Computer code, pictures, videos, dataserries, etc., shall be included electronically with the report.

Start date: 15 January, 2021
Supervisor: Thomas Sauder
Co-advisor(s): Astrid H. Brodtkorb

Due date: As specified by the administration.

Signature:



Digitally signed
by Sauder
Thomas Michel
Date: 2021.06.04
10:24:20 +02'00'

Preface

This work is a master thesis written as a part of my M. Sc degree in Marine Technology with a specialization in Marine Cybernetics at the Department of Marine Technology, Norwegian University of Science and Technology (NTNU). The thesis has been written during the spring semester of 2021.

The main goal of this thesis was to develop an automatic attitude controller for a foiling trimaran sailboat. A mathematical model of the trimaran was given by Thomas Sauder for the pre-project (Hella 2020). The code has since been further extended by myself.

The model has been used as a starting point in the development of a dynamic model in Simulink. The model has then been verified. To be able to compare and evaluate the effect of controlling foils, three different approaches for allocation the forces from the controller has been developed. Simulations in calm sea and with regular swell waves have been performed on the system. This gives great insight into how the trimaran behaves is, and it is interesting to see how different control approaches influence the performance of the trimaran.

All work presented in this thesis is done by me, unless stated otherwise in the text.



Amalie Hjellestad Hella

Trondheim , June 10th, 2021

Acknowledgments

I would like to express my gratitude to my supervisor Thomas Michel Sauder for all help and guidance during the last year. Thank you for your help with the programming, and for taking the extra time to help me solve the problems I faced.

I would also like to thank my co-supervisor Astrid H. Brodtkorb for valuable input.

Thanks to Emilien Lavigne at Mer Concept for answering our questions, and for the review of our results.

Thank you to my friends at office C1.058 for discussions and encouragement during the past year, as well as the fun times and great memories.

Abstract

Foils on sailboats that lift the hull out of the water are of massive interest in the present time and have been increasing over several years. When flying, the speed of the boat increases due to the reduced hydrodynamic resistance compared to "Archimedean" non-foiling conditions. In offshore racing, a foiling sailboat can, in addition to increase speed, have better performance in waves, but the stability of the boat needs to be good to avoid sudden water entries and violent reduction of speed.

The Ultim class gathers 32 meter long trimarans that are designed for offshore double- or single-handed racing in rough conditions. Today, the foils are controlled manually using hydraulic rams and manually operated winches. By controlling the foils automatically, the trimaran can achieve better stability in waves, which leads to more flying time, increased average speeds, and can also mean better safety for the sailors. This thesis models a generic Ultim trimaran and develops a control system to maintain the desired position and attitude for the trimaran. It includes studying the forces of the boat and the foils, and what the effects of changing them have on the performance of the boat.

By establishing a minimum viable model of the trimaran, it was used in the development of a control system. The model includes forces working on the trimaran and its foils. To validate the minimum viable model, a static equilibrium was found, for which the load distribution was analyzed. The loads are split between the weight of the trimaran, the aerodynamic loads from wind, and the lift and drag loads from the foils. By also looking at the trimarans sensitivity for changes in loads when the incident angle for the foils was changed, it gave valuable input to how the motions of the trimaran are coupled.

When developing the control system, three controller candidates were chosen to compare the performance. Controller 1 is a simple Proportional-Integrate-Derivative (PID) controller, where the loads in each degree of freedom (DOF) corresponds to one actuator acting in that DOF. Controller 2 is also a PID controller, but the allocation to actuators happens by using a configuration matrix established from the sensitivity analysis of forces and moments from the actuators on the motions of the sailboat.. Controller 3 is a combination of these two, using a PID controller and an allocation with values from the configuration matrix applied to the same actuators as in Controller 1.

By conducting two different test cases, the control system was verified. Subsequently, several test scenarios were simulated to look at the performance of the control candidates. The control system was exposed to disturbances such as difference in wind, reference changes, and waves to evaluate the performance of the system. The results show that the need for a more advanced controller increases when the conditions are more unstable, such as when exposed to waves and varying wind. Controller 1 performed generally very well but had larger variations in position when exposed to regular waves and varying wind, while Controller 2 performed better in these conditions.

Seeing as all three controllers were adequate for the tested scenarios, it can be concluded that this highly coupled and complex system can perform well with just a simple controller under these conditions. The trimaran is controlled well under the assumptions in this thesis, but the need for a more advanced controller is present in rougher conditions when the roll motion increases. The proposed system can be of value for the further development of an automatic control system for a foiling trimaran sailboat.

Sammendrag

For tiden er foiler på seilbåter som løfter dem ut av vannet veldig i vinden, og det har vært en økende trend de siste årene. Ved å fly over vannet, øker farten til båten. Dette er på grunn av den synkende hydrodynamiske motstanden som oppstår når båten løftes ut av vannet. I offshore konkurranser kan en foilende seilbåt, i tillegg til å øke hastigheten, også ha bedre ytelse i bølger. For å få det til er det viktig med god stabilitet for båten slik at en unngår plutselige krasjlandinger i vannet.

Ultim klassen samler 32 meter lange trimaraner som er designet for offshore singel eller dobbelhanded konkurranser i røffe forhold. I dag er foilene kontrollert manuelt ved å bruke hydrauliske pumper styrt av manuelle wincher. Ved å kontrollere foilene automatisk kan trimaranen oppnå bedre stabilitet i bølger, noe som fører til mer tid i foilende tilstand, høyere gjennomsnittshastighet og det kan føre til bedre sikkerhet for mannskapet. Denne masteroppgaven fokuserer på å modellere en generisk Ultim trimaran og utvikle et kontrollsystem for å oppnå den ønskede posisjonen til trimaranen. Dette innebærer å studere kreftene på båten og foilene, samt hvilke effekter det har å endre på vinkelen til foilene med tanke på ytelsen.

For å utvikle kontrollsystemet til trimaranen, ble det først etablert en matematisk modell av båten. Modellen inkluderer krefter som virker på båten og på foilene. For å validere denne modellen ble det funnet et statisk likevektspunkt. Lastene fra dette punktet ble så analysert. Lastene kan fordeles mellom vekten til trimaranen, de aerodynamiske lastene på skroget og de hydrodynamiske lastene (løft og drag) på foilene. Ved å se på sensitiviteten til lastene når angrepsvinkelen på foilene endret seg, fikk en et inntrykk at hvordan de koblede bevegelsene oppfører seg og dette gav verdifulle innspill til videre utvikling av kontrollsystemet.

Når kontrollsystemet ble utviklet, ble det brukt tre forskjellige kontroller kandidater for å sammenligne hvordan forskjellige tilnærminger til allokeringproblemet påvirker ytelsen til systemet. Kontroller 1 er en enkel Proporsjonal-Integrasjon-Derivasjon (PID) kontroller hvor lastene fra frihetsgradene korresponderer til en aktuator som virker i samme frihetsgrad. Kontroller 2 er også en PID kontroller, men allokeringen til aktuatorene gjøres ved hjelp av konfigurasjonsmatrisen fra sensitivitets analysen for foilene. Den siste kontrolleren, Kontroller 3, er en kombinasjon av disse to løsningene, hvor en PID kontroller brukes sammen med en allokering som henter verdier fra konfigurasjonsmatrisen korresponderende til spesifiserte frihetsgrader og bruker dem på de samme aktuatorene som for Kontroller 1.

Ved å gjennomføre to forskjellige test tilfeller ble kontrollsystemet verifisert. Deretter ble flere test scenarier gjennomført for å se på ytelsen til kontroller kandidatene. Kontrollsystemet var eksponert for forstyrrelser som varierende vind, endringer i referanse og bølger for å kunne evaluere ytelsen. Resultatene viste at det kan være nødvendig med en mer

avansert kontroller når forholdene blir mer ustabile, altså når den er utsatt før bølger og varierende vind. Kontroller 1 gjorde det generelt veldig bra da den var rask og hadde lite avvik fra referansen med unntak av i rull, men den hadde større, uønskede variasjoner i rull vinkel for ustabile forhold. Kontroller 2 gjorde det bra i ustabile forhold, og traff referansen i alle forhold, men gjorde det med større utslag på aktuatorene. Kontroller 3 gjorde det generelt likt som kontroller 1, men hadde større avvik i referanse, spesielt ved større endringer og ustabil vind og bølger.

Ettersom alle tre kontrollerne var tilstrekkelig i scenariene som ble testet, kan det konkluderes med at dette svært koblede og komplekse systemet kan yte godt selv med en enkel kontroller i disse forholdene. Under antagelsene presentert i denne rapporten er trimaranten godt kontrollert, men behovet for en mer avansert kontroller øker når forholdene blir tøffere og rull bevegelsen øker. Det foreslåtte systemet kan være av verdi i videre utvikling av et automatisk kontrollsystem for foilende trimaran seilbåter.

Table of Contents

Preface	iii
Acknowledgments	iv
Abstract	v
Sammendrag	vii
List of Figures	xiii
List of Tables	xvi
Nomenclature	xviii
1 Introduction	1
1.1 Motivation	1
1.2 Background	1
1.2.1 History of hydrofoils	1
1.2.2 Sailing hydrofoils	2
1.2.3 Modeling and control of hydrofoil vessels	3
1.2.4 Control systems of sailboats	5
1.2.5 The Ultim class of sailboats	5
1.3 Scope of work	6
1.4 Main Contributions	6
1.5 Organization of thesis	7
2 Dynamic and hydrodynamic model	8
2.1 Boat description	8

2.2	Reference frames	9
2.3	Dynamic model of a foiling vessel	12
2.4	Inertia, Weight and Coriolis-Centripetal loads	14
2.5	Foil loads	16
2.5.1	Lift and drag coefficients, C_L and C_D	16
2.5.2	Calculating the relative velocity and angle of attack	17
2.5.3	Lift and drag force	18
2.5.4	Drag on the superstructure	19
2.5.5	Effect of waves	19
3	Static equilibrium	20
3.1	Initial steady conditions	20
3.2	Reaching equilibrium	21
3.3	Load distribution	22
3.4	Validation of the forces and moments	23
3.4.1	Comparison with a dynamic velocity prediction program	23
3.4.2	Comparison with results from Mer Concept	24
3.5	Sensitivity of the loads to control inputs	25
3.5.1	Acting on the rudders	25
3.5.2	T-foil on rudders	26
3.5.3	Centerboard T-foil	26
4	Control System Design	28
4.1	Architecture	28
4.2	System components	30
4.2.1	Reference model	30
4.2.2	Computation of error	30
4.2.3	PID	30
4.2.4	Force Allocation	31
4.2.5	Actuator model	31
4.2.6	Wave filter	32
4.3	Control architecture candidates	33

4.3.1	Controller 1	33
4.3.2	Controller 2	34
4.3.3	Controller 3	35
5	Verification of the dynamic model, including controller	37
5.1	Initial conditions	37
5.2	Verification for cases	38
5.2.1	Case 1 - Change in yaw angle	38
5.2.2	Case 2 - Change in wind direction	40
5.3	Validity range	42
5.4	Discussion and conclusion	43
6	Comparison between controllers in calm waters	44
6.1	Indicators	44
6.2	Description of the tests	45
6.3	Result of the tests	45
6.4	Discussion of controller candidates regarding performance in calm water	52
7	Comparison between controllers when exposed to waves	55
7.1	Description of the tests	55
7.2	Results of the tests	56
7.3	Discussion of controller candidates regarding performance with waves	62
8	Conclusion	64
8.1	Concluding remarks	64
8.2	Further work	65
	Bibliography	66
A	Load distribution	I
B	Explanation of the code	XIII
B.1	initialize.m	XIII
B.2	staticEquilibrium.m	XIII
B.2.1	computeResidual.m	XIII

B.2.2 configurationMatrix.m XIV

B.3 Functions for calculating loads XIV

B.3.1 foilLoad.m XIV

B.3.2 aerodynamicLoadSuperstructure.m XIV

B.3.3 weightLoad.m XIV

B.3.4 coriolisCentripetal.m XIV

B.3.5 massDistribTrimaran.m XIV

B.4 Simulation XV

B.4.1 tests.m XV

B.4.2 figures.m XV

B.4.3 model.slx XV

B.4.4 Trimaran/ODETrimaran XV

B.4.5 referenceModel.m XV

B.5 Supporting functions XVI

B.5.1 Jbn.m, Rbn.m, Tbn.m XVI

B.5.2 skewSym.m XVI

List of Figures

1.1	Forlanini Hydrofoil 1906	1
1.2	Nacra17 (foto: Per Bakke)	3
1.3	Angle of attack α on foil (O. Faltinsen 2006)	4
1.4	Different foil types	5
2.1	Ultim trimarans	8
2.2	Degrees of freedom for marine vessel (Fossen 2011)	10
2.3	Body-frame and NED-frame	11
2.4	Foil-fixed reference frame	11
2.5	Length and distances on sailboat	15
2.6	Lift and drag coefficient as a function of angle of attack α	17
2.7	Illustration of foils in water or partially in water	17
3.1	Pie charts of forces	22
3.2	Pie charts of forces	23
3.3	Pie charts of forces when $U = 26$	23
3.4	Contributing forces to Z , heave for Kerdraon et al. (2020)	24
3.5	Jacobian of lift for forces on foil	26
3.6	Jacobian of lift for moments on foil	27
4.1	Block diagram	28
4.2	Model in simulink	29
4.3	Reference model (Fossen 2011)	30
4.4	Block diagram including wave filter	32
4.5	Wave filtering, excerpt from Fossen 2011	33

5.1	Attitude and position for boat for case 1	38
5.2	Result from PID controller for case 1	39
5.3	Commanded angles for actuators for case 1	39
5.4	Loads for case 1	40
5.5	Loads for case 2	41
5.6	Position for case 2	41
5.7	Commanded angles for case 2	42
6.1	Test 1; Position, attitude and velocity	46
6.2	Test 1; Control input	46
6.3	Test 2; Attitude	47
6.4	Test 2; Control input	47
6.5	Test 3; Attitude	48
6.6	Test 3; Control input	49
6.7	Test 4; Attitude	50
6.8	Test 4; Control input	50
6.9	Test 5; Wind speed and direction and boat velocity [m/s]	51
6.10	Test 5; Boat position and attitude	51
6.11	Test 5; Control input	52
7.1	Test 6; Position	56
7.2	Test 6; Control input	57
7.3	Test 7; Position	57
7.4	Test 7; Control input	58
7.5	Test 8; Position	58
7.6	Test 8; Control input	59
7.7	Test 9; Position	60
7.8	Test 9; Control input	60
7.9	Test 10; Velocity	61
7.11	Test 10; Control input	61
7.10	Test 10; Position	62
A.1	Forces in positive x-direction	I

A.2	Forces in negative x-direction	II
A.3	Forces in positive y-direction	III
A.4	Forces in negative y-direction	IV
A.5	Forces in positive z-direction	V
A.6	Forces in negative z-direction	VI
A.7	Positive moment in roll	VII
A.8	Negative moment in roll	VIII
A.9	Positive moment in pitch	IX
A.10	Negative moment in pitch	X
A.11	Positive moment in yaw	XI
A.12	Negative moment in yaw	XII

List of Tables

2.1	Boat Characteristics	9
2.2	Reference frame notation for 6-DOF marine vehicle	9
2.3	Foil description	12
2.4	Masses	14
2.5	Length and distances	15
3.1	Initial values	20
3.2	Forces [kN] and moments [kNm] before and after optimization	22
4.1	Limits for actuators	32
4.2	Actuators for each force component	34
4.3	Gains for naive controller	34
5.1	Studied conditions	37
5.2	Initial foil attitude for simulation (from {b} to {f})	38
6.1	Maneuvering test	49
7.1	Wave parameters	55

Nomenclature

Symbols

α	Angle of Attack
β	Drift angle of boat
β_{wave}	Wave propagation direction
β_{wind}	Wind propagation direction
η	Position and attitude
ν	Body-fixed velocities
ω	Wave circular frequency
ω_e	Encounter frequency
ϕ, θ, ψ	Roll, pitch, yaw angle
ρ_a	Density of air
ρ_w	Density of saltwater
τ	Load
Θ_{nb}	Euler angles (vector of roll, pitch and yaw angles)
ζ_a	Wave amplitude
C_D	Drag coefficient
C_L	Lift coefficient
g	Gravitational acceleration
K_p, K_d, K_i	Gains of a PID controller
U	Velocity of boat
u	Control input
b	Foil span
c	Foil chord

Acronyms

BG	Distance from CO to CG
----	------------------------

CB	Centerboard
CG	Center of gravity
CH	Centerhull
CO	Coordinate origin
CPM	Control plant model
DOF	Degree of Freedom
DVPP	Dynamic Velocity Prediction Program
EoM	Equation of motion
HF	High-frequency
IMO	International Maritime Organization
LF	Low-frequency
LP	Low-pass
MPC	Model Predictive Control
NED	North-East-Down
PID	Proportional-Integral-Derivative
PPM	Process plant model
SB	Starboard
TWA	True Wind Angle
TWS	True Wind Speed
VPP	Velocity Prediction Program

Chapter 1

Introduction

1.1 Motivation

Most sailboats are equipped with a course/heading autopilot, while everything else has to be handled manually. This includes trimming of the sails as well as raising and lowering of centerboards if that is possible.

For many sailboats, the course autopilot is enough, as it gives the option to not have someone at the helm at all times, and thus frees hands to perform other tasks. This may not be the case for sailboats such as high-performance foiling boats, for which the crew requires more assistance than the course autopilot can provide. An example of this is to control not only the yaw angle directly, but have a control system that takes more actuators into account such that more degrees of freedom are controlled. In this thesis, such a system is developed, with the aim of controlling a foiling trimaran sailboat.

1.2 Background

1.2.1 History of hydrofoils



Figure 1.1: Forlanini Hydrofoil 1906

The first boat with hydrofoils was made by Enrico Forlanini in 1906 as seen in Figure 1.1, which was a boat with ladder-like foils and achieved a speed of 42.5 mph (approx. 37 knots). The research and development of hydrofoils slowly continued in the years following,

and in 1955 the first hydrofoil to be approved by a classification society was the PT-20, a commercial passenger craft, using a V-shaped front foil and a rectangular rear foil (Yun and Bliault 2010). These vessels could reach a high speed of 40 knots, but the efficiency was reduced above this speed due to cavitation. Some other disadvantages were the limit for the propulsion, as it was difficult to have water jets with a surface-piercing hydrofoil, and that the size of the boat is limited due to the cavitation issue. The chance of cavitation increases when the pressure is reduced. When the foils become bigger, the speed for lift-off is increased which makes the pressure drop. Lastly the surface-piercing foils were disturbed by larger waves which can cause discomfort for the passengers.

To solve these issues, further development focused on *submerged* hydrofoils, and especially in the US Navy and the Russian Navy. The latter developed vessels for use on rivers and lakes with calm sea states. The prime time for hydrofoils was in the 1970s when many boats were built, some of which are still in use today. As the development of other more economic and stable vessels caught up, the hydrofoils were less interesting and development was reduced in the following years. Today, this has increased again, which is reflected in several start-ups focusing on hydrofoils to reduce energy consumption and accelerations in waves (*Candela Speed Boat* 2020; *FlyingFoil* 2020; *SEAir* 2021). Because of the reduced energy needs, hydrofoils could be part of the solution for express shipping in reaching the international Maritime Organization’s (IMO) goal of reducing emissions from international shipping (IMO 2020). This thesis focuses on high-performance foiling sailing vessels.

1.2.2 Sailing hydrofoils

The first known *sailing* hydrofoil was produced in 1938, using the same ladder-like configuration as the first hydrofoil boats (Sheahan 2013), while the first *offshore* sailing hydrofoil was Williwaw by David Keiper which sailed the South Pacific during the late 1960’s (Callahan 2020). In 1980, the trimaran Paul Ricard set a new record for transatlantic crossings. Due to its weight, adding hydrofoils to it would not make it foil, and instead, load-bearing planes were added to the starboard and port hulls. Another mentionable foiling sailboat is the Hydroptère which set the speed record for 500m and 1 nautical mile in 2009 with speeds above 50 knots. The record has since been broken again but 50 knots is still considered a symbolic limit to reach for sailboats, though the main objective is now to achieve the highest possible mean speeds over long time periods and be able to do so in rougher sea conditions.

Foils on high-performance sailboats have been used more in recent years. With the development of foils for smaller racing boats such as Waszp and the foiling Nacra17 being an Olympic boat (Figure 1.2), the community for foiling sailboats has grown rapidly. The development has happened both on multihulls and monohulls, as the latest edition of America’s Cup featured foiling monohulls. In addition, during the latest Vendée Globe there were used foils on the IMOCA60, which will also be used in The Ocean Race 2022-2023 (Limited 2021; S.L.U. 2021; Vendée 2021).

When flying, the speed of the boat increases due to the reduced hydrodynamic drag resistance, which leads to higher speeds, more delicate sail handling and maneuvers, more action, and thus is considered to be more ”spectator appealing”. This drives the racing closer to shore and opens up for new events such as SailGP and spectators in the Olympics. When foiling, the boats are as mentioned less influenced by the waves, but this also means that the stability of the boat in heave and pitch needs to be good so that they do not plunge into the sea.



Figure 1.2: Nacra17 (foto: Per Bakke)

1.2.3 Modeling and control of hydrofoil vessels

A mathematical model of the system, often implemented in a simulator, is a useful tool for understanding the system, especially for highly coupled and complex systems, like a foiling trimaran sailboat. It is normal to distinguish between different models, such as the simulation model or process plant model (PPM), which is a high-fidelity model with an accurate description of the vessel including marine craft dynamics, propulsion system, measurement system, and environmental forces. The simulation model is used for control system testing and verification. A control design model, also called control plant model (CPM), is a reduced-order model used to design the motion control system. For more details, see Fossen (2011) and Sørensen (2018).

There have been at least three previous master theses from NTNU, that have done work on hydrofoils, two of them are Håberg (2019) and Bøe (2019). They have used numerical tools to model the vessels. Bøe (2019) made a numerical model of a monohull sailboat with hydrofoils to be used as a training simulator for sailors not familiar with foiling sailboats. The potential flow approach (vortex lattice method) was used to find the forces on the foils (sails and hydrofoils). The equation of motion was then solved. The results from this work were that the modeling of forces to foils are good but the dynamic model of the boat had abnormal motions in some conditions.

Foils create lift (perpendicular to the incoming flow direction) and drag (in line with the incoming flow direction) forces. These forces can come from both hydrofoils that are surface piercing or submerged in water and from foils in air. The foils experience both lift and drag forces, and these can be calculated using several methods (O. Faltinsen 2006). For a flat plate using potential theory and assuming no cavitation or ventilation, the lift and drag coefficients can be written as

$$C_L = \frac{L}{\frac{\rho}{2}U^2A} \quad (1.1)$$

$$C_D = \frac{D}{\frac{\rho}{2}U^2A} \quad (1.2)$$

where U is the boat speed, $A = c \cdot b$ is the area of the foil, L is the lift force, D is the drag force and ρ is the density.

The lift and drag depends on the angle of attack on the foil α , which is defined as shown in Figure 1.3.

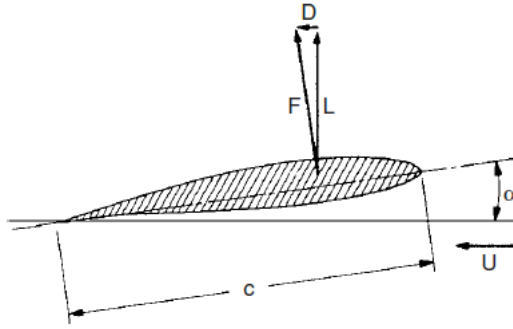


Figure 1.3: Angle of attack α on foil (O. Faltinsen 2006)

Control of a foiling vessel is achieved by controlling the incidence, and hence, the angle of attack of the foils. This can lead to better performance, as seen in Håberg (2019), where active control of the foil flaps lead to better dynamic motion of the foiling catamaran. Håberg (2019) uses numerical modeling to solve the hydrodynamic equation of motion and then applies a simple Proportional-Integral-Derivative (PID) controller. The theoretical study was conducted on a high-speed catamaran, but the theory can be applicable to a foiling sailboat as well. Smaller foiling sailboats, such as the Waszp, are equipped with a passive control system consisting of a rod measuring the distance to water, which controls the flap on the centerboard foil directly (WASZP 2021).

The motions on a high-performance sailboat are a lot of the time more complex and coupled, which calls for a model in ideally 6 degrees of freedom (DOFs), whereas on a hydrofoil it is often enough with four DOFs, excluding heave and pitch. When the foiling vessel is in flying condition, the motions exhibit strong couplings between the degrees of freedom and for a foiling vessel, the heave and pitch must also be considered for the vessel stability, as opposed to a regular surface vessel where these will balance themselves naturally when the wetted surface changes. Thus, the complexity of the system modeling and control increases.

The flying condition for a foiling vessel has similarities to aircraft theory, as the motions for both depend on foil forces, lift and drag. In an aircraft, the elevator is used for pitch control, the ailerons are used for roll control and the yaw angle is controlled by a combination of roll and pitch through "bank to turn". As we will see for a foiling sailboat, there are several actuators that contribute to e.g. roll, such that the complete system is more coupled (Beard and McLain 2012).

There are different types of foils used on sailing vessels that all have different properties. A T-foil has a straight vertical part with a horizontal flap at the bottom. L-foil is a foil that can look something between a L and a J in shape and often has an angle such that the lowest part is where it bends. An illustration of the two foils is shown in Figure 1.4.

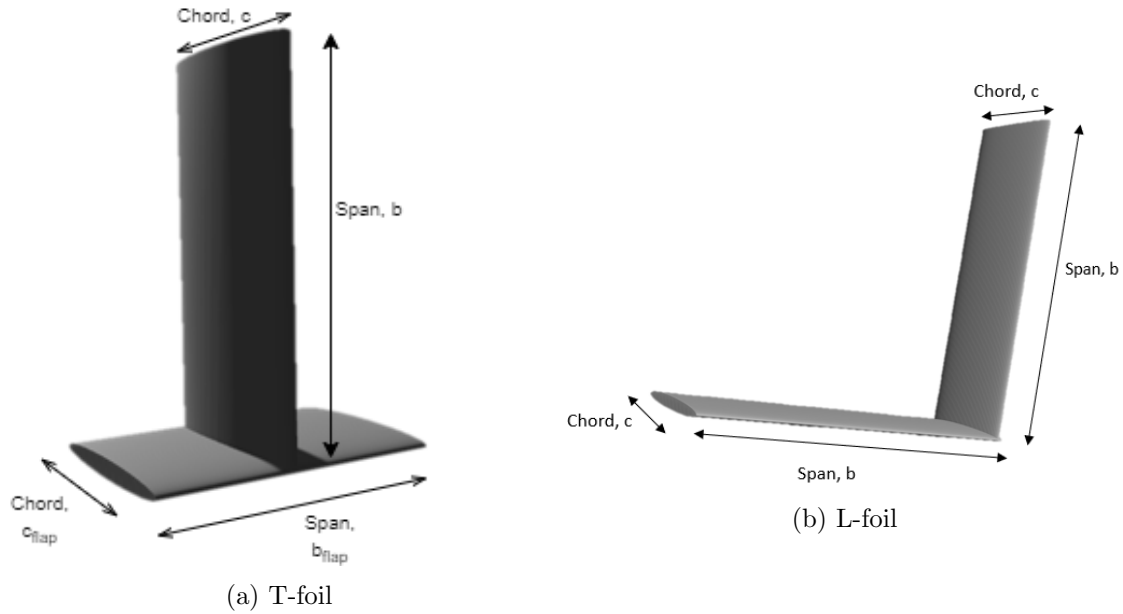


Figure 1.4: Different foil types

1.2.4 Control systems of sailboats

The difference between a foiling sailboat and a hydrofoil vessel is that the sail is the main propulsion. A sailboat is subjected to considerable aerodynamical forces on sail and rig, and hydrodynamical forces on the hull and foils. The sail provides a large moment in roll. The aerodynamic load on the sail has, in equilibrium conditions, the same module as the hydrodynamic loads on the foils that are much smaller, which is due to the difference in fluid density.

Sailboats are normally equipped with a heading autopilot as the only control system. In the industry, it is mostly PID controllers that are used in autopilots for sailboats as they are simple and inexpensive. These autopilots are tuned for some conditions, while a sailboat will most likely encounter a diverse range of conditions as the weather is unpredictable and sailboats often change the environment they are used in. As of today, gains in the PID must be adapted manually by the sailor through some interface.

In research, several different types of controllers have been developed and tested for sailboats. The advantages of the more advanced controllers are that they are more robust to handle the diverse conditions a sailboat is operating in (Trehin et al. 2019). These controllers often utilise more actuators and are made for autonomous sailboats, such that they consist of more than an autopilot. For example, Wille (2016) develops a course and roll controller for an autonomous sailboat using backstepping for the course controller, and state feedback linearization for roll control using the sail and rudder as actuators.

1.2.5 The Ultim class of sailboats

The Ultim class 32/23 trimarans are maximum 32 meters long and 23 meters wide and are designed for offshore racing with double or singlehanded sailing in rough oceanic conditions. Today, the foils are controlled manually using hydraulics driven by manual winch because no accumulation of energy is allowed except for course/heading autopilot (FFVoile

2020). It is interesting to see how these foils can be controlled using an automatic control system. With an automatic system, it could be expected that the stability in waves and wind gusts will be better, which leads to more flying time, higher average speed and can also mean improved safety for the sailors.

Because an automatic control system is not allowed in the Ultim class for anything else than the course control, the racing team Gitana regularly leaves (before re-entering) the official class to pursue offshore sailing where a control system for the foils are allowed, for example in the Jules Verne Trophy (Gitana 2020a). This means that such a system is under development and is being tested with the aim of automatically controlling the helm and the foils under conditions where the controller can be improved.

The Ultim trimaran has six foils that potentially can be controlled, located on the rudders, centerboard, and two large foils on the port and starboard hulls. These need to be modeled to understand how the foils act and what the effects of changing their incidence have on the behavior of the boat. In addition, the control structure needs to be modeled to prepare for control of the foils.

1.3 Scope of work

The main goal of this thesis is to

”Develop and verify a control system for the foiling trimaran sailboat that is suitable for automatic course and ride control and performs well in different environments.”

The controller should be sufficient to keep the sailboat in a foiling state over a certain amount of time, and under different disturbances which is covered by the test scenarios.

This goal is reached by developing a simple model for the trimaran, and three controllers with different approaches to the allocation of forces. The trimaran, its environment and the controllers are modelled and simulated using Matlab and Simulink, where they are tested for several scenarios.

The system is highly coupled between the degrees of freedom, so there is put some emphasis on understanding how this coupling works together with changes in foil incidence. This is discussed in relation with the development of the controllers.

1.4 Main Contributions

The main contributions of this thesis can be summarized as

- Development of a dynamic simulation environment describing an Ultim trimaran, with emphasis on studying the load distribution on the foils, and the effect of foil incidence on loads. This is presented in Chapter 2 and verified in Chapter 3.
- Development of a control system with three controller candidates
 - one based on direct allocation
 - one based on allocation using the load distribution

- one based on a combination of the other two
- Validation of the control system model through simulation of different cases. This is presented in Chapter 5.
- Simulations of scenarios with different disturbances to explore the performance of the model within the validity range.

1.5 Organization of thesis

The thesis is organized as follows:

Chapter 2 describes the boat, its relevant components and how the mathematical model of the boat is built. This is used as a starting point for the rest of the thesis.

Chapter 3 describes how the static equilibrium of the boat was found, and uses the equilibrium to validate the mathematical model from the previous chapter. It also presents the load distribution for equilibrium and shows the result of a sensitivity analysis of the control inputs. This is based on the results from the pre-project (Hella 2020).

Chapter 4 presents the architecture and components of the control system, as well as the three controller candidates used in simulations and tests.

Chapter 5 presents the results from two test cases which are used to verify the control system. It also presents boundaries for the validity of the model.

Chapter 6 and **Chapter 7** presents the results for different test simulations with regards to the performance of the three different controller candidates in calm sea and with regular (swell) waves, respectively. A discussion where the controllers are compared is included.

Chapter 8 presents the concluding remarks of the thesis, and elaborates on the main improvements and possibilities for further work.

Appendix A includes larger figures of the load distribution.

Chapter 2

Dynamic and hydrodynamic model

2.1 Boat description



Figure 2.1: Ultim trimarans

The characteristics for the sailboat used in this project are inspired by the three boats; *Macif 100*¹, *GitanaMaxi*, and *Sodebo Ultim 3* designed by Van Peteghem Lauriot-Prévost (VPLP) and the their respective teams. The main particulars for *Macif 100*, *GitanaMaxi* and *Sodebo Ultim 3* can be found in Table 2.1. The boat lifts off at a boat speed of about 20-25 knots and reach a maximum speed of 45-50 knots. They are mainly used in offshore racing, both for shorthanded² and for larger teams. 3D models of the sailboats are shown in Figure 2.1 (Actual 2021; Gitana 2020a; Sodebo 2021).

The modeled boat uses the main particulars of Macif 100, and is equipped with the following foils (Figure 1.4)

- Three rudders with a T-foil located on the central, port and starboard hull

¹Since the work on this thesis started, this boat has been sold and is now called Actual Ultim 3 (Actual 2020)

²Crews of two people or less

Sailboat	Macif 100	Gitana Maxi	Sodebo Ultim 3
Length	30 m	32 m	32 m
Beam	21 m	23 m	23 m
Draft	4.5 m	-	< 5 m
Air draught	35 m	37 m	36 m
Displacement	14.5 tonn	15.5 tonn	
Sail surface (close hauled)	430 m ²	450 m ²	447 m ²
Sail surface (down wind)	650 m ²	650 m ²	697 m ²

Table 2.1: Boat Characteristics

- Two large L-foils on the port and starboard hull, respectively
- One centerboard with T-foil on the central hull

The L-foils are inclined, to contribute to flight stability in a passive way. The centerboard counteracts leeway, and by adding a T-foil it also provides lift in z_b direction. This force is directed up or down depending on the wind direction, and can then be used to reduce the roll angle if the sail generates a too large side force.

2.2 Reference frames

The equations of motions need to be solved in 6-DOF. Surface vessels are generally controlled in 3-DOF, using surge, sway and yaw. For a sailboat, the roll angle must be included as the sail introduces a large roll moment that can, ultimately, cause capsizing. The pitch angle and flight height (heave) is an important aspect for performance, such that these three DOFs also needs to be factored in, which leads to the 6-DOF system (Heppel 2015).

The reference frames used is North-East-Down (NED) and body-fixed. The notations for the 6 Degree of Freedom (DOF) used is described in Table 2.2 and displayed in Figure 2.2 (Fossen 2011).

DOF		Forces and moments	Linear and angular velocities	Position and Euler angles
1	motion in x -direction (surge)	X	u	x
2	motion in y -direction (sway)	Y	v	y
3	motion in z -direction (heave)	Z	w	z
4	rotation about the x -axis (roll)	K	p	ϕ
5	rotation about the y -axis (pitch)	M	q	θ
6	rotation about the z -axis (yaw)	N	r	ψ

Table 2.2: Reference frame notation for 6-DOF marine vehicle

The transformation matrix $J_\theta(\eta) = \begin{bmatrix} R(\Theta_{nb}) & 0 \\ 0 & T(\Theta_{nb}) \end{bmatrix}$ between NED and body-frame is

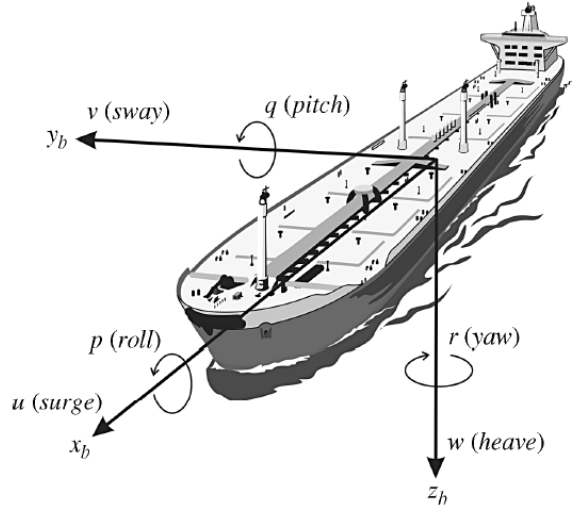


Figure 2.2: Degrees of freedom for marine vessel (Fossen 2011)

described by the Euler rotation in (2.1) and the angular velocity rotation in (2.2).

$$R(\Theta_{nb}) = \begin{bmatrix} \cos \psi \cos \theta & -\sin \psi \cos \phi + \cos \psi \sin \theta \sin \phi & \sin \psi \sin \phi + \cos \psi \cos \phi \sin \theta \\ \sin \psi \cos \theta & \cos \psi \cos \phi + \sin \phi \sin \theta \sin \psi & -\cos \psi \sin \phi + \sin \theta \sin \psi \cos \phi \\ -\sin \theta & \cos \theta \sin \phi & \cos \theta \cos \phi \end{bmatrix} \quad (2.1)$$

$$T(\Theta_{nb}) = \begin{bmatrix} 1 & \sin \phi \tan \theta & \cos \phi \tan \theta \\ 0 & \cos \phi & -\sin \phi \\ 0 & \sin \phi / \cos \theta & \cos \phi / \cos \theta \end{bmatrix} \quad (2.2)$$

The coordinate origin (CO) of the body-fixed reference frame is located below the mastfoot, at the waterline.

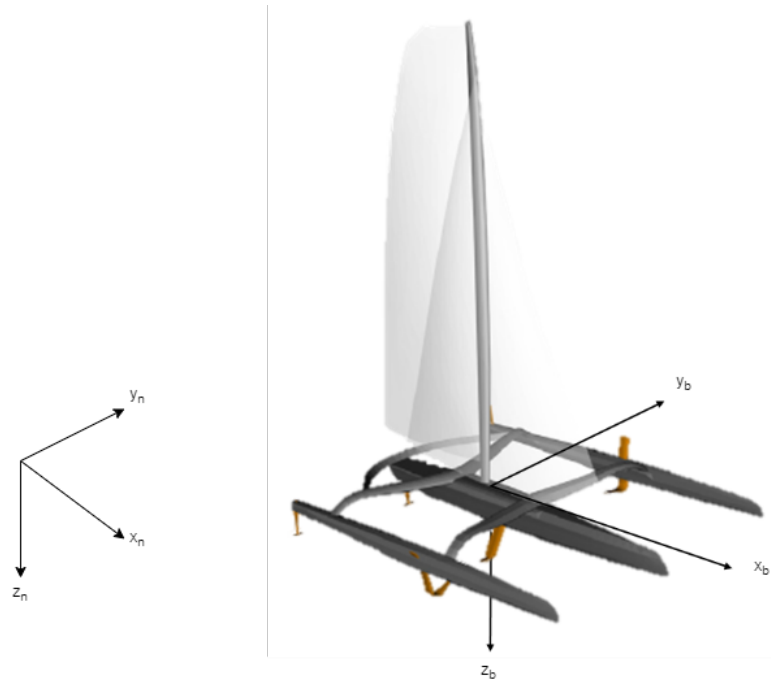


Figure 2.3: Body-frame and NED-frame

In addition, a foil-fixed reference frame $\{f\}$ is used to describe forces on the foils. This frame relates the attitude of the foil to the body-fixed frame. The rotation is the same as between NED and body-frame such that both (2.1) and (2.2) is applicable. The origin of $\{f\}$ is in the center of the foil, i.e. mid-chord and mid-span, while f_1 is along the foil chord, f_2 is along the span and f_3 is orthogonal to the foil (Figure 2.4).

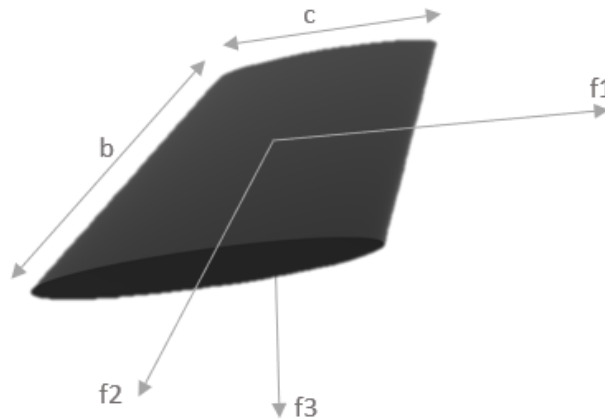


Figure 2.4: Foil-fixed reference frame

The positions of the foils and their nominal incidence are described by rotations from b to f and is given in Table 2.3. Due to symmetry, the foils on the port hull are not modeled. The positions are given in $\{b\}$, while the attitude is given in $\{f\}$.

Description	Position $[x_b, y_b, z_b]$	Attitude $[\phi_f, \theta_f, \psi_f]$ [deg]	Chord [m]	Span [m]
Sail	$[-1, -20 \sin 5, -20]$	$[-95, 0, -20]$	23	30
L-foil				
Horizontal	$[4, 8.5, 1.08]$	$[15, 4.5, 0]$	0.6	2
Vertical	$[4, 9.75, 0.58]$	$[100, 4.5, 0]$	0.6	2
Rudder starboard				
T-foil horizontal	$[-12.5, 10.5, 0.28]$	$[-5, 0, 0]$	0.5	0.5
T-foil vertical	$[-12.5, 10.5, -0.32]$	$[85, 0, 0]$	0.5	2.1
Rudder center				
T-foil horizontal	$[-11, 0, 2.1]$	$[0, 0, 0]$	0.5	0.5
T-foil vertical	$[-11, 0, 1.05]$	$[90, 0, 0]$	0.5	2.1
Centerboard				
T-foil horizontal	$[-1, 0, 4.2]$	$[0, 0, 0]$	0.5	1.1
T-foil vertical	$[0, 0, 2.1]$	$[90, -13, 0]$	0.5	4.2

Table 2.3: Foil description

2.3 Dynamic model of a foiling vessel

To make a control system for a boat, it is required to do a mathematical modeling of the system being controlled. To simplify the system, and make it possible to model within the scope of this thesis, a "minimum viable" model is made under the following assumptions.

Assumption 1. The sails are modelled as one foil and are preset.

Assumption 2. The boat is always foiling, i.e. hulls out of water.

Modeling in only the foiling state means the hydrodynamic loads on the hulls are neglected in the study of the forces. This also applies for the sail, where modeling it as a simple foil means the effects of twisting is not considered. By having constant wind and also constant target heading, it is possible to look at a static equilibrium for the initial states of the dynamic modeling.

Assumption 3. L-foil is preset.

The L-foil cannot be controlled automatically, and therefore it is set in one setting in this model. For the real boats, the cant (sideways inclination of the L-foil) can only be changed at quay, while the rake (trim of the L-foil) can be changed while sailing, but not dynamically. In addition, the L-foil can be lowered and raised while sailing but it is a demanding operation (especially when lowering the foil under speed). These possibilities is excluded when modeling the L-foil as preset.

The forces on a boat are the sum of inertia forces, weight forces, the hydrodynamic forces excited by the waves and current and aerodynamic forces on the topside structure and sail. These are expressed through excitation forces and through hydrostatic forces such as buoyancy and restoring loads. The generic equations of motion (EoM) for a vessel exposed to the environments are

$$\dot{\eta} = J_{\theta}(\eta)\nu \quad (2.3a)$$

$$M\dot{\nu} + C(\nu)\nu + D(\nu)\nu + g(\eta) = \tau + \tau_{wind} + \tau_{wave} \quad (2.3b)$$

Equation (2.3a) is the 6-DOF kinematic equation for rotation between the inertial frame

North-East-Down (NED) $\{n\}$ and the body-fixed reference frame $\{b\}$, while (2.3b) is the matrix equation of motion in $\{b\}$. The components in the equations are

- Vector of position and angles $\eta \in \mathbb{R}^6$
- Vector of velocities $\nu \in \mathbb{R}^6$
- The transformation matrix $J_\theta(\eta) \in \mathbb{R}^6$
- The system inertia matrix $M \in \mathbb{R}^{6 \times 6}$
- The coriolis and centripetal matrix $C(\nu) \in \mathbb{R}^{6 \times 6}$
- The damping matrix $D(\nu) \in \mathbb{R}^{6 \times 6}$
- The vector of gravitational forces and moments $g(\eta) \in \mathbb{R}^6$
- Vector of control inputs $\tau \in \mathbb{R}^6$
- Vector of generalized wind forces $\tau_{wind} \in \mathbb{R}^6$
- Vector of generalized wave-induced forces $\tau_{wave} \in \mathbb{R}^6$

The vector of position and angles η is given in $\{n\}$ and the vector of velocities ν is given in $\{b\}$. Both are displayed below.

$$\eta = \begin{bmatrix} x \\ y \\ z \\ \phi \\ \theta \\ \psi \end{bmatrix} \quad (2.4)$$

$$\nu = \begin{bmatrix} u \\ v \\ w \\ p \\ q \\ r \end{bmatrix} \quad (2.5)$$

For the sailboat considered in this thesis, all environmental loads are modeled through their actions on the foils, which means that the EoM reduces to

$$\dot{\eta} = J_\theta(\eta)\nu \quad (2.6a)$$

$$M\dot{\nu} + C(\nu)\nu + g(\eta) = \sum_{i=1}^{N_{\text{foils}}} \tau_{f_i} \quad (2.6b)$$

where τ_{f_i} is the lift and drag forces generated by the i th foil. As the sailboat is assumed to be foiling, the buoyancy forces in $g(\eta)$ is neglected. This is because the foils generates a small buoyancy force compared to the hydrodynamic foil loads.

As the boat is symmetric, the foils on the port hull is not included in the model. This is because the port hull is out of the water and does not contribute with any forces other than weight load, under the assumption that the boat is always in foiling state.

2.4 Inertia, Weight and Coriolis-Centripetal loads

The rigid-body coriolis and centripetal matrix C_{RB} consists of the coriolis term and the centripetal term represented by a skew-symmetric matrix ³. Note that the added mass coriolis and centripetal matrix C_A is not included as it is assumed to be zero when foiling.

$$C_{RB} = \begin{bmatrix} m_{tot}S(\omega) & -m_{tot}S(\omega)S(r_g^b) \\ m_{tot}S(\omega)S(r_g^b) & -S(I_b\omega) \end{bmatrix} \quad (2.7)$$

where $\omega = [p, q, r]^T$.

The gravitational force f_g^b acts in CG and is given as (2.8).

$$f_g^b = \begin{bmatrix} 0 \\ 0 \\ R^T(\Theta_{nb})m_{tot}g \end{bmatrix} \quad (2.8)$$

The resulting restoring loads are then

$$\tau_g = \begin{bmatrix} f_g^b \\ f_g^b \times r_{bg}^b \end{bmatrix} \quad (2.9)$$

where the center of gravity (CG) (p. 19 in Fossen 2011) of the sailboat is approximated by $r_g^b = [x_g, y_g, z_g]^T$.

The system inertia matrix consists of the rigid-body mass matrix M_{RB} and the added mass matrix M_A . As the sailboat is assumed to be in steady foiling state, the added mass from hydrodynamic forces are assumed to be zero. The resulting mass matrix is then $M = M_{RB}$. The total mass of the sailboat is given from the masses in Table 2.4 and is displayed in (2.10). These mass distributions are assumed to be representative of a typical Ultim.

$$m_{tot} = 2m_f + m_c + m_m + 2m_t + m_{co} = 14400\text{kg} \quad (2.10)$$

Label	Mass in tonnes	Description
m_f	1.85	Mass of a floater
m_c	3.3	Mass of the central hull
m_m	1.4	Mass of the mast and sails
m_t	1.75	Mass of the lateral beams
m_{co}	2.5	Mass of the cockpit

Table 2.4: Masses

The center of gravity (CG) is approximated by

$$\begin{aligned} x_g &= -\frac{m_{co}d_{co}}{m_{tot}} = -1.3[\text{m}], \text{ i.e. } 1.3\text{m behind the mast} \\ y_g &= 0 \\ z_g &= \frac{m_m l_m}{2m_{tot}} = -1.7[\text{m}], \text{ i.e. } 1.7\text{m above waterline} \end{aligned} \quad (2.11)$$

³Skew-symmetric matrix is a useful property for a nonlinear motion control system because of the quadratic form $\nu^T C_{RB}(\nu)\nu \equiv 0$.

which originated from $\sum m_i \overrightarrow{BG}_i = m_{tot} \overrightarrow{BG}$ by use of symmetry.

To estimate the moments of inertia, the distances between the components of the sailboat are needed. They are displayed in Table 2.5.

Label	Length in m	Description
l_f	27.6	Length of a floater
l_c	27	Length of the central hull
d_f	10.5	Distance between central hull and floaters
l_m	35	Height of mast
d_m	6	Distance between mast and transverse beams
d_{co}	7.5	Distance between mast and cockpit

Table 2.5: Length and distances

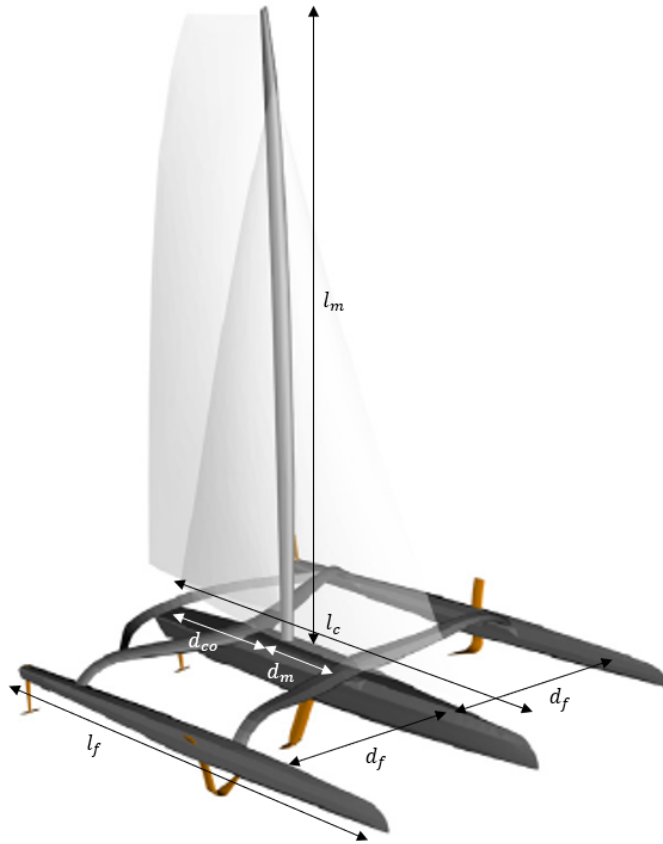


Figure 2.5: Length and distances on sailboat

The moments of inertia are then found by

$$\begin{aligned}
I_{xx} &= \int_V (y^2 + z^2) \rho_m dV \\
&\approx 2m_f d_f^2 + \frac{1}{3} m_m l_m^2 + \frac{2}{3} m_t d_f^2 \\
I_{yy} &= \int_V (x^2 + z^2) \rho_m dV \\
&\approx \frac{1}{6} m_f l_f^2 + \frac{1}{12} m_c l_c^2 + \frac{1}{3} m_m l_m^2 + 2m_t d_t^2 + m_{co} d_{co}^2 \\
I_{zz} &= \int_V (x^2 + y^2) \rho_m dV \\
&\approx 2m_f d_f^2 + \frac{1}{6} m_f l_f^2 + \frac{1}{12} m_c l_c^2 + 2m_t d_t^2 + \frac{1}{12} m_t d_t^2 m_{co} d_{co}^2
\end{aligned} \tag{2.12}$$

The mass matrix of the 6-DOF sailboat is given by

$$M = \begin{bmatrix} 0.0144 & 0 & 0 & 0 & -0.0245 & 0 \\ 0 & 0.0144 & 0 & 0.0245 & 0 & -0.0187 \\ 0 & 0 & 0.0144 & 0 & 0.0187 & 0 \\ 0 & 0.0245 & 0 & 1.1082 & 0 & 0 \\ -0.0245 & 0 & 0.0187 & 0 & 1.2736 & 0 \\ 0 & -0.0187 & 0 & 0 & 0 & 1.1260 \end{bmatrix} 10^6 \tag{2.13}$$

2.5 Foil loads

As opposed to a motorized marine vessel, a sailboat obtains its entire thrust force from flow around sails, represented by lift and drag force. Lift and drag force are from O. Faltinsen (2006), and is displayed in (1.1) and (1.2). The details in calculating the foil-induced forces are given in the following.

2.5.1 Lift and drag coefficients, C_L and C_D

The lift and drag coefficients C_L and C_D can be found in various ways, such as numerical methods or experimental methods. Here they were initially found using the graphs in Figure 2.6.

The graphs show the lift and drag coefficients as a function of angle of attack α in a steady flow past a 2D foil in an infinite fluid with turbulent boundary-layer flow conditions. For the lift coefficient C_L it is shown that it increases approximately from 0.5 when α is 0° to 1.5 when α is 15° where it stalls. The drag coefficient C_D varies between 0.01 for $\alpha = 0^\circ$ and increases quadratic to 0.025 for $\alpha = 20^\circ$.

By having a surface piercing L-foil, it can act as an active control system because of it's stabilizing effect due to the change in lift force with the submerged part (O. Faltinsen 2006).

As the foils can either be in air, in water or both, the exact submergence needs to be checked for each of the foils before calculating the lift and drag force. This is done by

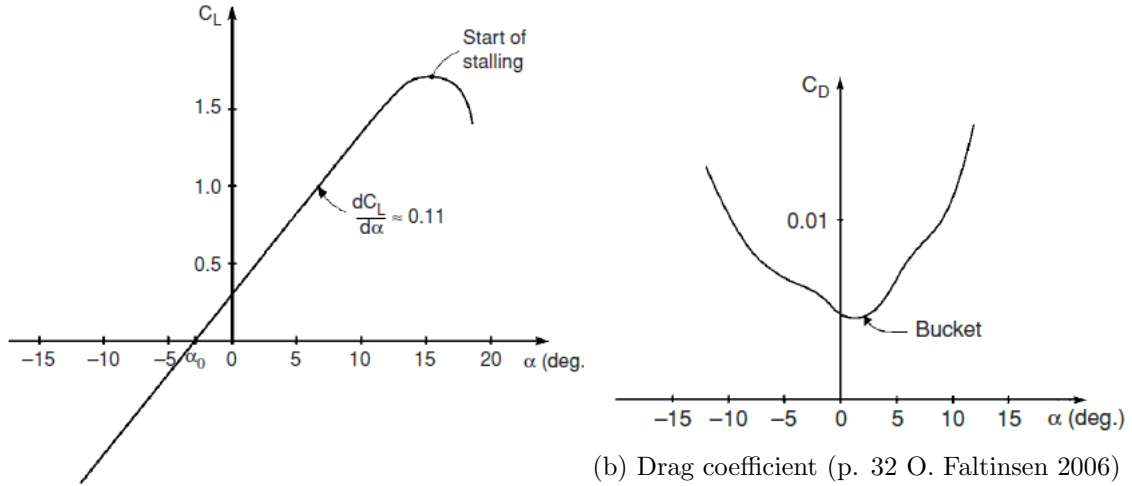
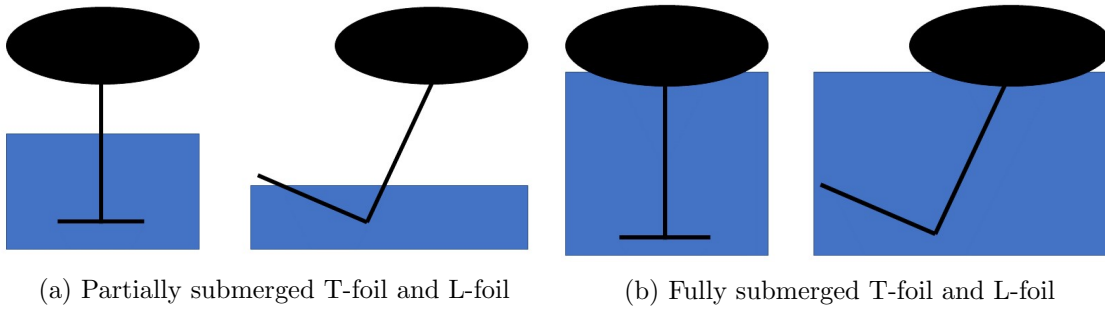
Figure 2.6: Lift and drag coefficient as a function of angle of attack α 

Figure 2.7: Illustration of foils in water or partially in water

comparing the position of the ends of each foil to the free surface. The comparison leads to three different cases: partially submerged, fully submerged or in air. For the case of partially submerged, a scale $\sigma \in [0, 1]$ is used to indicate how much of the foil is in water. σ is found by

$$\sigma = \frac{z_{top}^i}{z_{top}^i + z_{bottom}^i} \quad (2.14)$$

where z_{top}^i and z_{bottom}^i corresponds to the top and bottom position of the i -th foil ends.

2.5.2 Calculating the relative velocity and angle of attack

The velocity U_{wind} and direction of the wind β_{wind} given in NED and are rotated to the boat-fixed frame $\{b\}$.

$$U_{wind}^b = R_b^n(\Theta)^T \begin{bmatrix} U_{wind}^n \cos \beta_{wind} \\ U_{wind}^n \sin \beta_{wind} \\ 0 \end{bmatrix} \quad (2.15)$$

The lift and drag force is calculated in the foil-fixed reference frame, which is done in several steps. First, the velocity of the sailboat and wind speed is found in $\{b\}$ for each

foil position. The center of the i^{th} foil is denoted $F^{(i)}$ such that the distance from CO to $F^{(i)}$ is $BF^{(i)}$.

$$\nu_i = \begin{bmatrix} u \\ v \\ w \end{bmatrix} + \begin{bmatrix} \omega \times BF^{(i)} \\ \omega \times BF^{(i)} \\ \omega \times BF^{(i)} \end{bmatrix} \quad (2.16)$$

The relative velocity in body experienced by the foil is then $\nu_{r_i}^b = \nu_i - U_{wind}^b$ for a foil in air and $\nu_{r_i}^b = \nu_i - U_{waves}^b$ for a submerged or partially submerged foil. How to find the wave velocity is described in 2.5.5

$$U = \nu_{r_i}^f = R(\theta)\nu_{r_i}^b \quad (2.17)$$

The angle of attack α is found by looking at the angle between the relative velocity in f_1 and f_3 .

$$\alpha = \arctan \frac{U_{f_3}}{U_{f_1}} \quad (2.18)$$

2.5.3 Lift and drag force

Lastly, to calculate the lift and drag force, the foil area A is needed, which is $A = bc$. The resulting lift and drag is then given in the equations under dependent on if the foil is submerged or in air.

$$L = \frac{1}{2}\rho_w\sigma C_L U^2 A \quad (2.19) \quad D = \frac{1}{2}\rho_w\sigma C_D U^2 A \quad (2.21)$$

$$L = \frac{1}{2}\rho_a C_L U^2 A \quad (2.20) \quad D = \frac{1}{2}\rho_a C_D U^2 A \quad (2.22)$$

Here, ρ_a is density of air, ρ_w is density of saltwater, σ is the degree of submergence of the foil, C_L is the lift coefficient, C_D is the drag coefficient, U is the relative velocity of the fluid to the foil, given in (2.17), and A is the area.

When the lift and drag forces and moments are found in $\{f\}$, they are be rotated back to $\{b\}$ using the rotational matrix R_b^n .

The trimaran has asymmetric L-foils, in which case the lift/drag ratio is better, meaning that C_D can be decreased compared to a symmetric foil generating comparable lift. To simplify modeling at this stage, the C_D have also been decreased for the other foils too (T-foils, rudders, sails), as they represent less than 20% of the total drag force. Therefore this is also applied to this model.

2.5.4 Drag on the superstructure

The environmental forces on the superstructure (hulls, beams connecting the hulls, cockpit, mast, nets, etc...) consists of an aerodynamic drag only⁴. The air resistance or aerodynamical force is expressed as shown in (2.23)

$$\tau_{wind} = f_{air}^b = \begin{bmatrix} -\frac{1}{2}\rho_a C_d A \nu_r^2 \\ -\frac{1}{2}\rho_a C_d A \nu_r^2 \times BA \end{bmatrix} \quad (2.23)$$

where ρ_a is the mass density of the air and A is the area of the above-water hull form projected onto a transverse plane of the sailboat. C_D is the drag coefficient which in this case is modeled as 1, and ν_r is the relative velocity of the sailboat in {b}. $BA = [0, 0, -10]^T$ is the distance from CO to the assumed application point of the force on the mast.

2.5.5 Effect of waves

Waves can be modelled different ways. By using assuming deep water, horizontal sea bottom and a free-surface, the linear wave theory for propagating waves is derived. The velocity component of the wave particles are given in (2.24) (O. M. Faltinsen 1990).

$$\begin{aligned} u &= \omega \zeta_a e^{kz} \sin(\omega t - k\beta_{wave}) \\ w &= -\omega \zeta_a e^{kz} \cos(\omega t - k\beta_{wave}) \end{aligned} \quad (2.24)$$

Here, ω is the circular frequency of the wave, ζ_a is the wave amplitude, z is the vertical coordinate, $k = \frac{\omega^2}{g}$ is the wave number, t is the time variable and β_{wave} is the direction of wave propagation.

In the present work, for simplicity, the presence of waves is only accounted for though the induced particle velocity (and hence ambient fluid velocity around the foils), and the surface elevation is neglected.

⁴note that on some Ultims, the beams connecting the hulls are covered with "aerodynamic tarp" designed to generate some lift too

Chapter 3

Static equilibrium

To get an initial condition for the simulation of the control system, an equilibrium in steady-state conditions has to be found. This static equilibrium is also used to validate the mathematical model of the boat. Here, static refers to steady conditions, for which the boat has a constant, non-zero, velocity. This chapter is based on the results from the pre-project (Hella 2020).

The static equilibrium is found by considering a scenario with constant true wind speed (TWS) and true wind angle (TWA), and constant velocity and direction of the boat. As a part of the validation of the system, the steady-state equilibrium has been first sought by manually tuning the velocity, trim, heel, sinkage, leeway, L foil rake, sail angle, etc... Then, an automatic optimization was done by changing the foil angle for the hydrofoils with the aim of minimizing the residual in the forces and moments and further reach equilibrium for the model.

3.1 Initial steady conditions

The assumed conditions are displayed in Table 3.1. These conditions were chosen based on information gathered about the Ultim's performance, such that the conditions could be as authentic as possible. At a boat speed of 21 m/s (42 knots) and in 10 m/s wind, the boat is likely to be in stable flying conditions.

Speed	U_0	21 [m/s]
Drift angle	β_0	1.2°
Sinkage	z_{b0}	-1.6 [m]
Heel	ϕ_0	5°
Trim	θ_0	2°
Velocity	u_0	20.98 [m/s]
Velocity	v_0	0.5 [m/s]
Velocity	w_0	0.69 [m/s]
Wind speed	u_w	10 [m/s]
Wind direction	TWA	-120°

Table 3.1: Initial values

The drift angle β is the angle which describes the difference between the x_b axis and the

relative velocity direction for the boat. The wind direction is defined as the true wind angle (TWA) of -120° , which corresponds to $\beta_{wind} = 60^\circ$

To reach equilibrium, initial values for the optimization was needed. These were found from studying the trimarans mentioned in Section 2.1 through videos and online resources such as their websites (Gitana 2020a; PlanetSail 2020) and through correspondence with Mer Concept (Lavigne and Sauder 2020).

3.2 Reaching equilibrium

As the sailboat was not exactly in equilibrium with the conditions given in Table 3.1 (there was a residual net load on the boat), an optimization was performed on the model in Matlab, by using the initial conditions in Table 3.1 and Table 2.3 and then altering the foil attitude to achieve a balance in the forces and moments that is closer to zero. The optimization was terminated when the difference in value between two iterations was less than 10^{-10} , the number of iterations reached 10^6 or the function had been evaluated more than 10^8 times. The function to minimize is given in (3.1)

$$\min_x \sqrt{10^{-3}(X^2(x) + Y^2(x) + Z^2(x))} + \sqrt{10^{-3}(K^2(x) + M^2(x) + N^2(x))} \quad (3.1)$$

where x is the change in foil attitude, X, Y, Z are the net total forces on the boat and K, M, N are the net total moments for the sailboat. The optimization was solved with Nelder-Mead simplex algorithm using the Matlab function *fminsearch* (MathWorks 2020). The forces and moments are calculated as described in Chapter 2.

The components of x are the foils that were optimized, which are

- Rake angle of L-foil
- Rudder T-foil angle (both starboard and centerhull)
- Rudder angle (both starboard and centerhull)
- Centerboard T-foil angle

The initial values for the component of x were all zero, meaning no change in foil angles from the initial foil attitude. The rudder angles for the starboard and centerhull were constrained to have the same angles, using the assumption that they would be controlled as one. Similarly, the T-foils were constrained to have the same angles. By controlling the T-foils independently, the x vector could have had one more component. The final results was $x = [-0.9, -0.3, 1.3, 0.9]^T$ degrees change, which yielded the forces and moments in Table 3.2. Ideally, the results should have shown that the forces and moments were zero, but in a practical implementation this is hard to achieve because all other parameters but the foil angles are fixed (speed, trim, leeway, etc...). As the results are small compared to the lift forces from e.g. the sail, this is satisfactory as static equilibrium. We will see in the next chapters, that during dynamic simulation (when all parameters are free to vary), the Ultim reaches an equilibrium condition close to this one.

	X	Y	Z	K	M	N
Initial	0.7	19.0	-4.7	-127.1	39.6	317.3
Result	-0.1	5.7	2.1	0.3	2.1	-4.8

Table 3.2: Forces [kN] and moments [kNm] before and after optimization

3.3 Load distribution

The load distribution in {b} for static equilibrium has been analyzed and is displayed using pie charts showing the positive and negative forces and moments for each degree of freedom. Examples are shown in Figure 3.1 and Figure 3.2 and the full versions are in Appendix A.

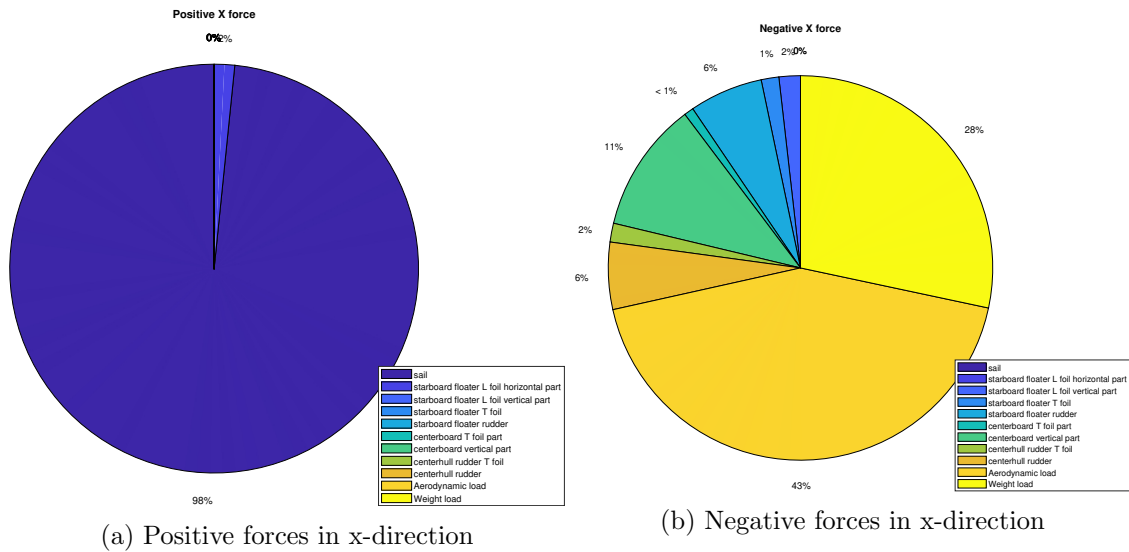


Figure 3.1: Pie charts of forces

The biggest contributor to the forward force is the sail, which is also the primary thrust force for the sailboat. This makes the boat move in positive x-direction. The counterforce in surge is the aerodynamic force and the weight force. Due to the trim angle, a part of the weight force is projected along x_b . The force from the sail is changing with the wind speed and wind direction. The sail is also the biggest contributor to positive sway force, where the centerboard is the counterforce. In heave, the weight is the force directed downwards and the lift force from the foils works upwards, with the horizontal part of the L-foil and the T-foil in the centerboard being the biggest contributors. In an Archimedean state, the weight would be counteracted by the buoyancy of the hulls in water.

For the moments, it is the L-foil that generates the largest moments in all directions together with the sail. The largest moments in pitch are provided by the sail and the horizontal part of the L-foil. For the yaw moment, the biggest contributor is the L-foil. General for the moments is that the control surfaces do not contribute a lot in equilibrium. This indicates that the Ultim is almost naturally in equilibrium without the need for the control surfaces.

An analysis of the static equilibrium for a boat speed of $U = 26$ m/s has also been performed, and the results from this showed that the equilibrium is closer to zero, but a boat speed of 26 m/s in a wind speed of 10 m/s would be unrealistic. 26 m/s corresponds to 52 knots, which is above the "limit" of 50 knots which is a speed that the Ultim trimarans

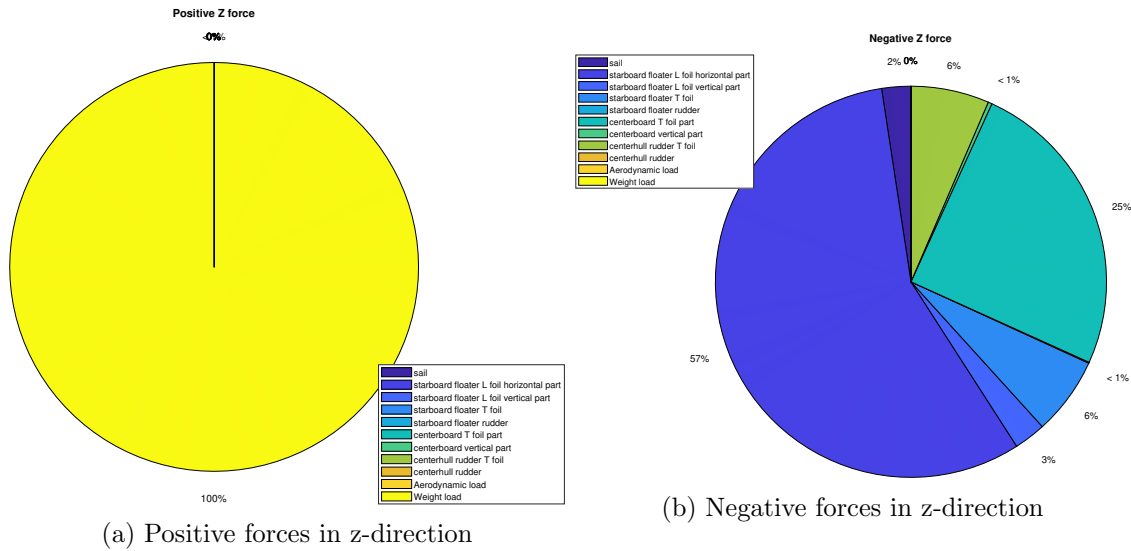


Figure 3.2: Pie charts of forces

can reach but is less likely to keep over some time. It was interesting though to see that the load distribution changed quite a lot from the on at boat speed $U = 21$ m/s.

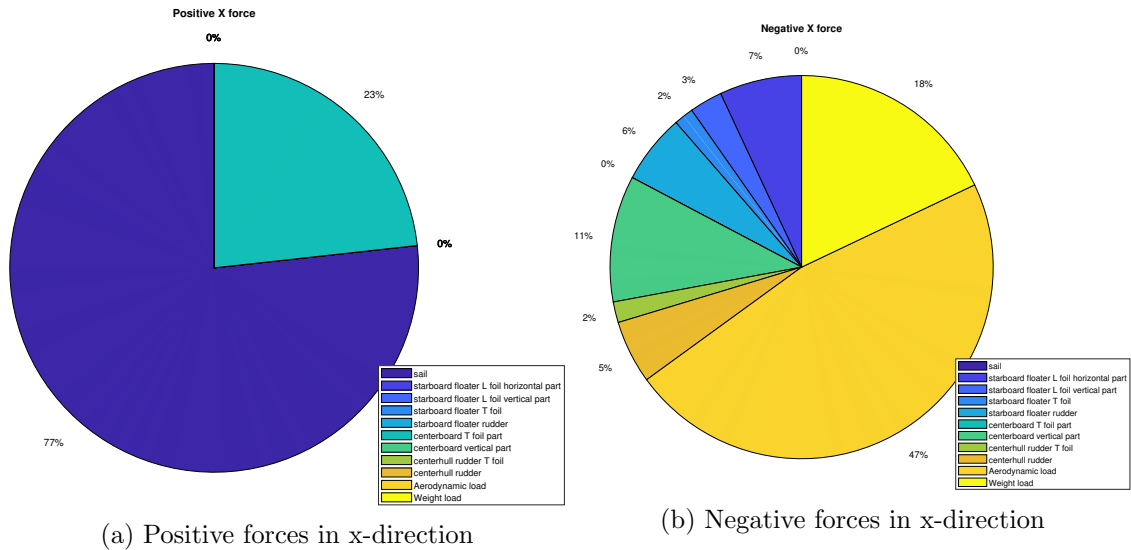


Figure 3.3: Pie charts of forces when $U = 26$

3.4 Validation of the forces and moments

3.4.1 Comparison with a dynamic velocity prediction program

A comparison with the dynamic velocity prediction program (DVPP) model in Kerdraon et al. (2020) has been made to make sure the model is viable. In this article, dynamic simulations were performed where the sailboat is in both Archimeadean, hybrid, or foiling state, where hybrid corresponds to a combination of the other two. The results are mostly in hybrid mode and are compared to the foiling mode for the minimum viable model, which is an important difference to be kept in mind.

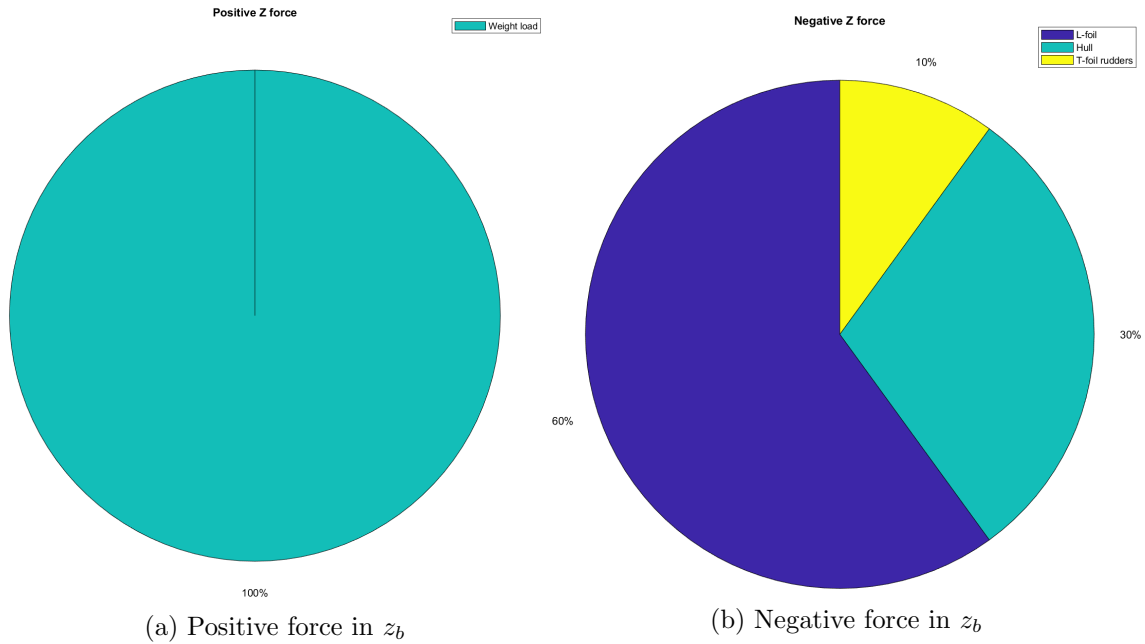


Figure 3.4: Contributing forces to Z , heave for Kerdraon et al. (2020)

The article looks at different cases of performance for the trimaran. The forces acting on the body are expressed as superposition between hull loads, appendage loads, and aerodynamic loads. An autopilot is implemented as a proportional-derivative (PD) controller to control the heading. Three different simulations were performed, one with a simple maneuver, one with unsteady wind conditions, and one with downwind sailing in waves.

From the simulation for downwind with TWA of 140° , the results show that the vertical forces (Z) as percentage of displacement was 60% from L-foil, 30% from hulls (hybrid state), and 10% from the T-foil rudders (Figure 3.4). When comparing this with the results in Figure 3.2, it corresponds with the resulting forces, where 60% is from the L-foils, 25% from the centerboard, and 12% from the rudders.

3.4.2 Comparison with results from Mer Concept

Mer Concept was responsible for and the operator of the Macif 100 trimaran until November 2020, and contact with Emilien Lavigne at Mer Concept was established when this project started. In e-mail and phone correspondence, assumptions and initial conditions were discussed such that the modeling would be as good as possible.

After conversation with Lavigne, changes were made to several aspects. For the foils, it was first assumed symmetric foils which lead to a high drag force. With asymmetric foils, which is the case for Macif, the drag coefficient and force is reduced which increases the velocity achieved in the given wind conditions. The weight distribution was altered, as the mast and sails contribute to about 10% of the weight, compared to 6-7% that was first assumed. Also, the central hull is located a little lower than the starboard and port hull, which means that the rudder on the central hull is contributing to the loads more than assumed.

After these alterations were performed, it was confirmed that the static equilibrium was realistic for the TWA of 120 degrees. The lift force distribution from Figure 3.2 corresponds

well with the experiences from Mer Concept.

3.5 Sensitivity of the loads to control inputs

A sensitivity study is performed by looking at how changing the incidence of the controlled foils will affect the forces and moments on the sailboat. This indicates how the foil angles affect the net load and the dynamic motion of the sailboat, which is useful information when doing control design. The model has very coupled motions, and understanding the interaction between different degrees of freedom is helpful when making a control system. In addition, this can help when making guidance strategies as the intuitive motion from a motorboat is not necessarily the same for a sailboat. To increase the speed of a motorboat, additional thrust is given in surge from the propeller, while for a sailboat the same increase in thrust will be from increasing the lift force on the sail. To do this, adjustments need to be made in the angle of attack for the sail, often through changing both the heading and the sail. Changing the heading can also lead to a bigger roll angle which needs to be compensated. Thus, the system is more complex and knowledge of the system is increasingly important.

The sensitivity study is done by looking at the Jacobian of the forces and moments acting on the boat in the foil angles. Using α from the static equilibrium state, the forces and moments on the foil is found for an $\alpha_{low} = \alpha - 0.1^\circ$ and for $\alpha_{high} = \alpha + 0.1^\circ$. By looking at the difference in load when changing the incidence of each foil, this allows to compare how different foils affect a given load component. The Jacobian for the forces is calculated in (3.2), and a corresponding calculation is done for the moments.

$$J = \frac{\delta F}{\delta \alpha} = \frac{F_{high} - F_{low}}{\alpha_{high} - \alpha_{low}} \quad (3.2)$$

The results are then presented in Figure 3.5 for the forces and Figure 3.6 for the moments. The L-foils, the vertical part of the centerboard and the sail are not considered in this analysis.

The next sections discusses the foil sensitivities.

3.5.1 Acting on the rudders

The rudder is expected to have a large effect on the yaw moment and sway force when steering i.e. change in rudder angle. From the figures, this is confirmed for the vertical part of both the rudder on the centerhull and the floater (starboard hull). The contributions are close to equal for the rudders in both sway and yaw, where the yaw moment is slightly larger for the starboard rudder. This corresponds well with the forces in equilibrium. Both rudders also influence the roll moment, which means that the boat will get a slight change in roll angle when changing heading using the rudder. A change in roll angle can also lead to a change in the lift for the L-foil, which will affect the heave of the boat. This contribution in roll is small, compared with the other moments, but can be significant if the change in yaw angle is large enough.

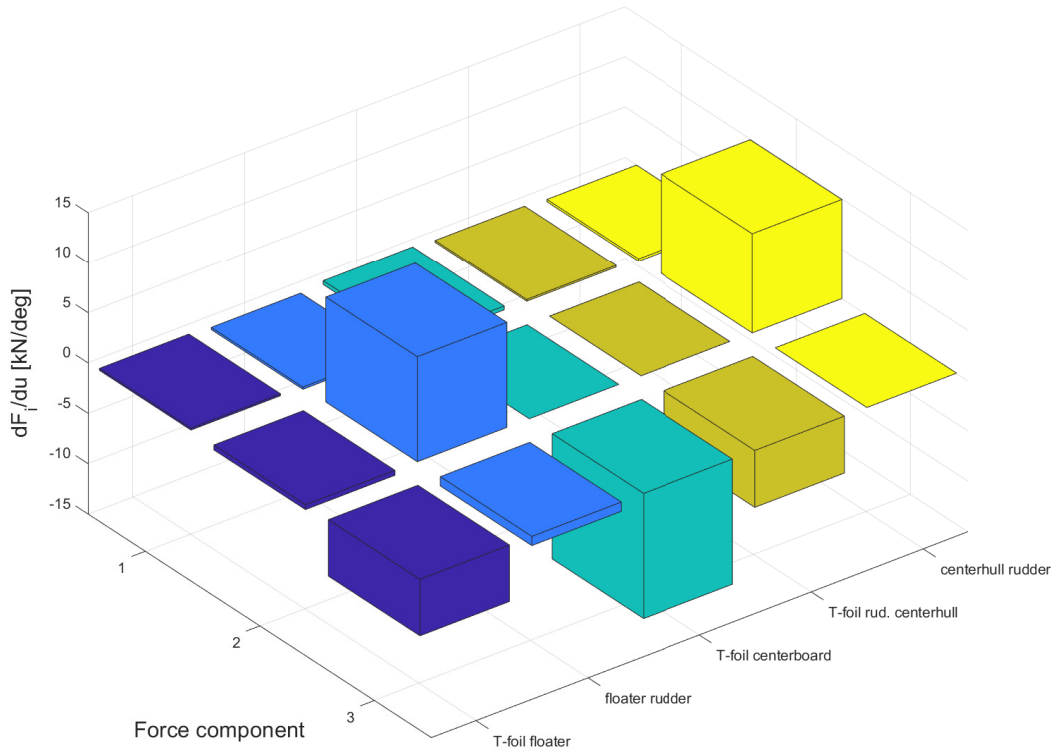


Figure 3.5: Jacobian of lift for forces on foil

3.5.2 T-foil on rudders

For the T-foil on the rudders, both the center hull and the floater has a change in heave force. This is expected as the lift forces on these are in heave direction and change with the angle of attack. Both also have a change in pitch moment, and the floater T-foil also has changes in roll. This change implies that the T-foil on the rudders can be used for heave and pitch control, and the floater T-foil can contribute to roll. This would mean that when the T-foils on the rudders are used to control the pitch angle, the roll angle will be affected, and nearly as much. For an ideal controller, this could be accounted for by controlling the two T-foils for rudders separately, and make the centerhull T-foil the primary actuator in pitch, such that the starboard T-foil gives a smaller control action to lessen the effect on roll.

3.5.3 Centerboard T-foil

In Gitana (2020b), it is stated that the centerboard T-foil is crucial for performance and foiling characteristics, which is reflected in the sensitivity analysis through the large changes in heave force. Changing the incidence of T-foil centerboard significantly affects the loads in heave and pitch, although the rudder T-foils (due to their distance to B) have much more effect on the pitch moment. As a side note, it is interesting to be aware of the fact that the desired direction of the lift force does depend on the conditions in which the boat is sailing. For some wind directions, the centerboard T-foil contributes to

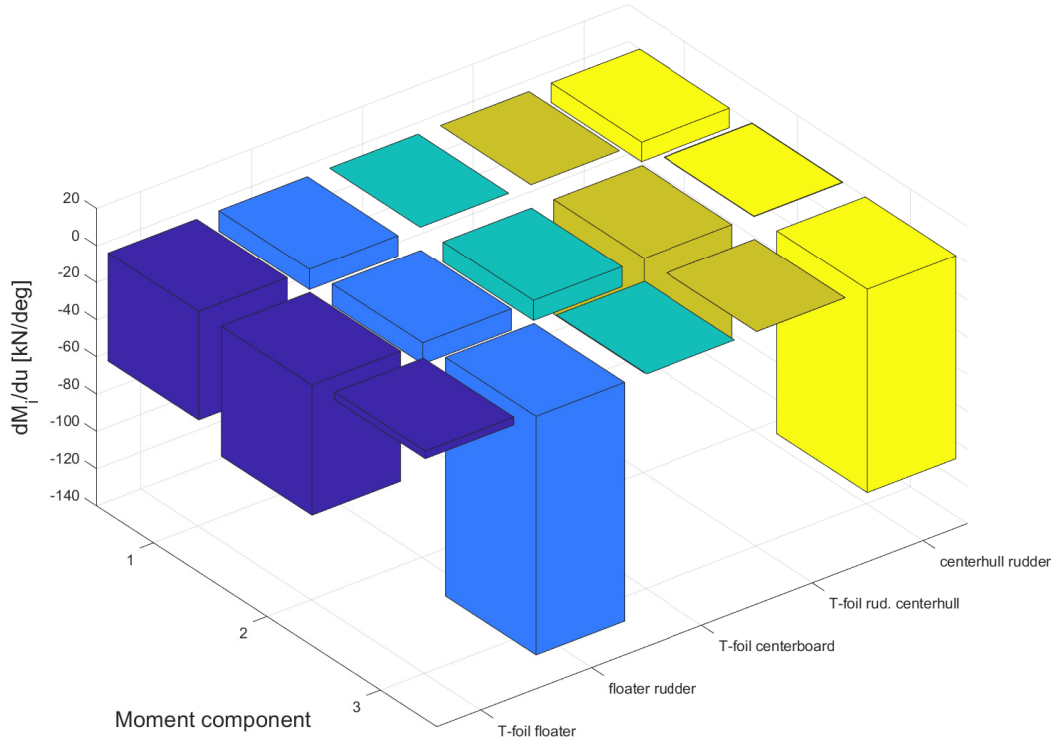


Figure 3.6: Jacobian of lift for moments on foil

helping keep the boat in the water (Lavigne and Sauder 2020). In this project, the lift force contributes to lifting the sailboat out of the water.

Chapter 4

Control System Design

The control system has been developed in Matlab and Simulink using the model described in Chapter 2.

4.1 Architecture

The control system is developed based on the block diagram in Figure 4.1, which displays a typical structure of a marine control system.

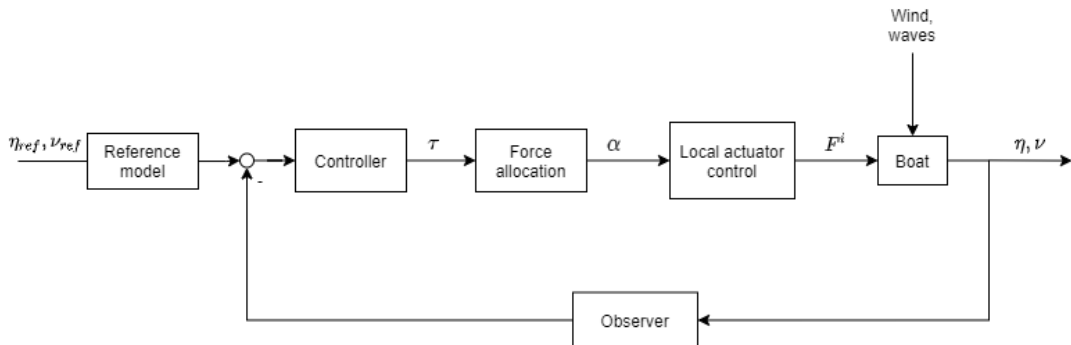


Figure 4.1: Block diagram

The boat block is represented by a mathematical model of the system, usually a process plant model (PPM). The disturbances, such as wind and waves are modeled in this block. A simpler model could be a CPM for this block. The controller computes the desired generalized load vector τ to be applied on the system given the error between the desired setpoint η_{ref}, τ_{ref} and the (estimated) system states. The setpoints are given by a guidance system and/or an operator. Then the allocation block computes the desired setpoints for each actuator in order to generate the commanded load. For the foiling sailboat, this is the desired angle of incidence for each foil to produce the desired lift and drag force. The local actuator control makes sure each actuator follows the desired setpoint, generating forces F^i that are applied to the boat model. The observer estimates non-measured system states, and feeds it back to the controller.

The control system is made using Simulink, where three different controllers are implemented. From the equation of motion in (2.3), $\dot{\nu}$ is found. To get the system states η and ν , a transformation using (2.1) and (2.2) is done.

The system states are assumed to be perfectly known, such that there is no observer for this system. The states are instead subtracted from the desired state directly and then fed into the controller. For this problem, surge and sway is not controlled, and the states are reduced to 4DOF into the controller.

In the controller, the desired load in each controlled DOF is found. The controller is a PID controller, and has been tuned manually, more on this in Section 4.2.3 and Section 4.3. The force allocation is where the commanded load is realized by acting on the incidence of the different foils.

The local actuator control is assumed to be perfect here (no delay, no actuator dynamics). This is then going into the boat block. The disturbances are in this case the wind and waves.

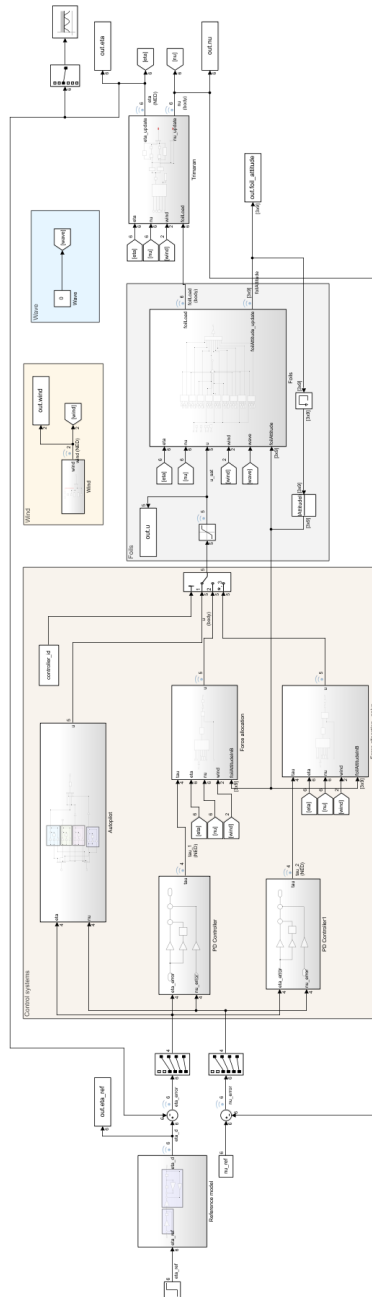


Figure 4.2: Model in simulink

4.2 System components

4.2.1 Reference model

A reference model was included to make sure that the changes in set point would be filtered such that the control system would be better prepared to handle discontinuous commands. It consists of a low-pass filter in conjunction with a second-order mass-damper-spring system as shown in Figure 4.3.

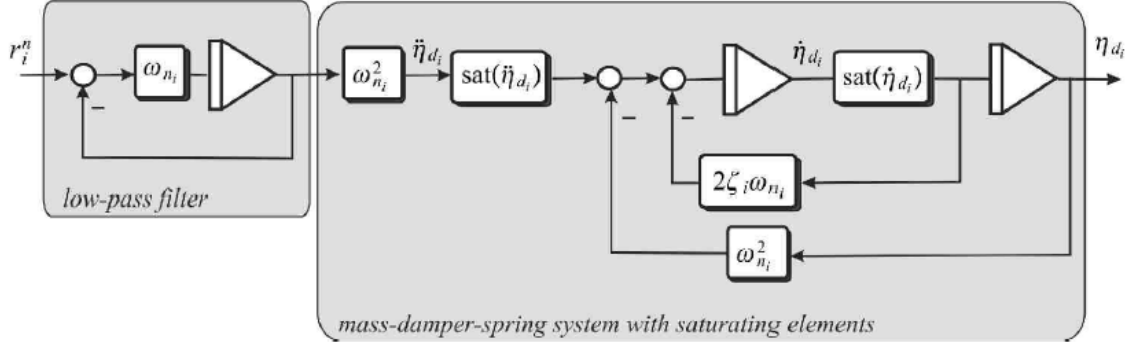


Figure 4.3: Reference model (Fossen 2011)

The natural frequencies ω_{n_i} are the diagonal of the matrix Ω , while the relative damping factors ζ_i are the diagonal of the matrix Δ .

$$\Delta = \text{diag}\{\zeta_1, \zeta_2, \dots, \zeta_6\}$$

$$\Omega = \text{diag}\{\omega_{n_1}, \omega_{n_2}, \dots, \omega_{n_6}\}$$

Adequate values for ω_{n_i} and ζ_i were found through trial and error. The goal was to find the combination of constants that made up a well functioning reference model.

4.2.2 Computation of error

The error between the desired position η_d and ν_d and the actual position η and ν was found by subtracting the actual position from the desired.

$$\eta_{error} = \eta_d - \eta \in \mathbb{R}^6 \quad (4.1a)$$

$$\nu_{error} = \nu_d - \nu \in \mathbb{R}^6 \quad (4.1b)$$

The controller is made for 4 DOF such that, after calculating the error, the vectors are reduced to \mathbb{R}^4 , excluding the error in surge and sway.

4.2.3 PID

Three controllers are implemented for the system, all of which are PID (proportional-integral-derivative) controllers. A PID controller calculates the desired thrust based on a desired setpoint with the control objective of getting the error between the current state and the setpoint to zero. A PID controller is shown in (4.2), where K_p is the proportional

gain, K_i is the integral gain and K_d is the derivative gain. The gains are diagonal matrices.

$$\tau = -K_p \tilde{x} - K_d \dot{\tilde{x}} - K_i \int_0^t \tilde{x}(\tau) d\tau \quad (4.2)$$

The proportional term uses the error in x , \tilde{x} , to create a proportional output. This does not eliminate errors due to constant disturbances, but decides how fast the controller is. To eliminate the error induced by constant disturbance, the integral term is added. For example, the integral term can correct for a constant unwanted error in pitch. A combination of proportional and integral terms may lead to overshooting, i.e. the signal exceeds the reference. This can be compensated by adding a derivative term.

4.2.4 Force Allocation

The desired loads $\tau \in \mathbb{R}^4$ given from the PID controller, are allocated to the different actuators using a force allocation method. The loads are allocated using (4.3), where $J \in \mathbb{R}^{n \times r}$ is a configuration matrix, $u \in \mathbb{R}^r$ is the control input and r is the number of actuators. The configuration matrix J was found by looking at the Jacobians of the forces and moments on the foils, in the same way as in Section 3.5.

$$\tau = Ju \quad (4.3)$$

If the number of DOFs are higher than the number of actuators ($n > r$), the system is *underactuated* and if the number of DOFs are lower than the number of actuators ($n < r$), the system is *overactuated*.

The sailboat has 5 foils that can be actively controlled:

- u_1 : Starboard (SB) rudder T-foil
- u_2 : Starboard (SB) rudder
- u_3 : Centerboard (CB) T-foil
- u_4 : Centerhull (CH) rudder T-foil
- u_5 : Centerhull (CH) rudder

which makes $u \in \mathbb{R}^5$ an overactuated system.

Details on how to obtain u from τ will be given later in the chapter.

4.2.5 Actuator model

The control input is applied to the attitude of the relevant foil and the new foil load is calculated. For each iteration, the general attitude of the foils stay the same, such that the applied change is added to the initial attitude.

For the actuators, the foils, a saturation limit is applied, which stops the applied angle to get higher than the limit.

Foil	Saturation [deg]
Starboard Rudder T-foil u_1	30
Starboard Rudder u_2	40
Centerboard T-foil u_3	30
Centerhull Rudder T-foil u_4	30
Centerhull Rudder u_5	40

Table 4.1: Limits for actuators

4.2.6 Wave filter

If the model is exposed to disturbances in the form of waves, it is important to make sure the control system is equipped to handle the disturbances without lessen the performance of the system. The waves are causing high-frequency disturbances, which the control system should not necessarily compensate for. It is therefore important to filter out the high-frequency wave-induced forces, such that the control system only compensate the slowly-varying forces. This is called wave filtering and is usually done using a model-based state estimator or a low-pass (LP) filter.

Since the model in this thesis does not have a state estimator or observer, a low-pass filter is more likely to be implemented. A low-pass filter cancels frequencies above a limit from entering the controller, leaving the slowly-varying forces to be accounted for when calculating the control action. To make the LP filter, the encounter frequency ω_e and the bandwidth frequency ω_b is needed. The LP filter is located before the controller (Figure 4.4).

The encounter frequency is the frequency in which the boat experience the waves. It is calculated as

$$\omega_e = |\omega_0 - \omega_0^2 \frac{U}{g} \cos \beta| \quad (4.4)$$

where ω_0 is the wave frequency, U is the boat speed, g is the acceleration of gravity and β is the wave encounter angle (rad). Usually it is desired to have $\omega_b \ll \omega_e$.

A first-order low-pass filter is displayed in (4.5)

$$h_{lp}(s) = \frac{1}{T_f s + 1} \quad (4.5)$$

where T_f is a time constant defined as $\omega_b < \frac{1}{T_f} < \omega_e$. An example of a filtered signal and non-filtered signal is shown in Figure 4.5.

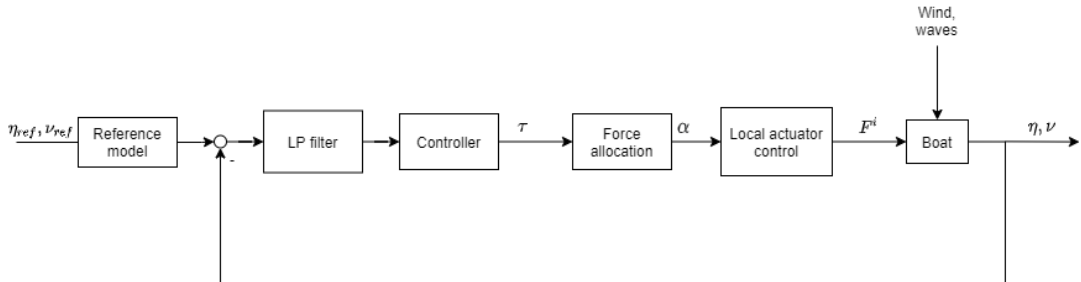


Figure 4.4: Block diagram including wave filter

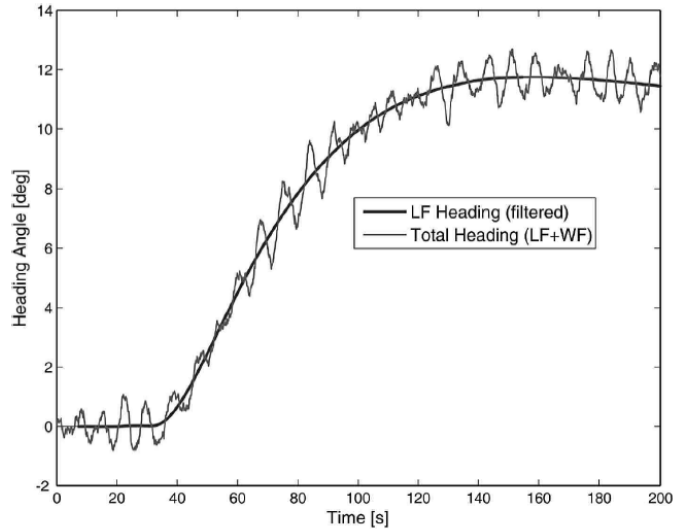


Figure 4.5: Wave filtering, excerpt from Fossen 2011

4.3 Control architecture candidates

When doing research on control methods for sailboats and hydrofoils, several methods were mentioned including fuzzy logic and model predictive control, but the most used were PID. From the research, it was clear that although the methods are there for more advanced controllers, the PID controller is easy to use, tune, and most likely the cheapest option. Another side of the story is that most sailboats have autopilots, where only the heading/course is controlled, and thus the need for more advanced controllers is not present.

As a starting point, a PID controller is good, for the reason stated above. Due to the complexity of the motions for the trimaran, the PID was assumed to be too simple for this system, and the initial thought was therefore that a more complex controller might be needed. But, it would be interesting to see if a simple controller would be able to handle the complex system at hand. To do this, it was decided that a PID controller would be applied to the system, but with different approaches to see which would be more efficient to make an automatic course and flight control system.

The two approaches were a "naive" allocation following the PID controller (Controller 1) and a PID controller combined with a force allocation based on the heave and attitude-dependent Jacobian matrix for the foils (Controller 2). Another controller was added as a mix of the two (Controller 3), with a PID controller in conjunction with a force allocation based on the "naive" allocation used in Controller 1. This makes it possible to compare the allocation approaches and the controller approaches.

4.3.1 Controller 1

The first controller is a simple and intuitive controller. This means that the error in set point gives a gain to one single actuator (Table 4.2). For each degree of freedom, there is a PID-controller deciding the control input or the change of angle for each of the control surfaces (Equation 4.6). The connection between DOF and actuator is displayed in Table 4.2, and here it can be seen that the system is underactuated for this controller

set-up, since the five foils have merged to three control inputs.

DOF	Actuator
Heave	3 – Centerboard T-foil -
Roll	- -
Pitch	1 – Starboard rudder T-foil 4 – Center rudder T-foil
Yaw	2 – Starboard Rudder 5 – Center rudder

Table 4.2: Actuators for each force component

$$\tau_1 = K_{p,1}z_{error} + K_{d,1}w_{error} + K_{i,1} \int z_{error} \quad (4.6a)$$

$$\tau_3 = K_{p,3}\theta_{error} + K_{d,3}q_{error} + K_{i,3} \int \theta_{error} \quad (4.6b)$$

$$\tau_4 = K_{p,4}\psi_{error} + K_{d,4}r_{error} + K_{i,4} \int \psi_{error} \quad (4.6c)$$

The allocation is $u = [0.5\tau_3 \ 0.5\tau_4 \ \tau_1 \ 0.5\tau_3 \ 0.5\tau_4]$ is the resulting control inputs. The reason that roll is not actively controlled for this controller is that from the load distribution seen in Section 3.3, the only control surface contributing in roll is the starboard rudder, but this is a small contribution. The rudder contributes more to the yaw moment, and since it is assumed that the rudders are controlled together for this controller it leaves no control surface for roll.

The gains were found by manually tuning based on trial and error. K_p was tuned first, starting with the heave gain, as the main goal is to keep the flying height. When a satisfactory behavior in heave was achieved, pitch was tuned and lastly the yaw gain was found, K_d was tuned second, and then K_i last.

DOF	K_p	K_d	K_i
Heave	2e3	20	200
Pitch	20e3	0.2e3	2e3
Yaw	2e3	20	200

Table 4.3: Gains for naive controller

4.3.2 Controller 2

The second controller is the “smartest” one. It consist of a PID-controller generating a commanded global load vector, which is realized by solving the complete force allocation problem.

$$\tau = K_p\eta_{error} + K_d\nu_{error} + K_i \int \eta_{error} \in \mathbb{R}^4 \quad (4.7)$$

The PID controller calculates the total load τ needed to reach the set points. The gains are diagonal matrices as displayed under.

$$K_p = \begin{bmatrix} 200e6 & 0 & 0 & 0 \\ 0 & 10e6 & 0 & 0 \\ 0 & 0 & 0.8e9 & 0 \\ 0 & 0 & 0 & 1.5e9 \end{bmatrix} \quad (4.8) \quad K_d = \begin{bmatrix} 2e3 & 0 & 0 & 0 \\ 0 & 1e3 & 0 & 0 \\ 0 & 0 & 2e3 & 0 \\ 0 & 0 & 0 & 2e3 \end{bmatrix} \quad (4.9)$$

$$K_i = \begin{bmatrix} 5e6 & 0 & 0 & 0 \\ 0 & 200e3 & 0 & 0 \\ 0 & 0 & 20e6 & 0 \\ 0 & 0 & 0 & 20e6 \end{bmatrix} \quad (4.10)$$

In the force allocation, the forces are allocated to the five control inputs. The method from Section 4.2.4 is used, such that the control inputs can be found by calculating the Moore–Penrose pseudoinverse of J and multiply it with the load vector from the PID-controller (Equation 4.11).

$$u = J^\dagger \tau \quad (4.11)$$

By using this method, where the rudders are controlled independently, the system is overactuated.

The gains were found by manually tuning, starting with K_p . When the transient was sufficiently small, the tuning was considered good. Some adjustments to the gains were made when doing initial tests.

4.3.3 Controller 3

The third controller is a semi-naïve controller. It consists of a PID-controller generating a general load vector τ and a force allocation. The allocation is semi-naïve because it uses same allocation as Controller 1 (Table 4.2), while the loads are from the configuration matrix J .

The allocation is done by picking the relevant elements from the configuration matrix J . For example, the centerboard T-foil is the actuator for heave, such that the element in J corresponding to the heave component for the centerboard T-foil is picked and multiplied with the heave component in τ to find the change in incident angle for the centerboard T-foil.

$$u(3) = J^\dagger(3,3)\tau(1) \quad (4.12)$$

The PID-controller is as (4.2), with gains

$$K_p = \begin{bmatrix} 5e6 & 0 & 0 & 0 \\ 0 & 0 & 0 & 0 \\ 0 & 0 & 0.7e9 & 0 \\ 0 & 0 & 0 & 5e6 \end{bmatrix} \quad (4.13) \quad K_d = \begin{bmatrix} 5e3 & 0 & 0 & 0 \\ 0 & 0 & 0 & 0 \\ 0 & 0 & 5e6 & 0 \\ 0 & 0 & 0 & 1e3 \end{bmatrix} \quad (4.14)$$

$$K_i = \begin{bmatrix} 200e3 & 0 & 0 & 0 \\ 0 & 0 & 0 & 0 \\ 0 & 0 & 80e6 & 0 \\ 0 & 0 & 0 & 200e3 \end{bmatrix} \quad (4.15)$$

Chapter 5

Verification of the dynamic model, including controller

5.1 Initial conditions

The initial conditions used for the cases are given in Table 5.1. The conditions are the one's acquired from the static equilibrium, and the control input added to the attitude of the foils.

Speed	U_0	21 [m/s]
Drift angle	β_0	1.2°
Sinkage	z_{b0}	-1.60 [m]
Heel	ϕ_0	4.5°
Trim	θ_0	2.3°
Heading	ψ_0	-0.03°
Surge vel.	u_0	21.19 [m/s]
Sway vel.	v_0	0.53 [m/s]
Heave vel.	w_0	0.81 [m/s]
Wind speed	u_w	10 [m/s]
Wind direction	TWA	-120°

Table 5.1: Studied conditions

Since the control input u from the static equilibrium is added to the foil attitude, the initial value in the simulation is zero as displayed in (5.1). The initial attitude for the foils are given in Table 5.2.

$$u = [0 \ 0 \ 0 \ 0 \ 0] \quad (5.1)$$

Foil	ϕ	θ	ψ
Starboard rudder T-foil	-5	-0.57	0
Starboard rudder	85	0	1.33
Centerboard T-foil	0	0.81	0
Centerhull rudder T-foil	0	-0.57	0
Centerhull rudder	90	0	1.33

Table 5.2: Initial foil attitude for simulation (from {b} to {f})

5.2 Verification for cases

Test cases are done to determine if the model behaves as expected during the different steps.

5.2.1 Case 1 - Change in yaw angle

The first test case performed is a case where the commanded yaw angle changes from 0 to 15 degrees after 150 simulation seconds. The test case uses controller 2. When the yaw angle receives a new reference, it is expected that the system is affected such that the boat will move towards the new reference. By following step by step and compare with plots from the simulation, it is possible to see if the system follows the expected behavior. In this case, a small portion of the simulation is looked at, just before and after the change in command.

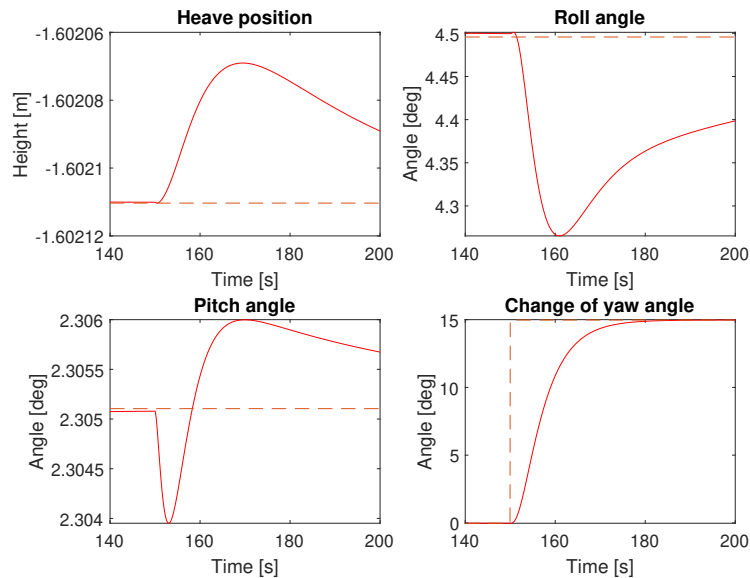


Figure 5.1: Attitude and position for boat for case 1. Heave, roll and pitch reference returns to reference

The first step in the case for the simulation model is a change in command from 0 to 15 degrees, which is initiated at 150 seconds of simulation time. At $t = 149$ seconds, $\eta_{error}, \nu_{error}$ is approximately zero, and the system has stabilized in a state without disturbances. As the initial conditions are close to equilibrium, the commanded angles to the actuators are small, and only small adjustments have been made since the start of the simulation. At $t = 150$ the commanded yaw angle is changed to 15 degrees. The

commanded η is first passing through a reference model, which makes the change happen over the course of approximately 20 seconds, rather than in an instant. This is to prevent the error in position to get very large from one instance to another, and thus prevent the actuators to overcompensate the change.

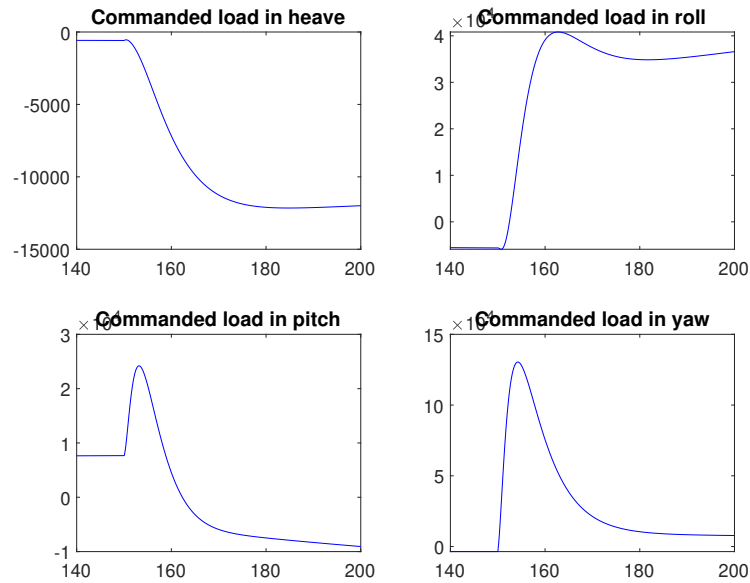


Figure 5.2: Result from PID controller for case 1

The next step in the model is to calculate the error between the reference and the actual (calculated) position. It is the size of the error that passes through the PID, and determines how much force the actuators must give to make the boat move toward the reference. When the error between set-point and actual position changes, it causes an increase in τ calculated in the PID controller.

For this case, when the yaw angle changes it instantly leads to an increase in commanded load in yaw. Due to the coupled motions of the trimaran, and the sensitivity of the foils, it induces changes in other degrees of freedom. These changes is what leads to commanded loads in heave, roll and pitch in Figure 5.2.

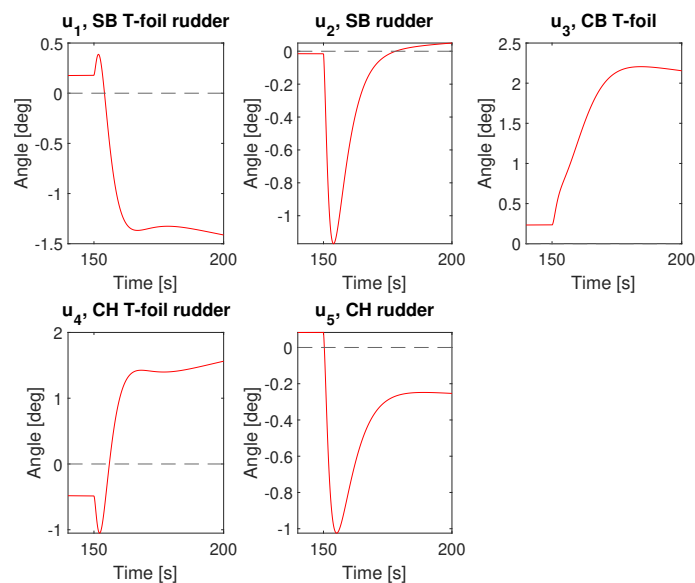


Figure 5.3: Commanded angles for actuators for case 1

The loads τ from the controller, are turned into changes of incidence for each foil in the force allocation. For controller 2, the configuration matrix of Jacobians is used to decide the angles for the different actuators. In Section 3.5 one could see that all the foils affect differently in each direction, such that it is expected that the allocation gives different values for the angles for all foils. This can be seen in Figure 5.2 and Figure 5.3.

The commanded angles are added to the foil angles in the local actuator control. Here, the new foil loads are calculated. These are part of the EoM that are solved next. When solving the EoM, the new position and velocity for the boat is found. It is expected that the load distribution changes as the boat is changing direction (yaw angle). The loads are plotted in Figure 5.4 and this change is seen in the figure.

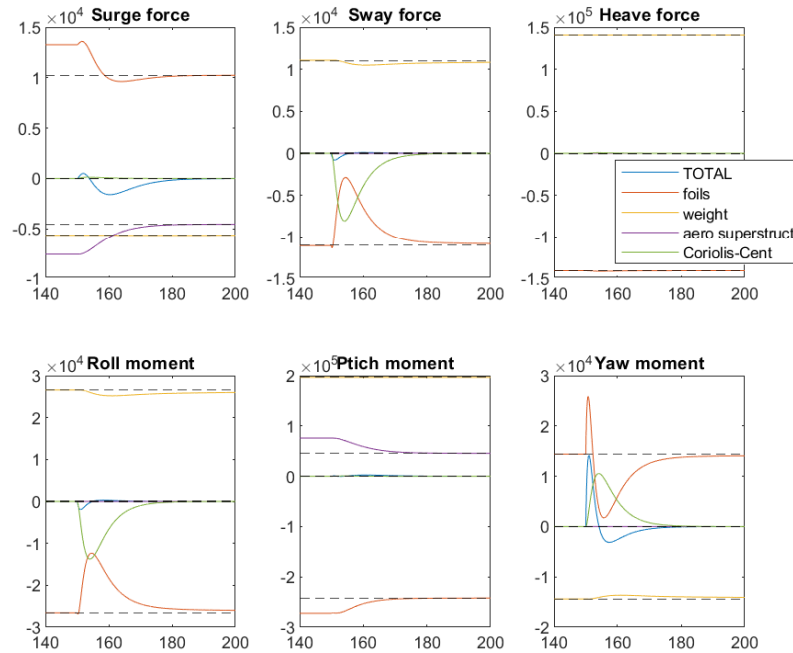


Figure 5.4: Loads for case 1

Generally, one can see from the figures of the simulation that the system has an expected response for this case.

5.2.2 Case 2 - Change in wind direction

The second case, is a situation where the wind direction suddenly changes at 150 seconds simulation time. In this case, Controller 1 is used. The direction changes from the initial direction of 120 degrees TWA to 100 degrees TWA, which means that it changes such that the wind is hitting the boat more from in the side than from behind. There is no change in the reference value for η and ν , such that the system will try to make sure the boat does not change its configuration as a result of the change in wind direction.

In the model, the wind is added as a disturbance on the boat in the sail load calculations, such that when the alteration in wind direction happens, the boat's loads and position calculated in the EoM will be affected first. When the wind direction is altered, the forces on what's above water will be affected. It is expected that the sway forces and roll moment

will increase as a consequence of the change.

Generally, the disturbance will set the system out of its stable state before the control system will work towards the system returning to its original state. In this case, the system is underactuated such that the lack of control in roll could mean that the roll angle does not return to its previous state.

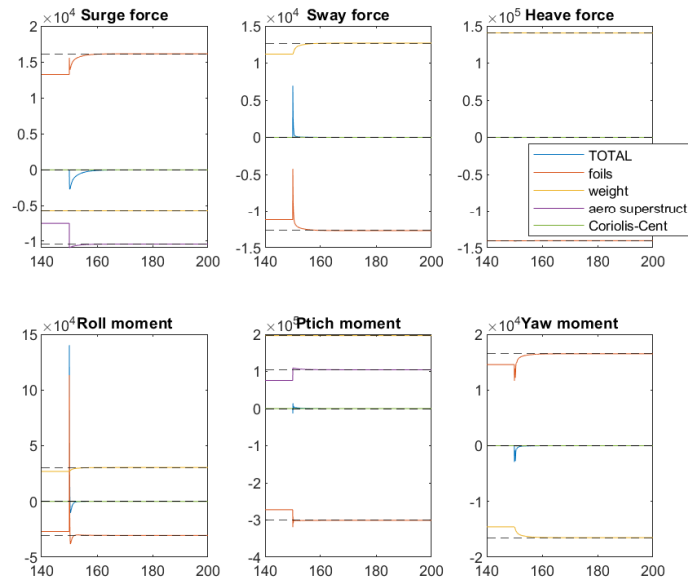


Figure 5.5: Loads for case 2

Looking at the simulation in Figure 5.5, one can see that the loads change at the simulation time of 150 seconds. The changes in the load can be seen in relation to a change in position, see Figure 5.6. The boat has a small change in position, which soon goes back to the reference value, with the exception of the roll angle which has a significant change. The change in load for heave is too small to appear in the plots, which corresponds with the change in heave position being half a millimeter.

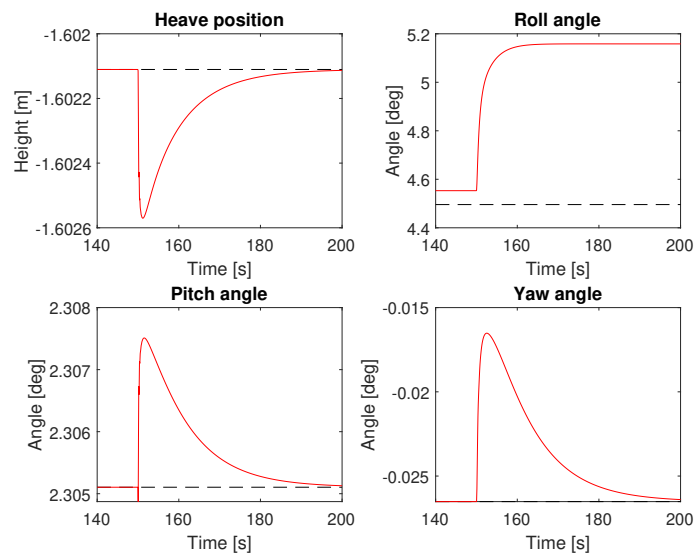


Figure 5.6: Position for case 2

When there is an error in position and velocity it leads to a reaction in the PID controller such that the actuators receive a commanded angle. In this case, with Controller 1, it is actuator 1 and 4 that controls sway, actuator 2 and 5 that controls the yaw angle and actuator 3 controls the heave position.

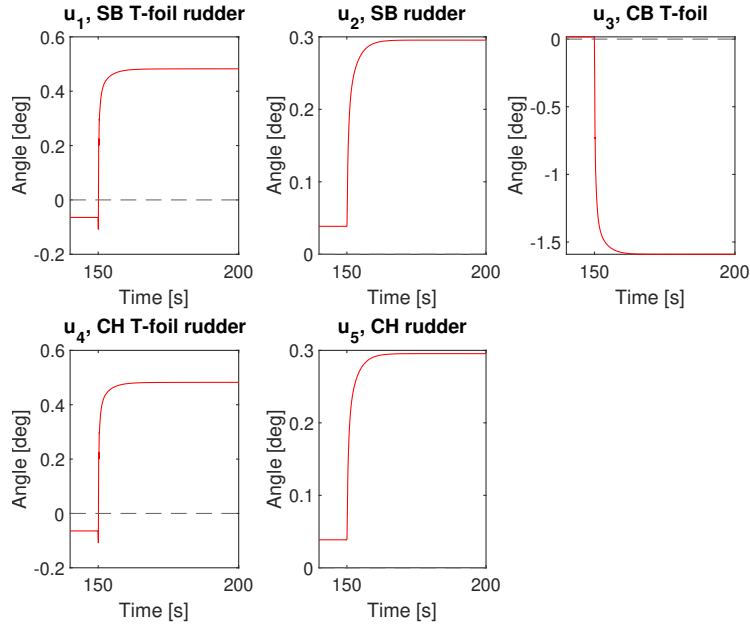


Figure 5.7: Commanded angles for case 2

5.3 Validity range

The simulation model is valid as long as the hull is out of water and the T-foils are fully submerged. This corresponds to heave positions given in NED-frame between 0 and -2.2, given that roll and pitch is constant. If the hulls touch the water, the model becomes invalid as the buoyancy forces are not modeled. In that case, the simulation stops.

Due to dihedral, the floater is located 0.91 m above the center hull when the roll angle is zero. This means that at static equilibrium, when the roll angle is 5 degrees, the starboard and center hull has the same heave position. Due to this, the roll angle ϕ for this model cannot exceed

$$\phi_{max} = -\sin^{-1}\left(\frac{z}{10.5}\right) + 5 \quad (5.2)$$

as this is the limit for when the starboard hull touches the water while the center hull is still flying, also known as hybrid mode. For a reference heave position of -1.6 m and zero trim, the corresponding roll angle limit is 13.7 degrees. The roll angle cannot be negative, since that would mean the port hull and/or foils are in water, and contributing to the loads, which is not modeled.

For the pitch angle it is desired that the angle stays small enough to keep the wind from catching on to the superstructure between the hulls. This may lead to the trimaran being lifted in the front, and then plunge into the water. It is expected that this happens in stronger winds than modeled here, and is not considered for the limits in this system.

The yaw angle is determined by the wind angle. Since the model assumes wind from port, the wind angle can in principal be between 0 and -180 degrees relative the heading.

5.4 Discussion and conclusion

From the test cases, it can be seen that the model and main controller components behaves as expected when given a change in the commanded set-point or change in wind direction. It stabilizes at the new set-point quickly, and the commanded actuator angles are consistent with the errors in position and attitude.

Chapter 6

Comparison between controllers in calm waters

In this chapter, a comparison between the three different controllers will be made with regard to the performance during different test scenarios in calm waters.

6.1 Indicators

To say that the performance of a controller is acceptable, indicators of the performance have been defined. The indicators are based on what would be realistically acceptable while sailing the boat in a race, where the performance should be of the highest order at all times. The indicators are applied to the position and attitude, and the applied angle for each actuator.

The first indicator is if the system reaches the reference, and how fast the reference is reached. This is evaluated based on the desired position from the reference model. Following this, it was determined if the response overshoots, and how large the potential overshoot is. Connecting to the validity, it is checked if the boat hits the water. If so, the simulation should have stopped.

It is desired that the error in all DOFs are as small as possible, and it is therefore also used as an indicator if the DOFs that are not altered get an error. The size of the error is then evaluated. Next, the commanded angles to the actuators are evaluated. It is desirable to have as small commanded angles as possible.

A goal with the model is to have a steady velocity, and preferably the highest possible velocity for the given conditions. As this is not accounted for by the controllers, they cannot be evaluated at their ability to keep a velocity over time, but rather their potential for maintaining or reaching a high velocity compared to the other controller candidates, and how much velocity the controller loses. The boat's speed is a scalar velocity, and can be seen in (6.1) where $V = [u, v, w]$.

$$U = \sqrt{((R_b^n(\eta)V) \cdot n_1)^2 + ((R_b^n(\eta)V) \cdot n_2)^2} \quad (6.1)$$

For the four DOFs evaluated, it is desirable if the response uses less than 100 seconds

to change position/direction when the reference is altered. The deviation from reference should be less than one degree or 0.2 meter when exposed to disturbances.

6.2 Description of the tests

The tests performed on the model are

- Change in heave reference
- Change in roll reference
- Change in pitch reference
- Change in yaw reference
- Noisy wind speed and direction

The test are performed to evaluate how well the system performs with different disturbances, and to study the perturbations that are induced by such disturbances. The test were done by initiating a change in reference for position or wind at a predefined simulation time. The magnitude for the disturbance was decided in the MATLAB script before starting the simulation.

6.3 Result of the tests

Test 1 - Change in heave

Test 1 involves checking if the model is capable of making a change in heave position. The position was altered 10 cm.

In Figure 6.1, the result for heave position is displayed, together with the roll, pitch and yaw angle for all three controllers. It is clear that all controllers follows the reference in heave, and thus manages the change well. However, it is different how the other direction are affected by the change. Controller 1 and Controller 3 do not control roll, and this can be seen in the result, as both of these have a large change in roll angle when the heave position changes. Controller 2, on the other hand, has a small error before going back to reference. For pitch and yaw, the changes in angles are minor and insignificant.

It is clear that the motions are coupled for this system, as there was a change in roll and pitch angle when the heave position was altered.

Figure 6.2 shows the commanded control input for the test, where the result for Controller 1 and 3 coincide. The plot shows that Controller 2 clearly commands larger angles than Controller 1 and Controller 3. It is also interesting to see that the rudder angles (u_2 and u_5) for Controller 2 goes in different directions. It shows that even though they, according to the sensitivity analysis in Section 3.5, contribute close to equal in yaw, there are contributions related to other load components that make up the final commanded angle such that they are very different from each other. For Controller 1 and 3, the rudder angles are equal as expected.

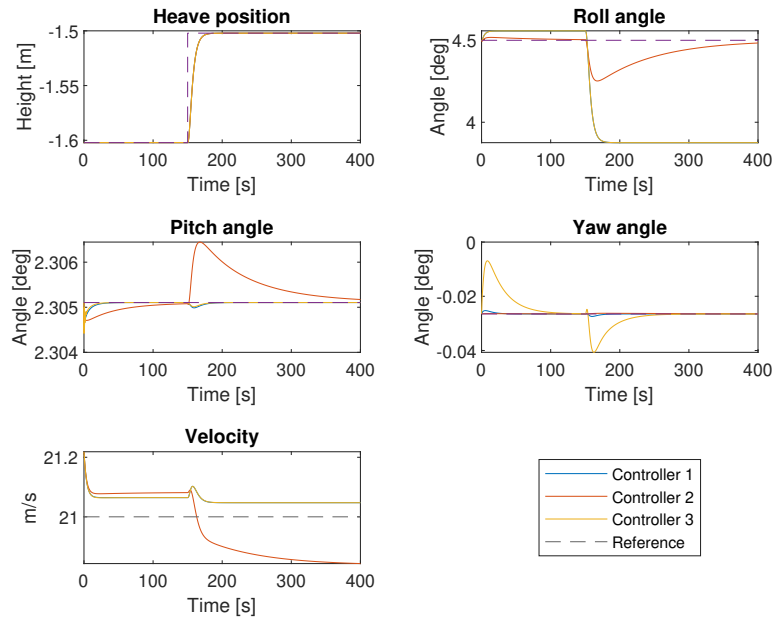


Figure 6.1: Test 1; Position, attitude and velocity

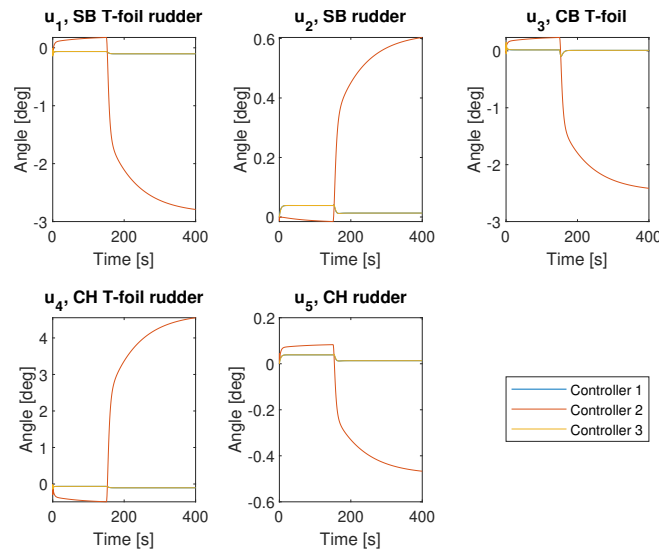


Figure 6.2: Test 1; Control input

From the velocity plot in Figure 6.1, it can be seen that Controller 2 has reduces velocity when the change happens. This can be due to the large commanded angles leading to higher drag force on the foils.

Test 2 - Change in roll

The second test checks whether or not the model is capable of following a change in roll reference, and the effect it will have on the other directions as well as the resulting control input. The commanded change in roll angle is 3 degrees. This was chosen as test value because it is inside the validity range for the model, while still being large enough to have impact on the state of the boat.

Since neither Controller 1 nor Controller 3 have any active control in roll, meaning there

are no actuators working in roll, it was not expected to see any change in position when the reference changes. For these controller, the result would rather represent the steady-state values for the model given the desired position.

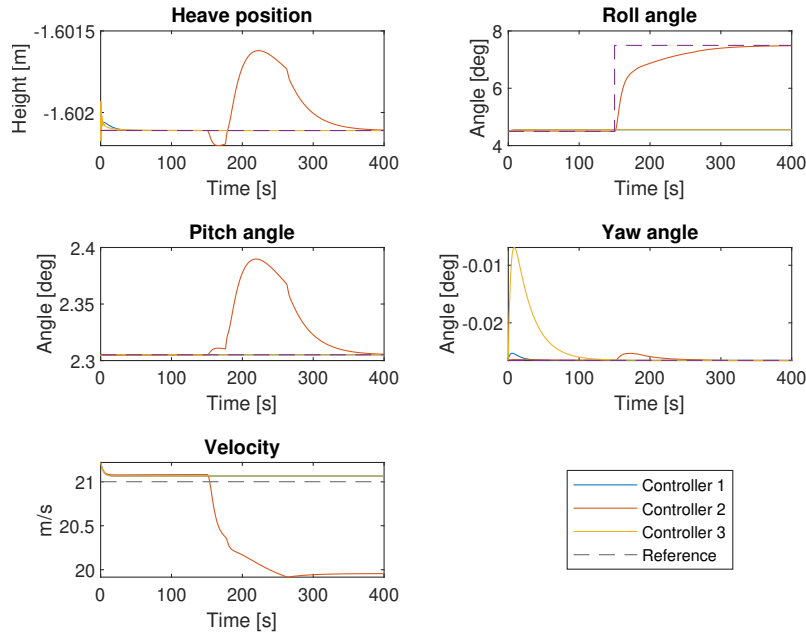


Figure 6.3: Test 2; Attitude

The results for position, attitude and velocity is displayed in Figure 6.3 and for control input in Figure 6.4. As expected, there are no change for Controller 1 and Controller 3, while Controller 2 reaches the new reference a little after 300 seconds, over 150 seconds after the change was initiated. The impact on heave and yaw is not substantial, and the pitch angle increases almost 0.1 degree, but returns to reference after about 200 seconds. The velocity is reduced about 1 m/s, which is consistent with the fact that the foils have a higher incidence angle, and thus have more drag.

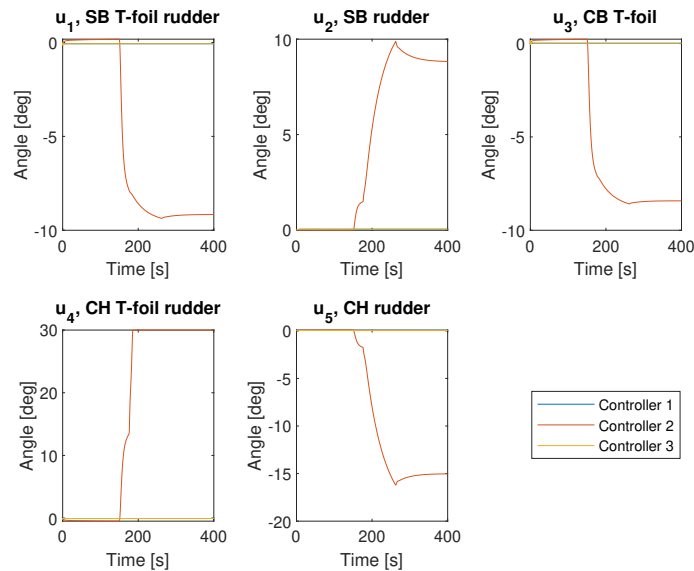


Figure 6.4: Test 2; Control input

Going into more detail on the control input, it can be seen that the rudders have large adjustments in opposite directions. The centerhull T-foil rudder goes to saturation only

short time after the change is initiated, which is an unwanted behavior for the actuator. This can be an indication that the set of actuators available is not adequate to control roll only. The saturation could possibly be avoided by reducing the gain in roll or reducing the commanded change.

Test 3 - Change in pitch

This test involves changing the pitch angle -0.5 degrees, which results in a change of height between the fore and aft of the hull of 27 cm.

When the reference in pitch is changed, all three controller candidates manages to follow the reference (Figure 6.5), with some delay due to the reference model and tuning. The other directions are affected in the moment, but only slightly and quickly goes back to reference position. The degree of disturbance for the candidates vary, but they are all small enough to be insignificant during racing. From the plots, it can be seen that the initial transient at $t=0$ has larger deviations from reference than the one happening when the change is initiated at $t=150$ s. The velocity of the boat has insignificant changes for this scenario.

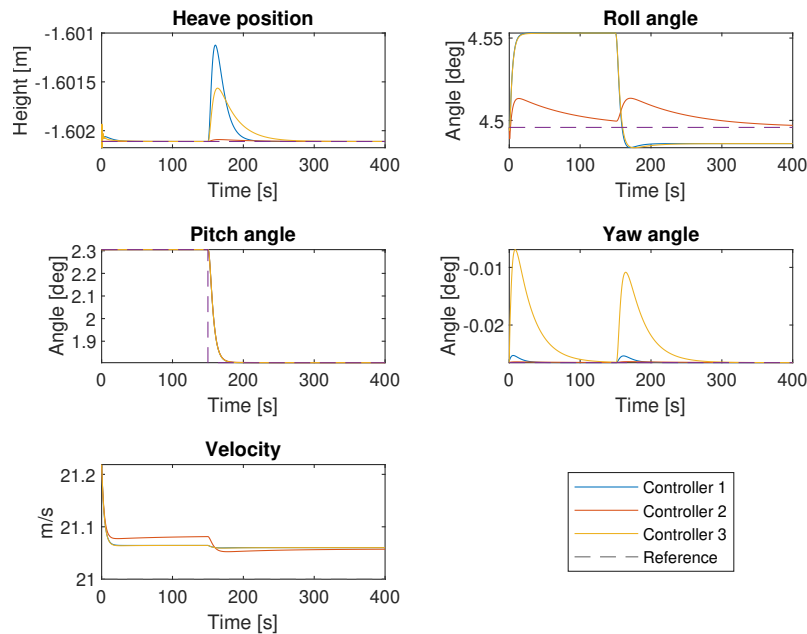


Figure 6.5: Test 3; Attitude

If looking at the control inputs in Figure 6.6, it can be seen that the commanded angles are small. The small angles indicate that the placement of the actuators are efficient to control pitch. Controller 1 and 3 have close to the same response.

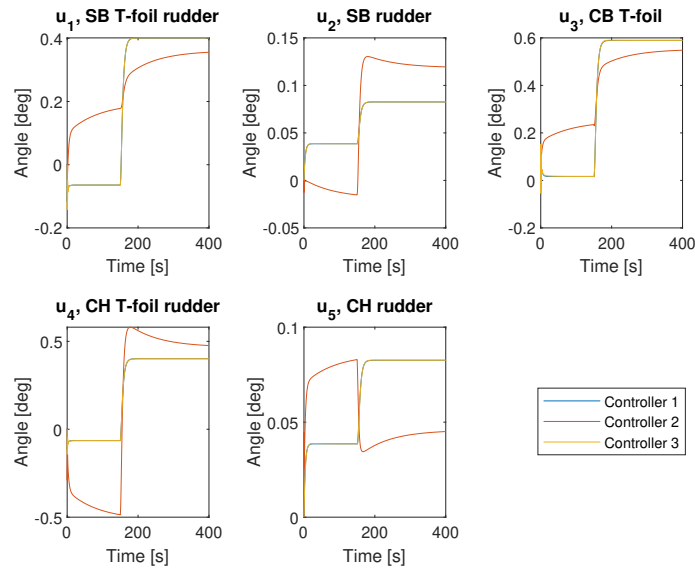


Figure 6.6: Test 3; Control input

Test 4 - Change in yaw

A maneuvering test, resembling a zig-zag test is performed. This is done by commanding changes in yaw angle in the manner shown in Table 6.1. The test is useful to see how well the boat can perform maneuvers, and how several maneuvers in a row will affect the performance.

Commanded yaw angle	Simulation time
10	150
-20	200
20	250
-10	300

Table 6.1: Maneuvering test

It can be seen in Figure 6.7 that the boat reaches the yaw angle after about 25 seconds for all maneuvers. The three controller candidates have the same performance for yaw angle, while the reaction in heave, roll and pitch differs from each other. The largest deviation is in roll, where a change in yaw angle of 20 degrees leads to a change in roll angle of a little over 0.6 degrees. The changes are still insignificant for the boat when racing.

The velocity of the boat varies with the yaw angle due to the relative wind angle on the boat which changes. When the boat turns to east (positive yaw angle), the relative wind angle on the boat increases and this leads to more power in the sails, and the opposite when turning west (negative yaw angle).

Controller 1 and controller 3 have, as in the other tests, the same commanded angles to the actuators. The most noticeable with the plots in Figure 6.8 are that the commanded angles for Controller 2 are close to equal for u_2 and u_5 , and these are close to the other controllers. This could be indicating that when the rudders are primarily used to control the yaw angle, they behave in the same way, while when the primary focus is on another degree of freedom they will behave differently.

Generally, the commanded angles are small compared to the change in reference, and the

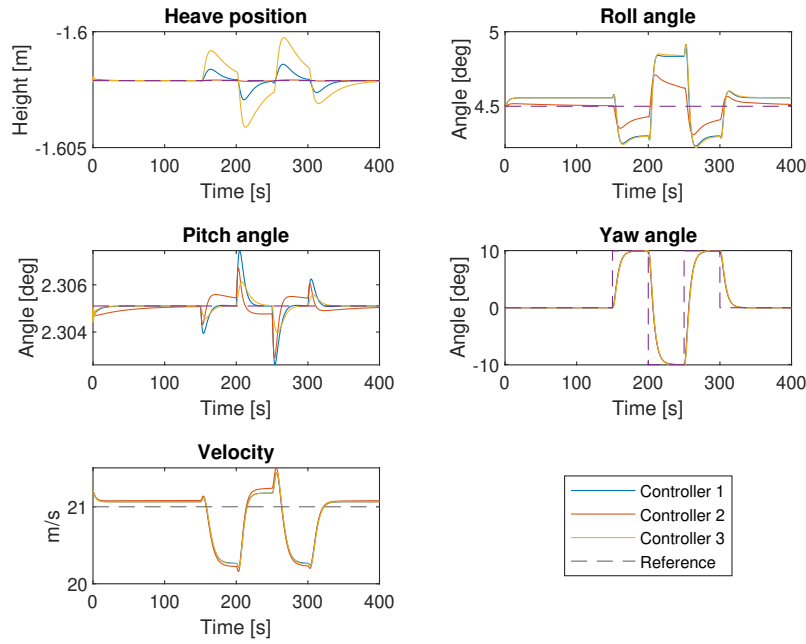


Figure 6.7: Test 4; Attitude

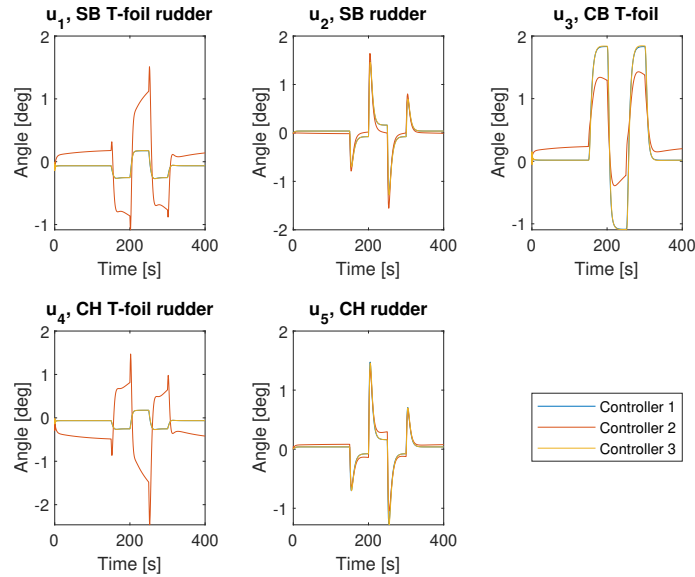


Figure 6.8: Test 4; Control input

controllers shows good performance for the test. The trimaran manages to stay foiling and not enter the water, and the velocity loss is not very large.

Test 5 - Noisy wind speed and direction

This test will show how good the performance of the boat is in an environment with external disturbances that are in continuous change. It is demonstrated by a noisy wind speed and direction. The wind starts at 10 m/s with a maximum value of 12 m/s and a minimum value of about 9.5 m/s. The wind direction varies between about 135 and 115 TWA. Through the test it is observed how position and velocity changes, as well as how much control input is given to the actuators to stay on reference. The result is summarized

in Figure 6.10 and Figure 6.11.

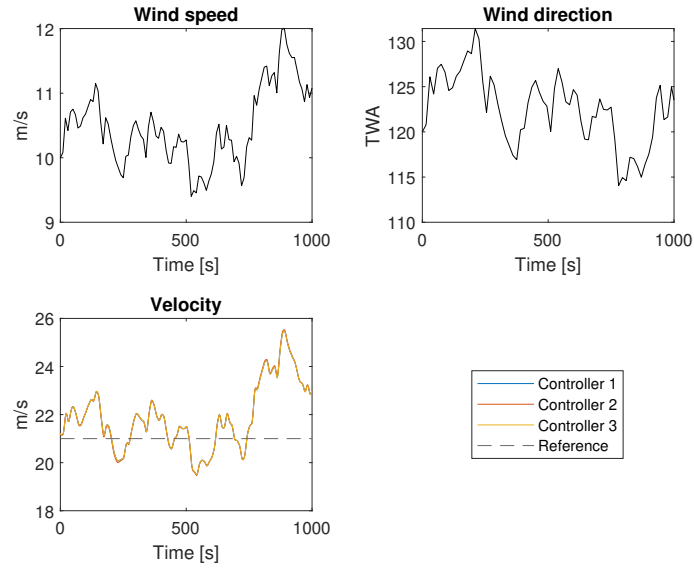


Figure 6.9: Test 5; Wind speed and direction and boat velocity [m/s]

It can be seen that the boat's speed varies correspondingly with the wind speed. This is a good indication of the performance of the boat in these conditions, as it manages to maintain a position that takes advantage of the extra power from the wind. For the wind direction interval in this test, it does not seem to affect the velocity of the boat, since it follows the wind speed. This may be due to the apparent wind angle (AWA) not being influenced by small changes in TWA due to the high speed of the boat.

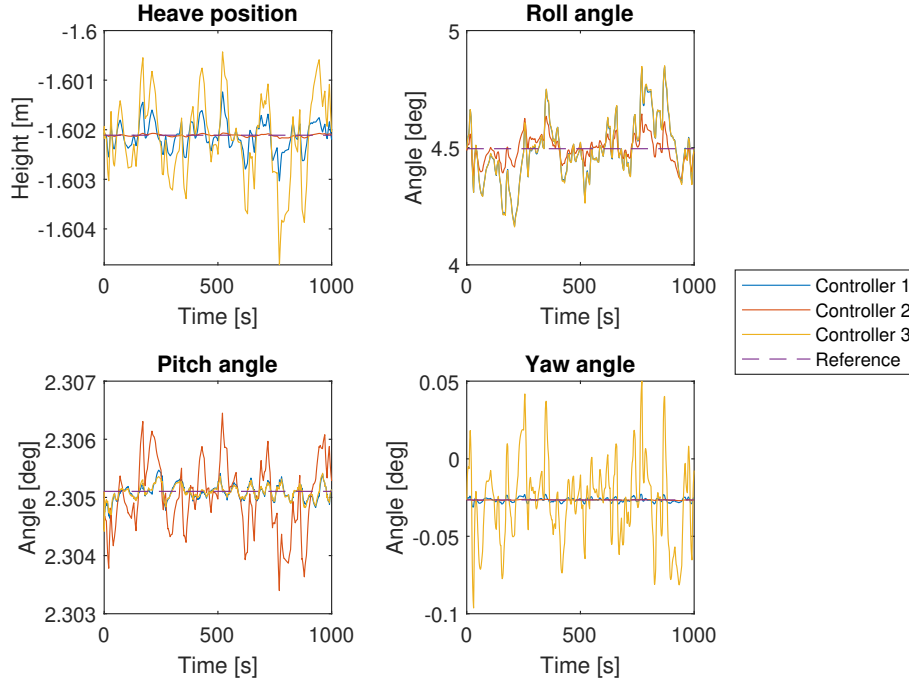


Figure 6.10: Test 5; Boat position and attitude

It is not clear from the plots that a single controller candidate stands out in terms of performance, as the variations vary in size and direction. Generally, all the variations are small. Except for roll, they are most likely not noticeable for the crew on board the boat,

as they are of a small magnitude. The rudder works to counteract the changes in yaw angle due to the change in wind direction. The response changes in yaw between 0.05 and -0.1 for Controller 3 and small changes around 0.025 for Controller 1 and 2. Considering a 0.05 degree deviation leads to 8 cm deviation from desired position after 100 m, this is a small error in response.

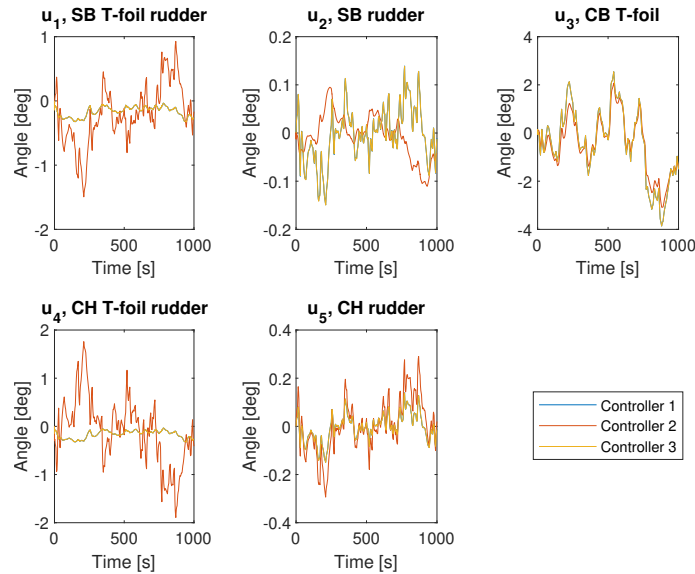


Figure 6.11: Test 5; Control input

It is interesting to see that the control inputs for controller 1 and 3 is nearly identical, while the response on the boat is different. This is due to the accuracy of the plots, as the difference is for instance 0.002 for u_1 and 0.07 for u_2 at one timestep, which is visible in the position response plot, but not in the control input plot. Controller 2 has larger commanded angles for the rudder T-foils, which corresponds with the larger deviation in pitch.

6.4 Discussion of controller candidates regarding performance in calm water

This section will discuss the performance of the controller candidates in calm waters.

Generally, the controllers manage to obtain the desired position. There are deviations from the reference for the degrees of freedom not changed, but they are for the most part insignificant. None of the tests show any overshoot when changing reference, and all the tests were performed without the hulls touching the water. The non-existent presence of overshooting may be due to the reference model delaying the signal enough for the control system to not overcompensate the change.

Note that controller 2 is the only one that manages to reach the references in all cases. But looking specifically at the difference between the three controller candidates, it looks like Controller 2 has poorer performance within the same operational areas as Controller 1 and Controller 3. The commanded angles to actuators are larger and with more rapid jumps. A large control output alone does not necessarily lead to more deviation from reference for a position. With active control in roll, it leads to more perturbations in pitch as these are very coupled motions for this system, and use the same actuators to control

the motion. The use of actuators for Controller 2 leads to reduced velocity

For controllers 1 and 3, it is assumed that the rudders are connected, such that they cannot be controlled independently, and the number of actuators is reduced to three. In addition, the actuators are only allowed to control one degree of freedom. This means that the actuators only act when an error occurs for the direction they produce the largest force. For controllers 1 and 3, it means that since there are no actuators in roll, the three actuators produce the largest forces in heave, pitch, and yaw.

Initially, there was some issues with Controller 2, which lead to the roll gain being reduced for the controller to work. A high gain in roll caused the response to have chattering, and the system had a smaller operational area. By reducing the roll gain it was possible to increase the gain in heave, and the performance overall for the system was increased. The roll reference angle is not reached as fast as wanted and it may have a constant deviation from reference due to this. Another possible solution could have been to implement anti wind-up. Anti wind-up keeps the integral gain from increasing, or winding up, when the error from set-point is not reduced and u is saturating. In this case, it was possible to solve the problem by reducing the roll gain.

When the assumption to have dependent rudders was made, it was also assumed that the T-foils should be dependent. For some high-performance multihull sailboats, this is not the case. The F50 catamarans have rudders that are steered together, while the T-foils are independent of each other, and are thus used to trim separately (SailGP 2019). If this was implemented for controller 1 or 3, it could mean that the T-foils on the rudders can be used to control both roll and pitch. This could increase the performance of the boat, when exposed to disturbances for roll, such as large wind gusts.

Another assumption for the model is that the sail is modeled as a foil, and is preset. When the sail is preset, it means that the most efficient actuator for controlling the roll angle (and forward force) is left out of the equation. This leads to a smaller operation area for the model or at least lessens the performance for some operational areas. By using the sail as an actuator, the performance would be increased, and the safety and comfort for the crew could be better (Wille, Hassani, and Sprenger 2016). By assuming the roll angle must be at least over 10 degrees before the risk of capsizing, the results for the tests would indicate that the roll angle is low enough that there is no risk of capsizing with the studied conditions and it should be comfortable for the crew to be on board.

The operational area for the model is less extreme than the intended environment the trimaran would race in. Modeling of the environment has not been a priority in this thesis and would be something to include in further work.

Dynamic simulations give the impression that there are more than one equilibrium states for the system, and that when the conditions change, the system wants to find a new equilibrium to fit those conditions. This is consistent with Kerdraon et al. (2020). This implies that real-time simulations in various conditions are needed to get a complete view of the complex system and its behavior.

For the tests, it can be seen that several things that influence the boat's velocity. It decreases when the wind decreases, or when the boat changes its heading towards the east, which means that the TWA increases. It can also be seen that the velocity decreases when the roll angle is increased and the other directions are kept constant. Generally, the most influence is from the apparent wind speed and angle. This could be linked to the trim of the sail. For a TWA of 120 degrees, the trim of the sail is good, and a change in

wind speed will increase or decrease the speed. When the TWA is changed, it would be ideal to change the trim of the sail to compensate for the change in TWA, such that the angle of attack for the sail gives the most lift (forward thrust) possible for the conditions. By adding the sail as an actuator, this could be implemented in the control system.

Chapter 7

Comparison between controllers when exposed to waves

This chapter presents a comparison between the three different controllers with regards to the performance during different test scenarios when exposed to waves.

7.1 Description of the tests

For the next tests, small swell (regular waves with low amplitude) were added. The wave parameters are given in Table 7.1, and the method described in Section 2.5.5 were used. With a propagation direction of 180 degrees it corresponds to head sea waves, which gives an encounter period of 7.14 s when the boat speed is 21 m/s.

Wave amplitude ζ_a [m]	0.15
Wave period T [s]	14
Propagation direction β_{wave} [deg]	180

Table 7.1: Wave parameters

While the waves are added to the boat model, they are not included in the configuration matrix, and thus not accounted for in the allocation. This is because the controller does not know anything about the disturbances the trimaran is exposed to. This way, the waves is accounted for through the error from desired position.

When Controller 2 was exposed to waves and steady conditions without any changes in reference, an error occurred after about 10 seconds. The error came from the trimaran plunging into water due to saturation in the actuators, and the simulation was terminated. To prevent this from happening, and to be able to perform the tests, the gains for heave was reduces to $K_p = 50e6$ and $K_i = 1e6$. The other gains were kept as they were.

7.2 Results of the tests

Test 6 - Change in heave

This test is identical to Test 1, only with waves. It is clear from Figure 7.1 that there are more disturbance for the system, as the positions are varying more. Looking at the period of the variations, they correspond with the encounter period, which gives a good indication that the effect of the waves are applied correctly to the system. The waves are regular, which is reflected in the fact that the high-frequency part of the response is varying periodically. By not accounting for the high-frequency perturbations and only looking at the low-frequency response, there is little error between the positions and reference. The varying response can be compared to constant vibrations caused by the waves. Compared to the response in Test 1, the roll angle has the same deviation, while the pitch and yaw angle has slightly larger deviations. They are still small enough to be insignificant.

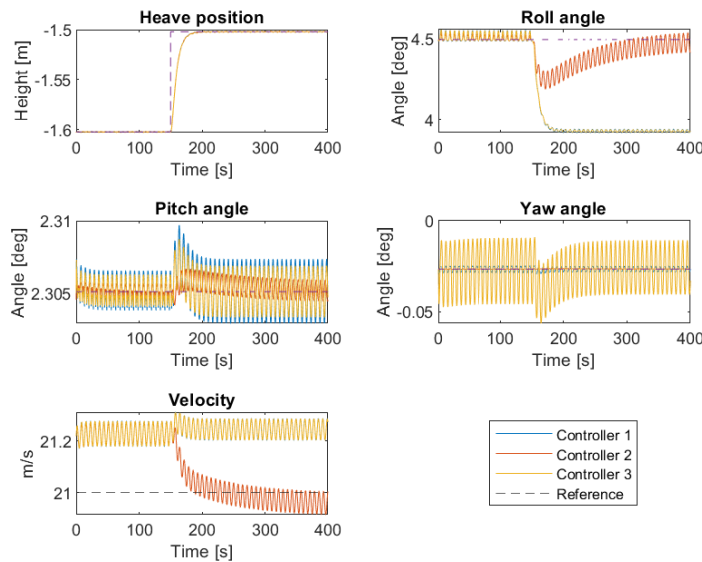


Figure 7.1: Test 6; Position

The velocity is reduced for Controller 2 when the positions are altered, which is the trend for the controller.

Comparing the commanded angles for test 1 and test 6, the result is very similar as well. The high-frequency response for the actuators corresponds with the encounter frequency. The shape of the response is the same, but the low-frequency values for waves are slightly larger. This may be due to the waves applying extra loads to the system that the actuators must compensate for.

Test 7 - Change in roll

This test applies a change of 1 degree in roll, which is a smaller change than in Test 2. When the change for roll were the same as for the tests in calm water, large perturbations happened. Controller 2 is the only one with actuators for roll, and it is therefore only this controller that reaches the reference. It takes, on the other hand, about 200 seconds, which is quite long. To compare, the desired position from the reference model takes about 30

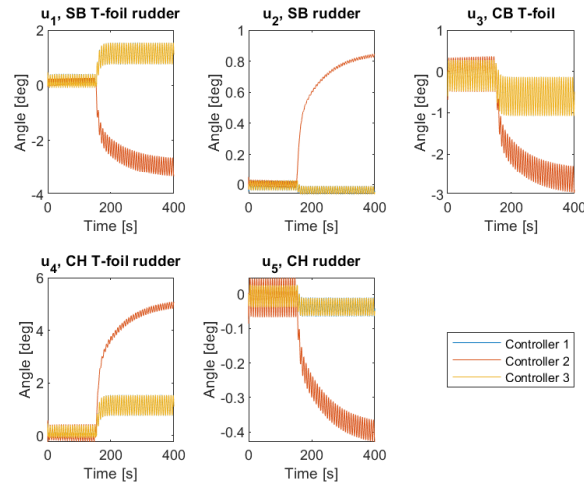


Figure 7.2: Test 6; Control input

seconds to reach the new reference. This slow change is due to the roll gain being small, to prevent the trimaran from getting unstable and plunging into the water.

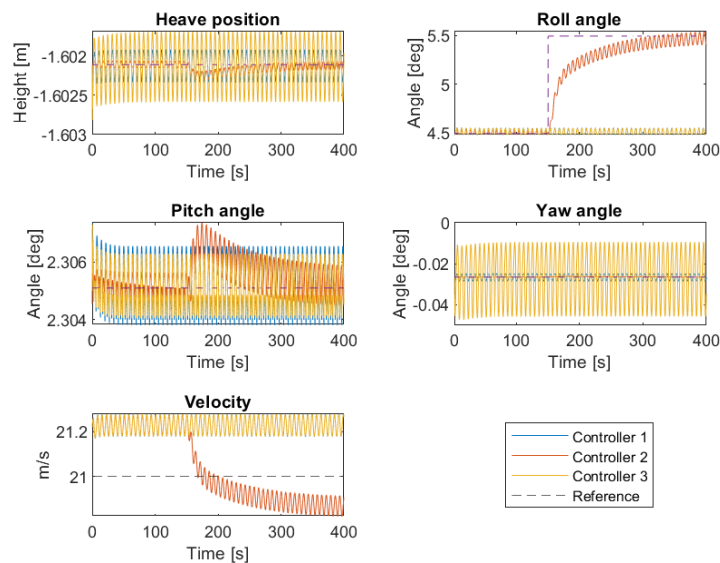


Figure 7.3: Test 7; Position

It is Controller 3 that has the largest perturbations in position, something that may be from the response of the actuators being a small second behind the response for controller 1. This gives controller 1 the opportunity to act against the perturbations before controller 3, and they do not get the possibility to grow as much. Still, the changes are insignificantly small here, which indicates that the controllers work very well at keeping the attitude constant in spite of the waves.

The size of the commanded angles to the actuators are higher than the corresponding test without waves, while the low-frequency responses are the same. This implies that more power is needed to correct the change in position for the boat. The waves apply forces to the boat, which makes the forces the actuators should compensate for larger, and thus larger control outputs. It can be said that the response oscillate around a mean that is

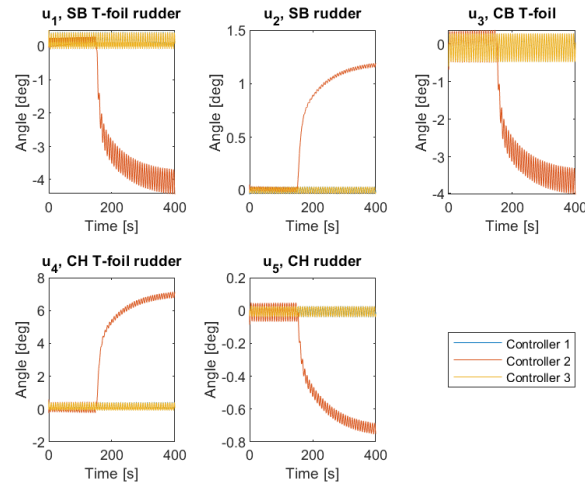


Figure 7.4: Test 7; Control input

the control input given in calm waters.

Test 8 - Change in pitch

For this test, the aim was that the controllers would make the boat follow the reference in pitch while it was changes from 2.3 degrees to 2.25 degrees, and maintaining the reference position for all directions after the change with as little control action as possible. In addition, the boat is exposed to waves. This change is smaller than for the corresponding test in calm water, Test 3. When the change was the same, the trimaran touched the water when using Controller 2 in pitch.

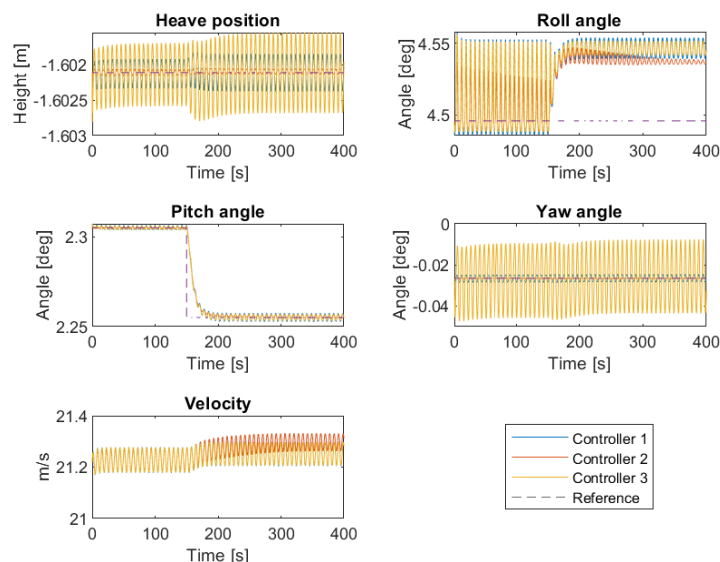


Figure 7.5: Test 8; Position

Looking at the results displayed in Figure 7.5 and Figure 7.6, it can be seen that the pitch reference is reached. The perturbation in the other degrees of freedom is small, with Controller 3 having the largest high-frequency oscillations. The response for controller 1

and controller 3 is good. The roll angle is increased as the pitch angle is decreased, but this is an expected response from the coupled motion, and the error is small enough for the system to maintain a good response. For this test, the velocity for Controller 2 was increased a little.

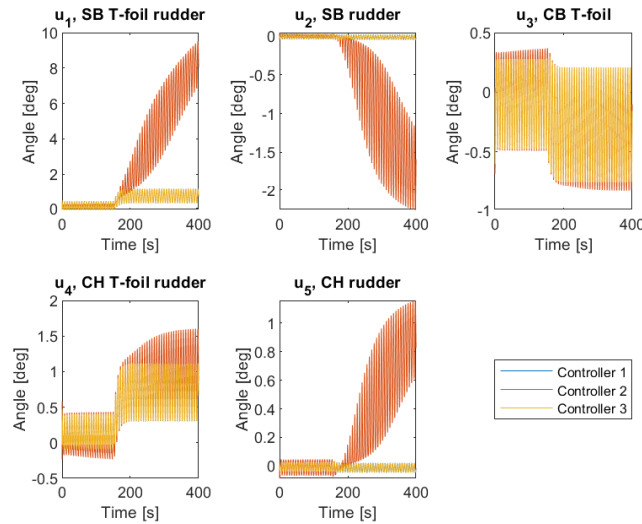


Figure 7.6: Test 8; Control input

The commanded angles are small and has small rapid changes that is acceptable behavior for the actuators, and coincides with the wave-frequency. The HF response are small enough to not exhaust the actuators. Controller 2 has increased control input for u_1 , u_2 and u_5 , which is not consistent with the attitude response, which has a constant mean.

Test 9 - Change in yaw

The maneuvering test performed in test 4, was also done for the system while exposed to waves. The control system takes approximately the same time to reach the new yaw angles as in test 4, about 50 seconds. It reaches without major perturbations for the other directions. The roll angle for controller 1 and 3 is the largest with a 0.4 degree change when the yaw angle changes 20 degrees. This change in roll corresponds to a 7 cm change in flight height for the floaters, which is an expected behavior when doing maneuvers while sailing.

Looking at the control output, the commanded angles are varying with the wave encounter frequency. The angles are within the saturation limits, but some of the rapid changes are undesirable large. Such as u_1 for Controller 2 for the last yaw change, there are several rapid jumps between 0 and 6 degrees. This could be damaging the actuators in the long run.

The control output for u_2 and u_5 (rudder angles) are the same for Controller 1 and Controller 3, as expected. While for Controller 2, u_2 is slightly larger than u_5 and has opposite direction. It corresponds with most of the tests, where u_2 and u_5 are opposite for controller 2, but it differs from test 4, which had u_2 and u_5 being the same. In test 4, the errors in heave and pitch were smaller, which could be a contributing factor for this.

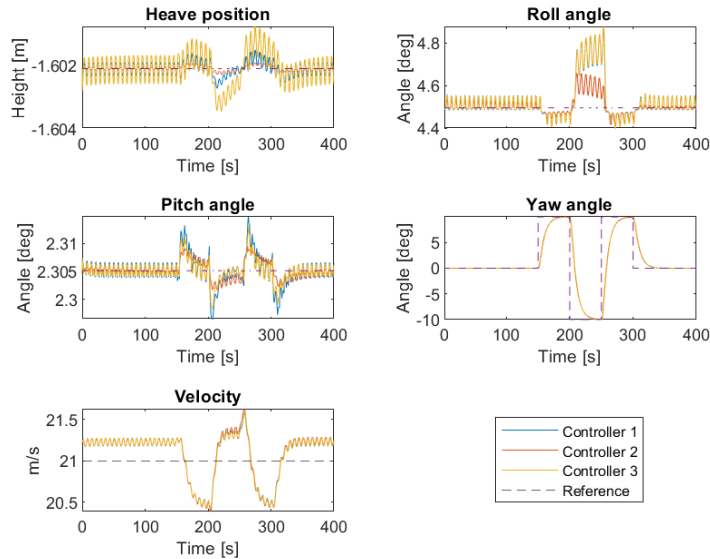


Figure 7.7: Test 9; Position

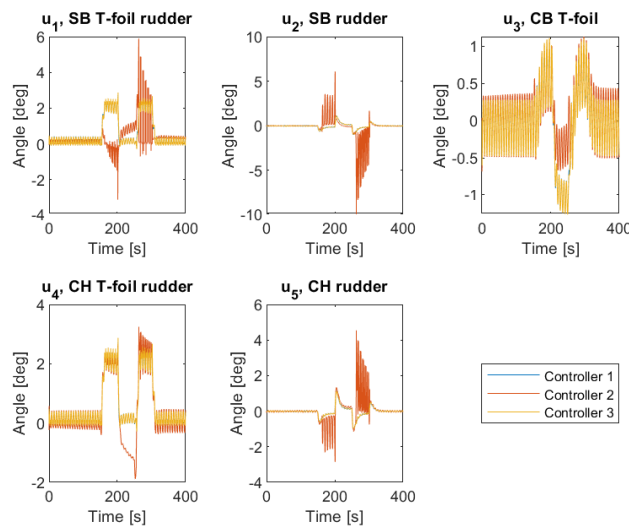


Figure 7.8: Test 9; Control input

Test 10 - Noisy wind speed and direction

With noisy wind speed and direction, the result are rapid changes in the control system.

The results show small perturbations for all controllers. The mean response is mostly at the reference attitude. Comparing it to Test 5, the trend is more high-frequency response in Test 10 due to the waves. The velocity follows the wind speed, which indicates that the boat exploits the increased power from the wind to increase the forces in surge and sway.

It appears that controller 2 has the largest peaks, with some rapid changes for the rudders. They are still small enough that it is no problem for the control system to handle.

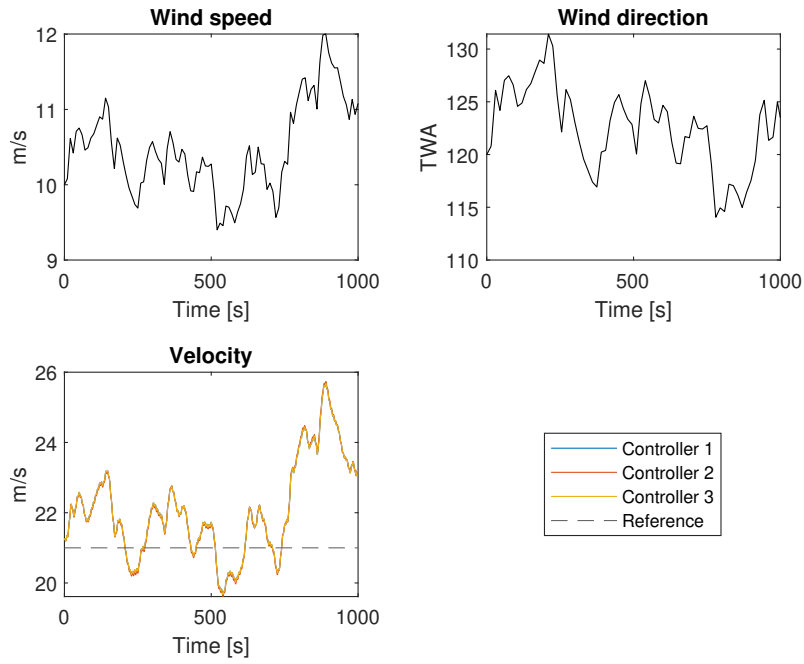


Figure 7.9: Test 10; Velocity

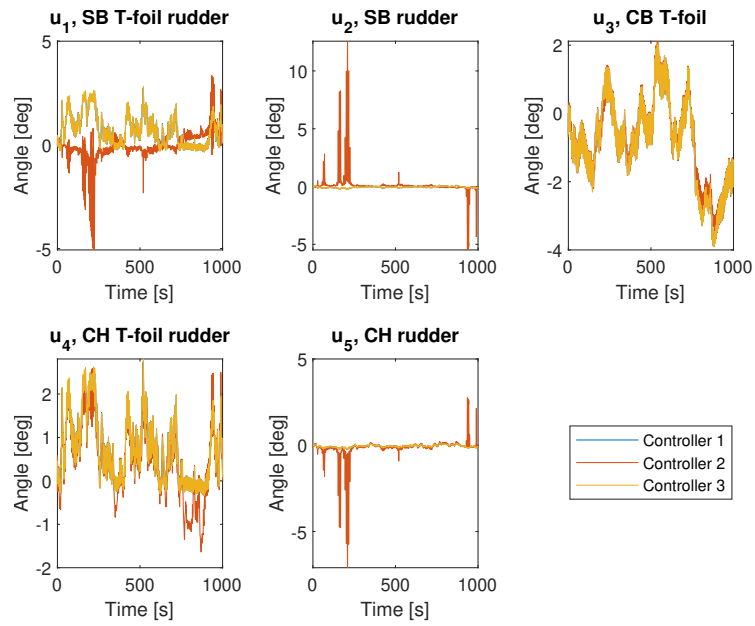


Figure 7.11: Test 10; Control input

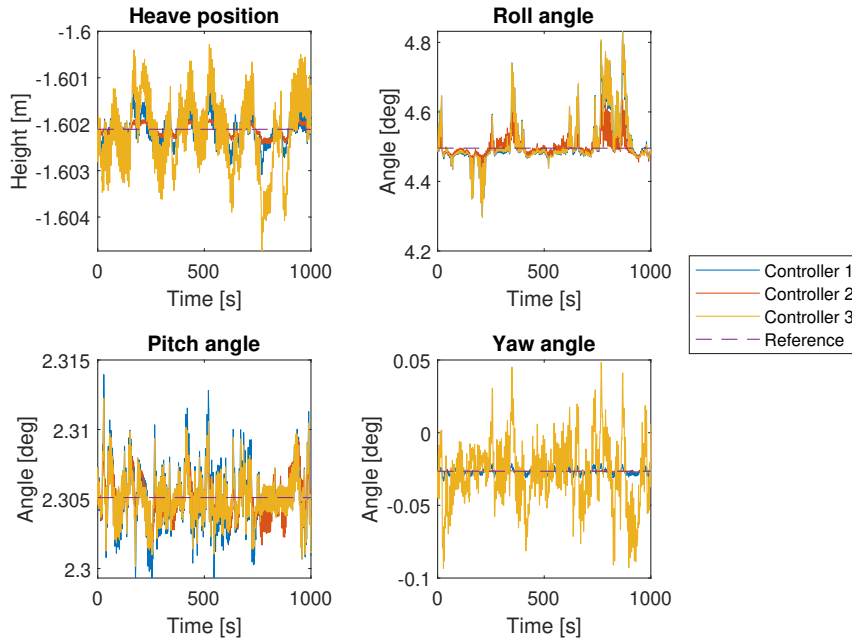


Figure 7.10: Test 10; Position

7.3 Discussion of controller candidates regarding performance with waves

For the test performed when exposed to waves, the experience is that the results are good for small changes in reference. Generally, the reference is reached, and the perturbation for the other degrees of freedom is small.

Controller 2 can follow the commands for all test, but produce large foil angles. By only looking at the control input, Controller 1 and Controller 3 have the lowest angles. When the model is exposed to waves, they also produce the least rapid jumps, which leads to less strain on the actuators. Between the two controllers, Controller 1 is easier to implement. By evaluating the foil sensitivities and using the result, the force from the PID for Controller 1 are assigned to one DOF based on the sensitivities and there is no need for a separate force allocation.

The velocity depends on the attitude of the trimaran and the wind. When the roll angle is desired to be kept constant while heave or pitch changes, the velocity is reduced for Controller 2. Comparing to test results in calm water, it does not seem to affect the velocity of the trimaran much to be exposed to waves. It rather seems like the velocity is kept higher for the tests with waves.

As there is little data for comparison, it makes setting the boundaries for the model harder. From videos, it looks like the boats are under little influence from even bigger waves (offshore conditions), and it seems as it would be realistic for the boat to be as stable as the tests make it out to be. The conditions in the tests are very calm, and it is therefore to be expected that the influence from the environment is small compared to harder conditions. By comparing with the values from Kerdraon et al. (2020), it looks like roll, pitch and rudder angles from the tests agree with results from other similar trials.

When the model is exposed to waves, it might be desirable to have a wave filter to filter out the high-frequency wave motions. A phase delay in the model due to a filter can make the

system unstable, and the control system cannot react to the disturbance before the errors become too big. The variations in response for the actuators due to the waves are small enough for the result to be good without a filter. The actuators are not overcompensating in this case, and thus filtering is not necessary.

Chapter 8

Conclusion

The main goal of this thesis was to

”Develop and verify a control system for the foiling trimaran sailboat that is suitable for automatic course and ride control and performs well in different environments.”

This chapter concludes the work done in this thesis and presents some suggestions for further work.

8.1 Concluding remarks

The focus of this thesis has been to model and control a foiling sailboat, with the aim of keeping the boat in a foiling state when exposed to different disturbances. The sailboat is based on the Ultim class of trimarans, which are intended to race in offshore conditions. The history of foiling vessels and different approaches to making a control system have been investigated.

A dynamic simulation environment was developed, and it has been verified through comparison with a DVPP and input from Mer Concept. Five of the foils were chosen to be used as actuators. Due to the complexity of the system, the sensitivity of the incidence angle of the controlled foils has been used to analyze the coupled motions of the trimaran.

The control system architecture has been presented and is made in Simulink using the dynamic simulation environment. Three controller candidates have been used to compare the performance of the proposed control system using several test scenarios. These candidates were chosen to be able to compare the effect of coupled motions of the boat by looking at a simple approach, an advanced approach, and a combination of those, for the allocation of forces. All three candidates used a PID controller to find the loads.

The model has been exposed to changes in reference, in wind, and to waves, and the results show that the control system is effective in maintaining the desired position and direction of the trimaran. The three controller candidates show some differences in performance, with Controller 2 having larger incident angles to the actuators and controllers 1 and 3 have poorer performance in roll due to the force allocation. Controller 2 is effective in gusty conditions, where the roll control is more needed, while Controller 1 is effective and simple for more stable conditions.

To conclude, all of the proposed controller candidates manage to keep the trimaran foiling in the test scenarios, with some limitations due to the validity range of the dynamic simulation model. The trimaran is controlled well under the assumptions in this thesis, but the need for a more advanced controller is present in rougher conditions when the roll motion increases, when waves become larger, and more complex maneuvers are to be studied (i.e. tacking, jibing, etc...).

8.2 Further work

Below are some points for further investigation.

Modeling

- The waves are added to the model as induced particle velocity, and the surface elevation is not accounted for. By including the surface elevation, the model can be more accurate.
- The model has a reduced validity range. By including the port hull in the modeling, it could be possible to expand the range to include sailing on the starboard tack. The sail would then have to be able to change form incident angle of 20 degrees to -20 degrees.
- Improved modeling of the hydrodynamic (contact of the hull with water) and aerodynamic forces (modeling several sails, the twist in sails, and on the long run, using CFD).

Control

- In the actuator dynamics, a delay due to the hydraulic system is not accounted for, and would be something to include in a later edition of the control system. This could make the model more realistic.
- To further expand the range, the sail could be included as an actuator. This would improve the control of roll, and the risk of capsizing can be reduced.
- The L-foil can be included as an actuator by controlling the rake angle using a flap.
- When the roll angle is changed, this induces a change in heave. For Controller 1 and 3, the change in roll cannot be controlled, while the change in heave can. An objective for the control system, can be that it is the combination of heave, roll, pitch and yaw that is controlled, rather than the set point for each of the DOFs. If so, it could be possible to use sliding mode control.
- A goal with the thesis was to understand the dynamics of the trimaran, to be able to make the best possible control strategy. To start with, a simple controller was made to establish the needs for a more advanced controller. The simple controller was efficient in maintaining the reference position, but due to the ambition of maximizing the velocity it could be beneficial to use an optimizing strategy such as the model predictive control (MPC).

Bibliography

- Actual (2020). *Le Trimaran Macif devient officiellement Actual Leader 2*. Visited 26.04.2021. URL: <https://www.team-actual.fr/news/wnc2gcwcyo3icbzu3oek3cdymdrwtf>.
- (2021). *L'actual Ultim 3*. Visited 25.05.2021. URL: <https://www.team-actual.fr/lactual-ultim-3>.
- Beard, Randal W. and Timothy W. McLain (2012). *Small Unmanned Aircraft: Theory and Practice*. Princeton University Press. ISBN: 9780691149219.
- Bencatel, R., S. Keerthivarman, I. Kolmanovsky, and A. R. Girard (2021). “Full State Feedback Foiling Control for America’s Cup Catamarans”. In: *IEEE Transactions on Control Systems Technology* 29.1, pp. 1–17. DOI: 10.1109/TCST.2019.2955059.
- Bøe, Mikael (2019). “Numerical modelling of sailing hydrofoil boats”. Master thesis. Department of Marine Technology, the Norwegian University of Science and Technology (NTNU).
- Callahan, Steven (2020). “Hydrofoils for Sailboats”. In: *Cruising World*. Retrieved 16.03.2021. URL: <https://www.cruisingworld.com/story/how-to/hydrofoils-for-sailboats/>.
- Candela Speed Boat* (2020). Visited 05.12.2020. URL: <https://candelaspeedboat.com/>.
- Faltinsen, O. M. (1990). *Sea Loads on Ships and Offshore Structures*. Cambridge University Press.
- (2006). *Hydrodynamics of High-Speed Marine Vehicles*. eng. Cambridge: Cambridge University Press.
- FFVoile (2020). *Règles de Classe Ultim 32/23*. Retrieved from FF Voile by e-mail 13.11.20.
- FlyingFoil (2020). *Flying Foil*. Visited 12.11.2020. URL: <https://flyingfoil.no/>.
- Fossen, T.I. (2011). *Handbook of Marine Craft Hydrodynamics and Motion Control*. eng. 1. Aufl. Hoboken: Wiley.
- Gitana (2020a). *Gitana Team website*. Visited 02.11.2020. URL: <http://www.gitana-team.com/en/>.
- (2020b). *Hors Quart*. Watched 19.11.2020. URL: https://youtu.be/4ndTXJQm_dg.
- (2020c). *Servo-control, switching from 2D to 3D*. Watched 02.11.2020. URL: <https://youtu.be/N9w7AM4drHA>.
- (2021). *Making an ocean Maxi-trimaran fly, the main principles*. Watched 19.04.2021. URL: <https://www.youtube.com/watch?v=q-8VcIbp0TU>.
- Håberg, Ida Oline (2019). “Foil Motion Control of High-Speed Catamarans”. Master thesis. Department of Marine Technology, the Norwegian University of Science and Technology (NTNU).

- Hella, Amalie Hjellestad (2020). “Modeling of foiling trimaran sailboat”. Project thesis. Department of Marine Technology, the Norwegian University of Science and Technology (NTNU).
- Heppel, Peter (Mar. 2015). “Flight dynamics of sailing foiler”. In: HPYD5. URL: https://www.researchgate.net/publication/274640126_FLIGHT_DYNAMICS_OF_SAILING_FOILER.
- IMO (2020). *Reducing greenhouse gas emissions from ships*. Visited 03.12.2020. URL: <https://www.imo.org/en/MediaCentre/HotTopics/Pages/Reducing-greenhouse-gas-emissions-from-ships.aspx>.
- Kerdranon, Paul, Boris Horel, Patrick Bot, Adrien Letourneur, and David Le Touzé (2020). “Development of a 6-DOF Dynamic Velocity Prediction Program for offshore racing yachts”. In: *Ocean Engineering* 212, p. 107668. ISSN: 0029-8018. DOI: <https://doi.org/10.1016/j.oceaneng.2020.107668>.
- Lavigne, Emilien and Thomas Sauder (2020). *Personal correspondence with Mer Concept*. Correspondence by mail and telephone in the period june-october.
- Limited, America’s Cup Event (2021). *America’s Cup*. Visited 28.05.2021. URL: <https://www.americascup.com/en/home>.
- MathWorks (2020). *fminsearch*. URL: <https://se.mathworks.com/help/matlab/ref/fminsearch.html>.
- PlanetSail (2020). *The full story - Brest Atlantique*. Watched 09.06.2020. URL: <https://youtu.be/Lnww0H6HQCY>.
- S.L.U., The Ocean Race (2021). *The Ocean Race*. Visited 28.05.2021. URL: <https://www.theoceanrace.com/>.
- SailGP (2019). *How to sail an F50 catamaran*. Watched 09.04.2021. URL: https://www.youtube.com/watch?v=dujJu3j81tQ&ab_channel=SailGP.
- SEAir (2021). Visited 16.03.2021. URL: <https://www.seair-boat.com/>.
- Sheahan, Matthew (2013). “The foiling phenomenon – how sailing boats got up on foils to go ever-faster”. In: *Yachting World* (April). URL: <https://www.yachtingworld.com/special-reports/the-foiling-phenomenon-66269/4>.
- Sodebo (2021). *Sodebo Ultim 3*. Visited 25.05.2021. URL: <https://ultim3.sodebo.com/>.
- Sørensen, Asgeir J. (2018). *Marine Cybernetics: Towards Autonomous Marine Operations and Systems*. Trondheim, Norway: Department of Marine Technology, the Norwegian University of Science and Technology (NTNU).
- Trehin, Mathilde, Johann Laurent, Hugo Kerhascoet, and Jean-Philippe Diguët (Mar. 2019). “An Energy Aware Autopilot for Sailboats”. In: SNAME Chesapeake Sailing Yacht Symposium.
- Vendée, SAEM (2021). *Vendée Globe*. Visited 28.05.2021. URL: <https://www.vendeeglobe.org/en>.
- WASZP (2021). *Manuals and Guides*. Visited 28.05.2021. URL: <https://www.wazsp.com/ask-wazsp/manuals>.

- Wille, Kristian L. (2016). “Autonomous Sailboats - Modeling, Simulation, Control”. Master thesis. Department of Marine Technology, the Norwegian University of Science and Technology (NTNU).
- Wille, Kristian L., Vahid Hassani, and Florian Sprenger (2016). “Roll Stabilization Control of Sailboats”. In: *IFAC-PapersOnLine* 49.23. 10th IFAC Conference on Control Applications in Marine SystemsCAMS 2016, pp. 552–556. ISSN: 2405-8963. DOI: <https://doi.org/10.1016/j.ifacol.2016.10.493>. URL: <https://www.sciencedirect.com/science/article/pii/S2405896316320833>.
- Yun, Liang and Alan Bliault (2010). *High Performance Marine Vessels*. eng. 1. Aufl. New York, NY: Springer-Verlag. ISBN: 9781461408680.

Appendix A

Load distribution

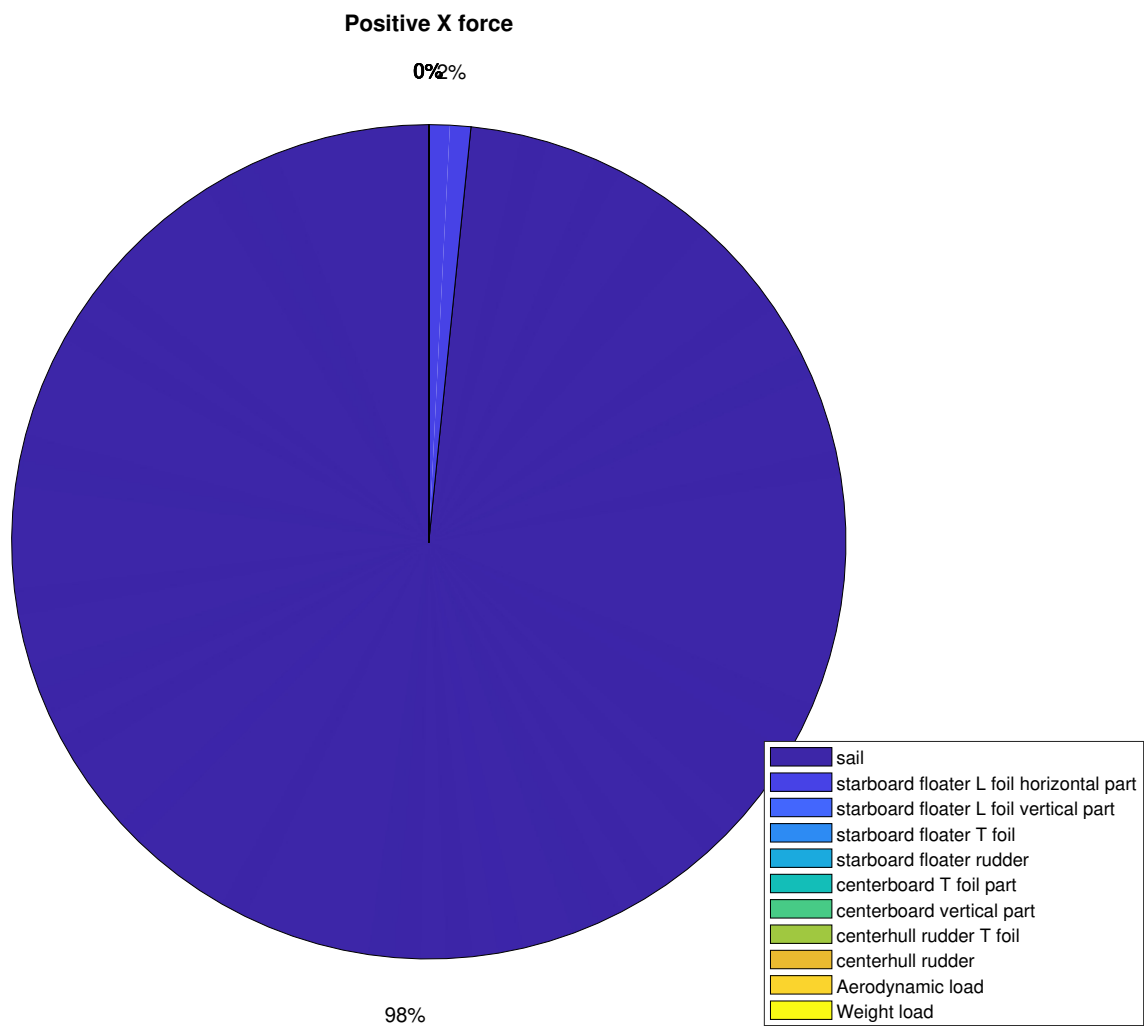


Figure A.1: Forces in positive x-direction

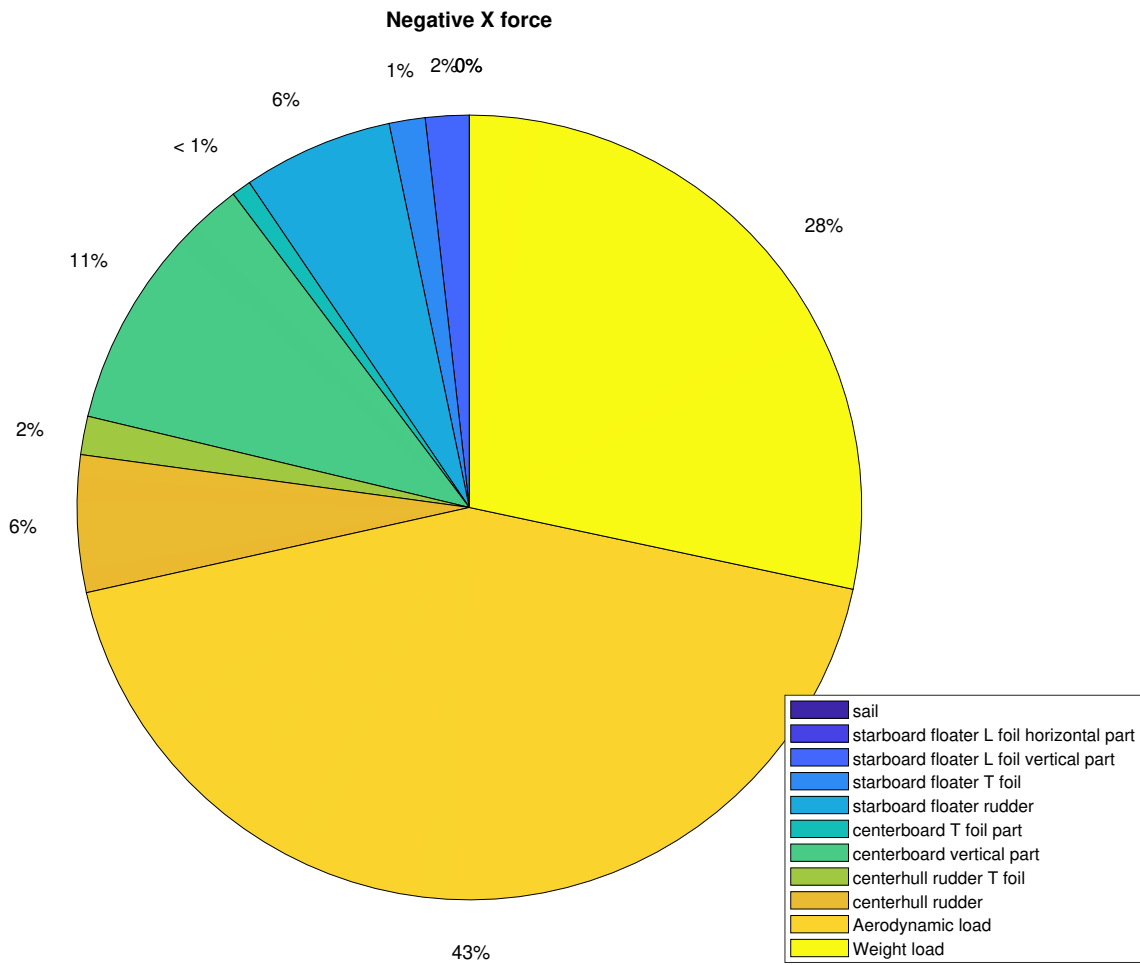


Figure A.2: Forces in negative x-direction

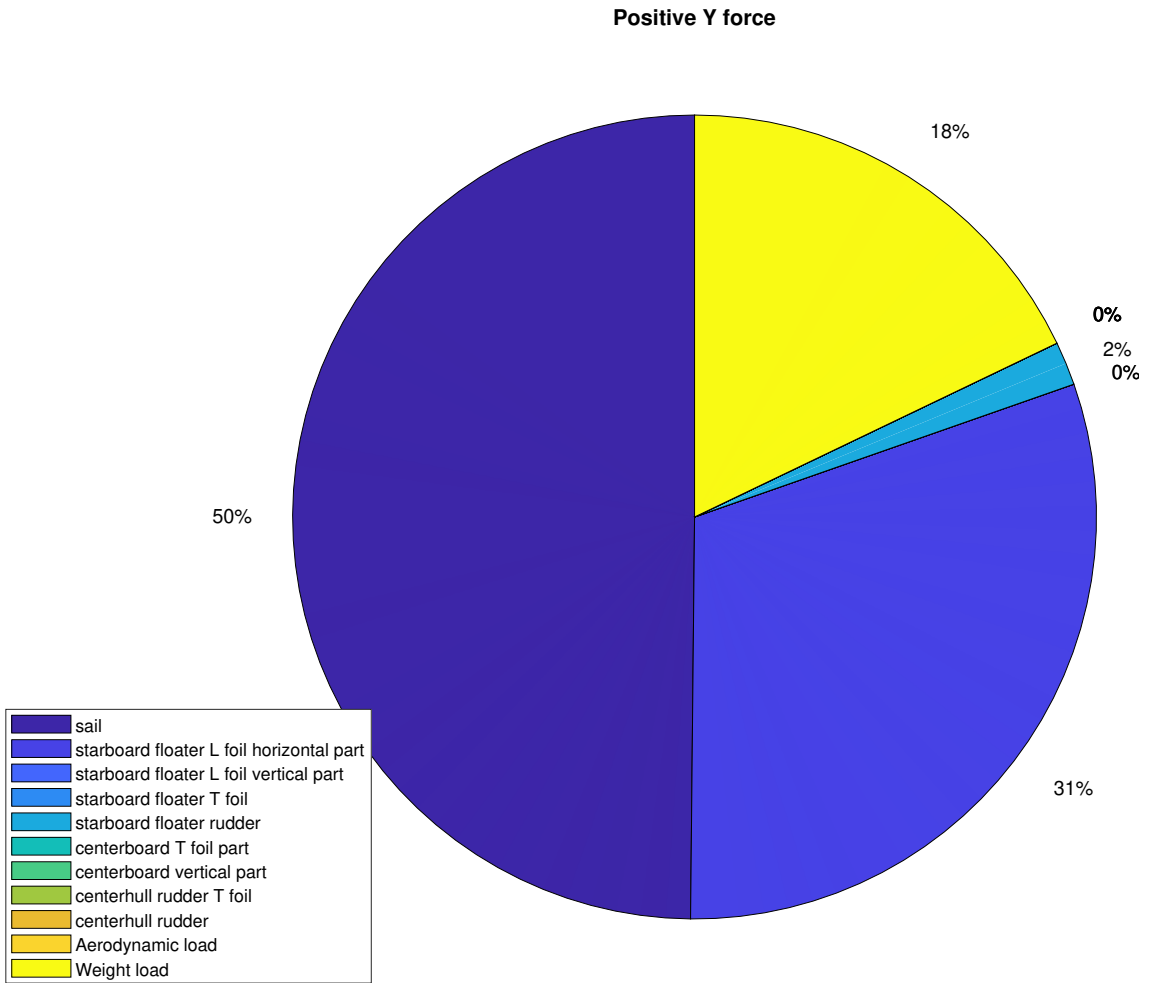


Figure A.3: Forces in positive y-direction

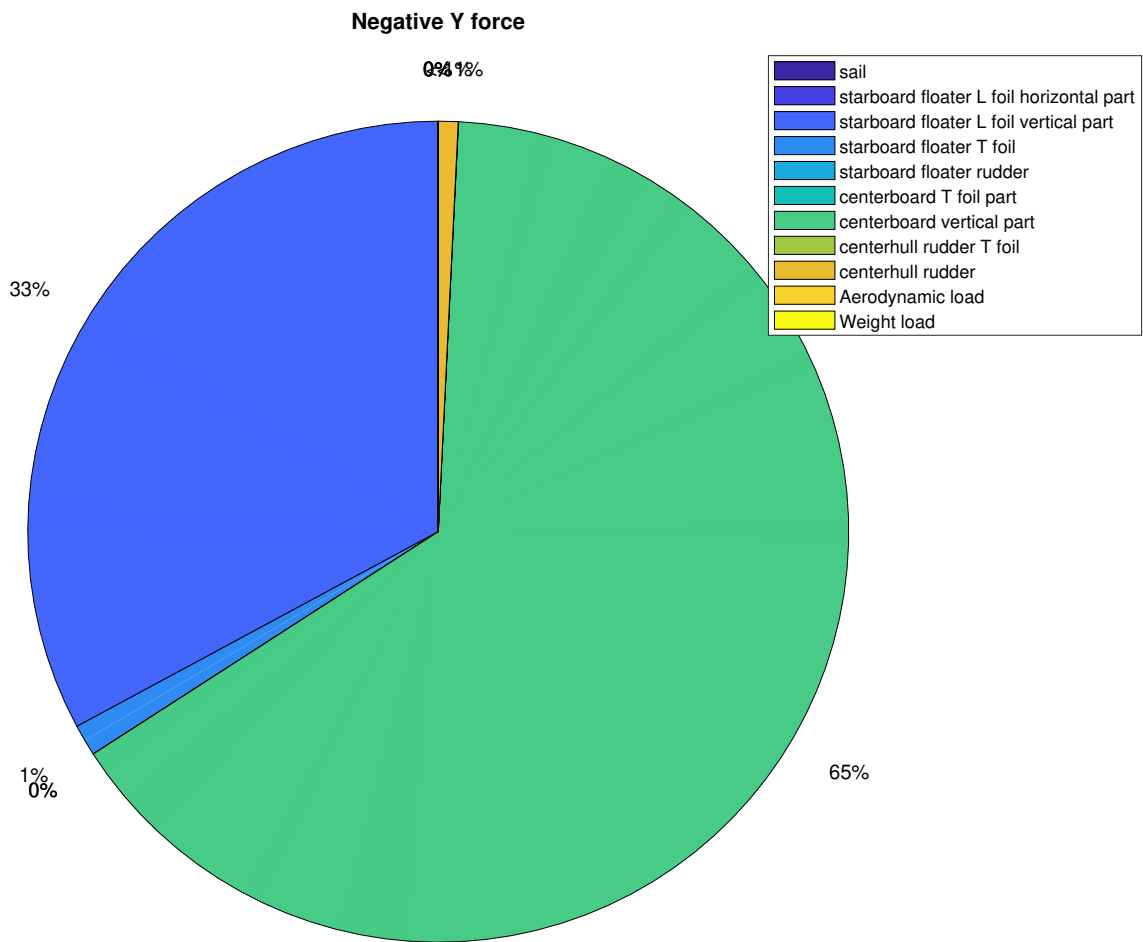


Figure A.4: Forces in negative y-direction

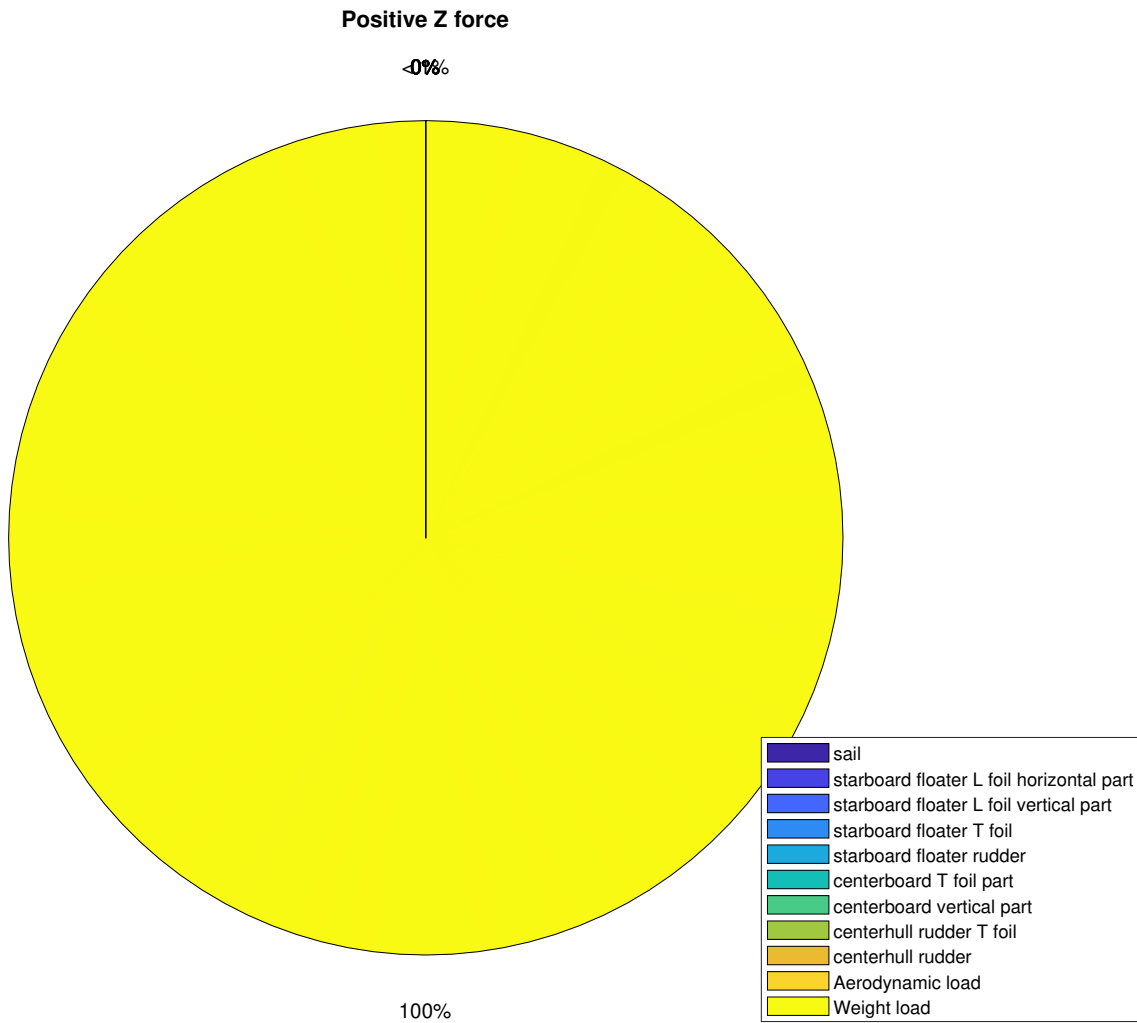


Figure A.5: Forces in positive z-direction

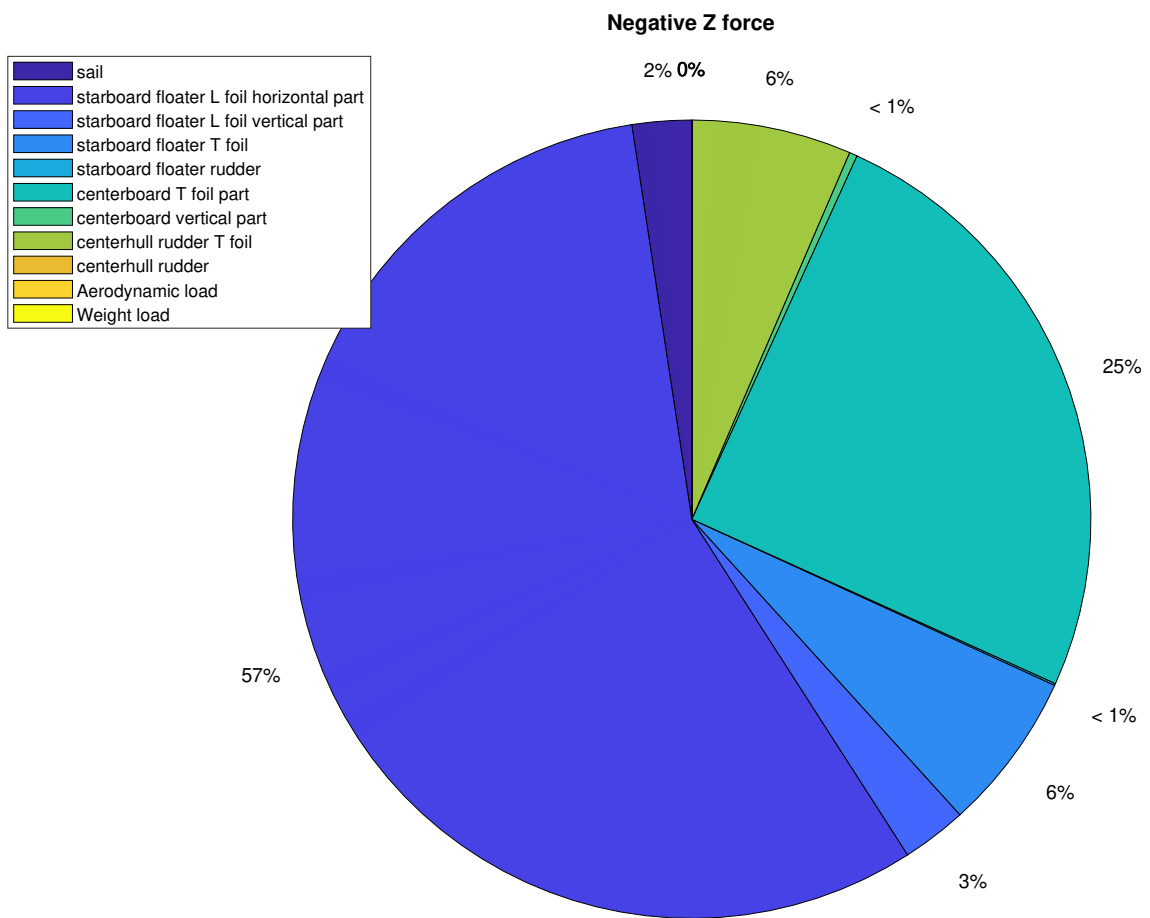


Figure A.6: Forces in negative z-direction

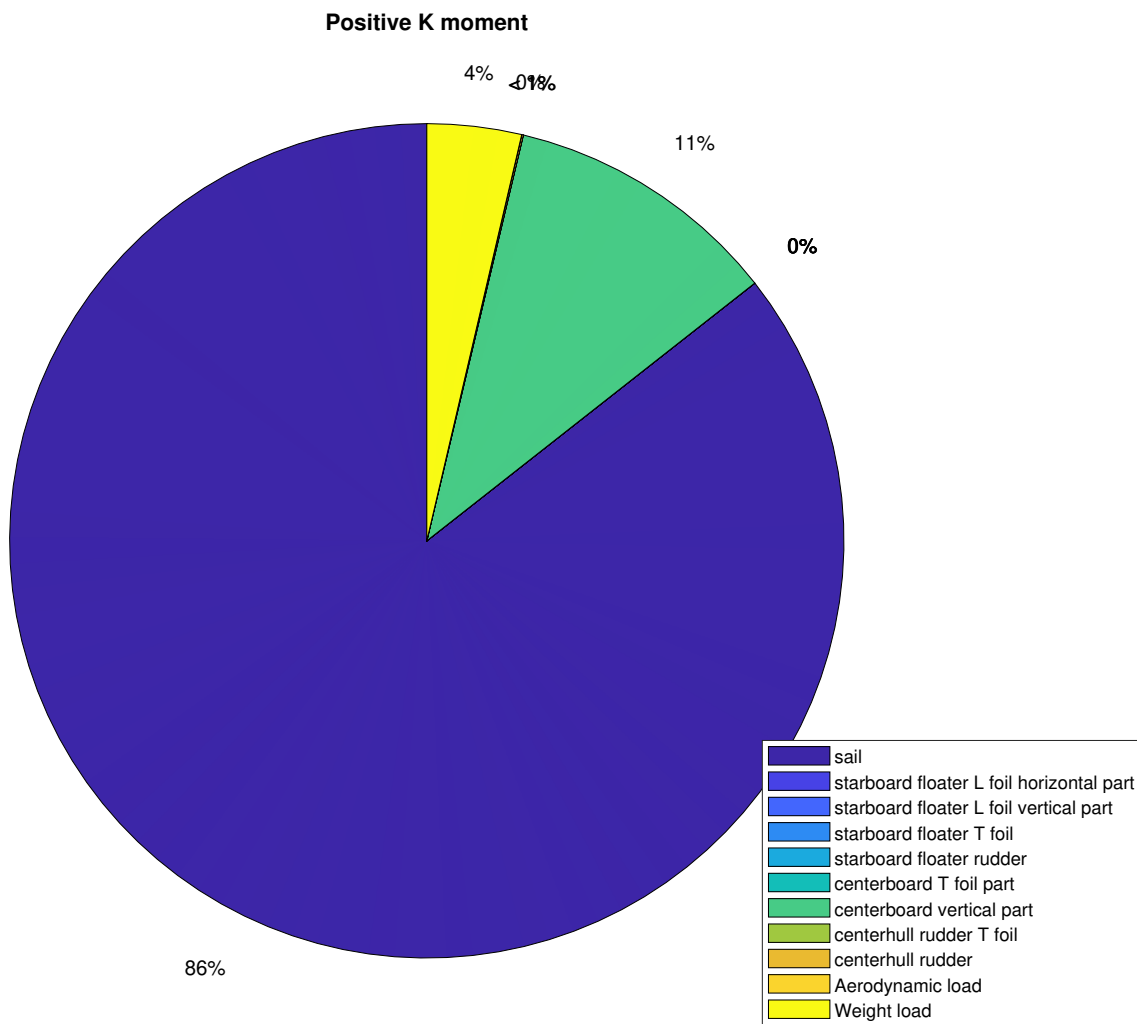


Figure A.7: Positive moment in roll

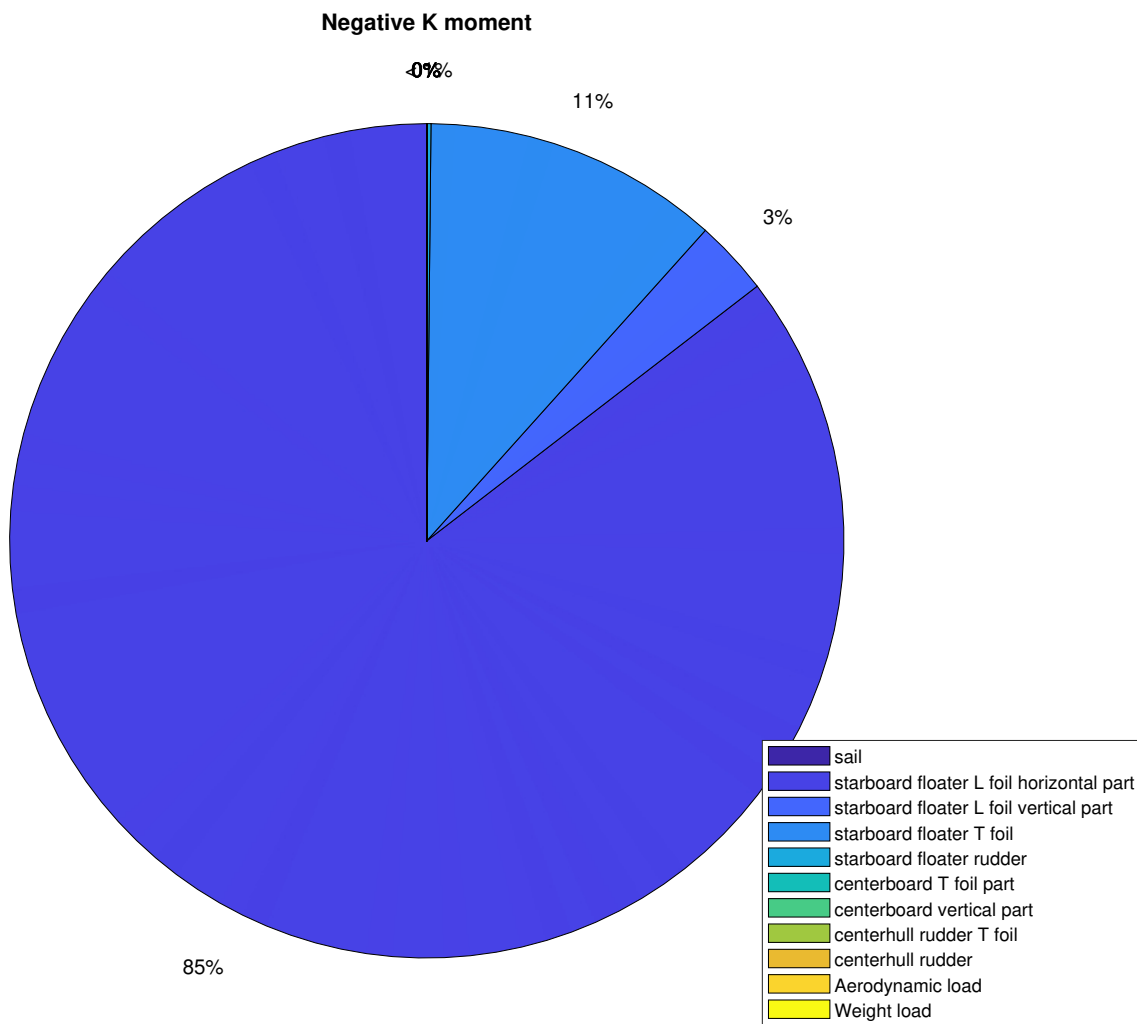


Figure A.8: Negative moment in roll

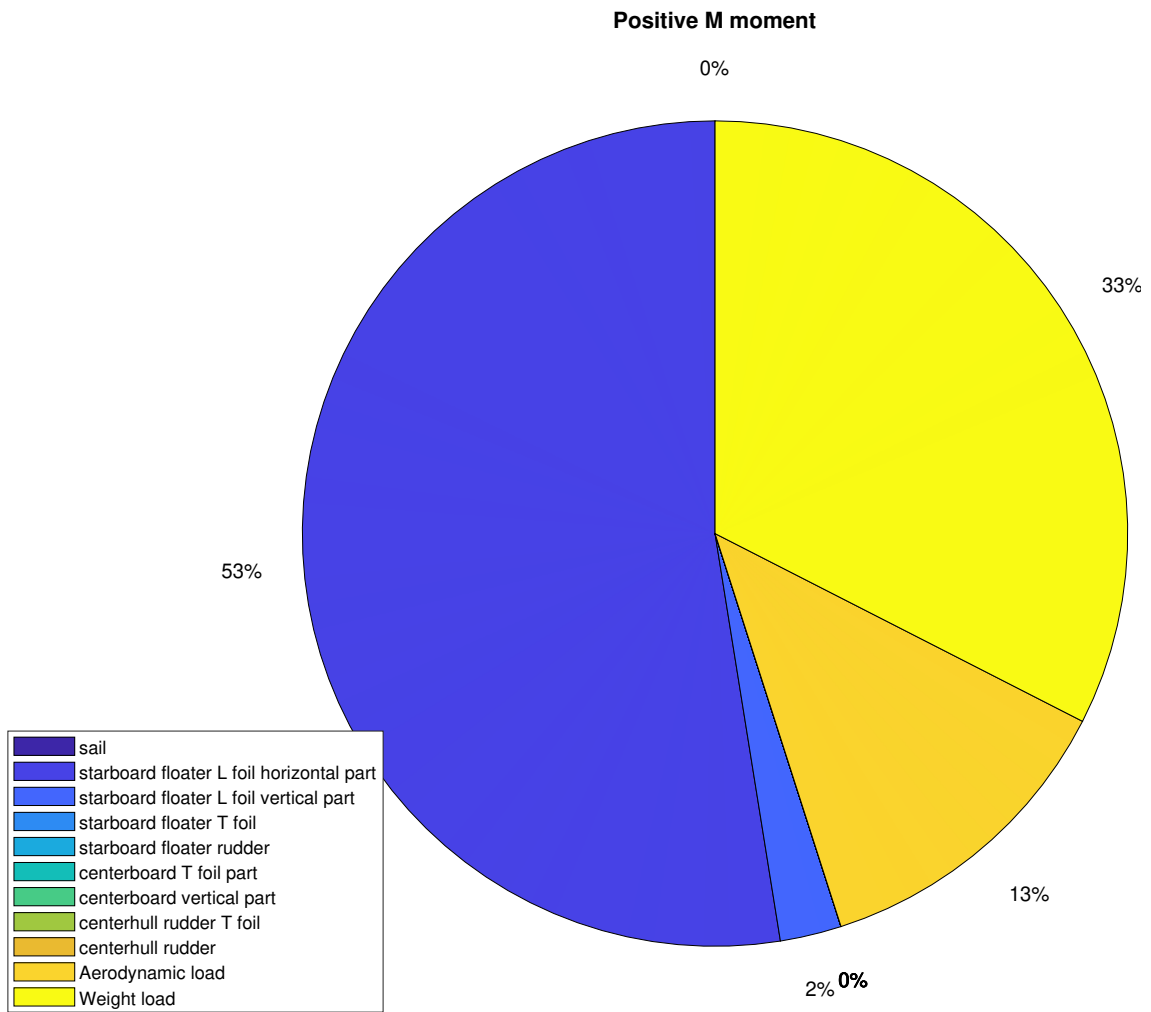


Figure A.9: Positive moment in pitch

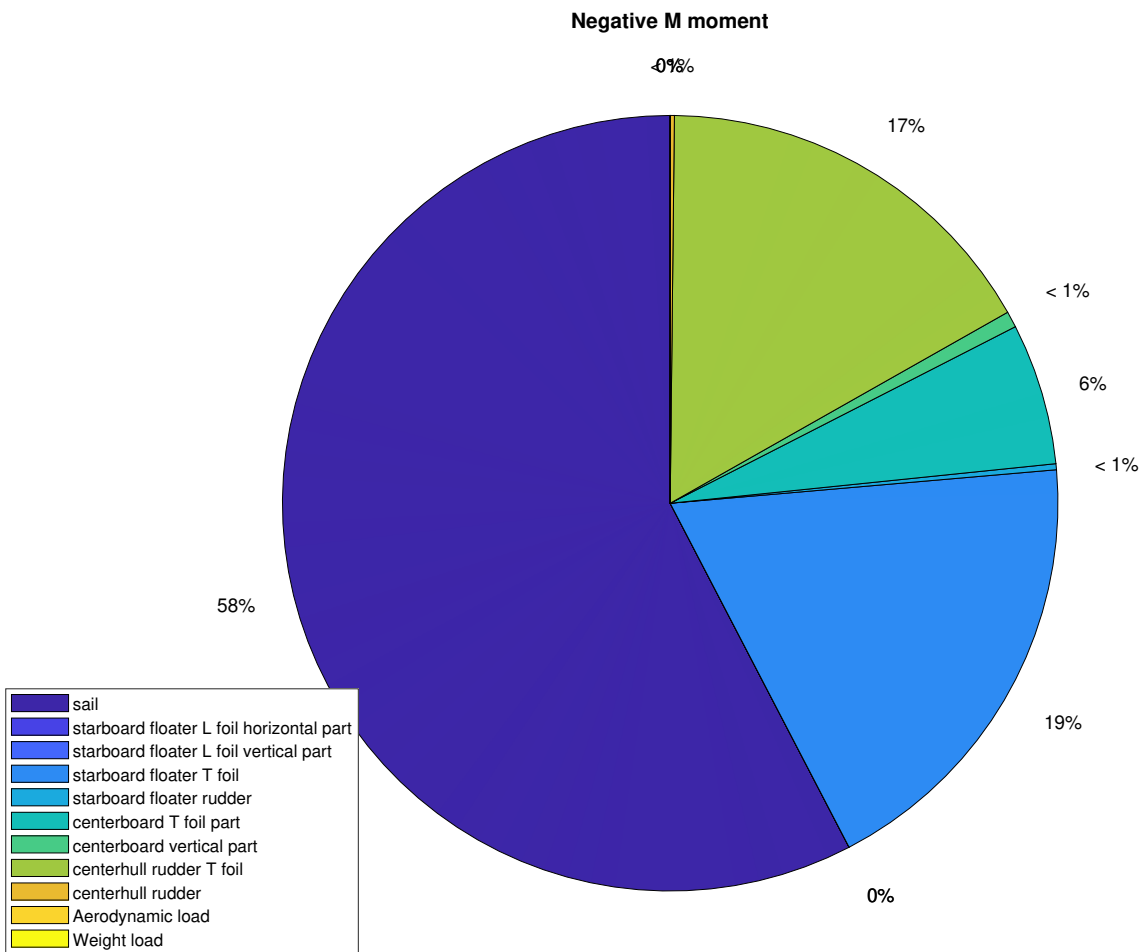


Figure A.10: Negative moment in pitch

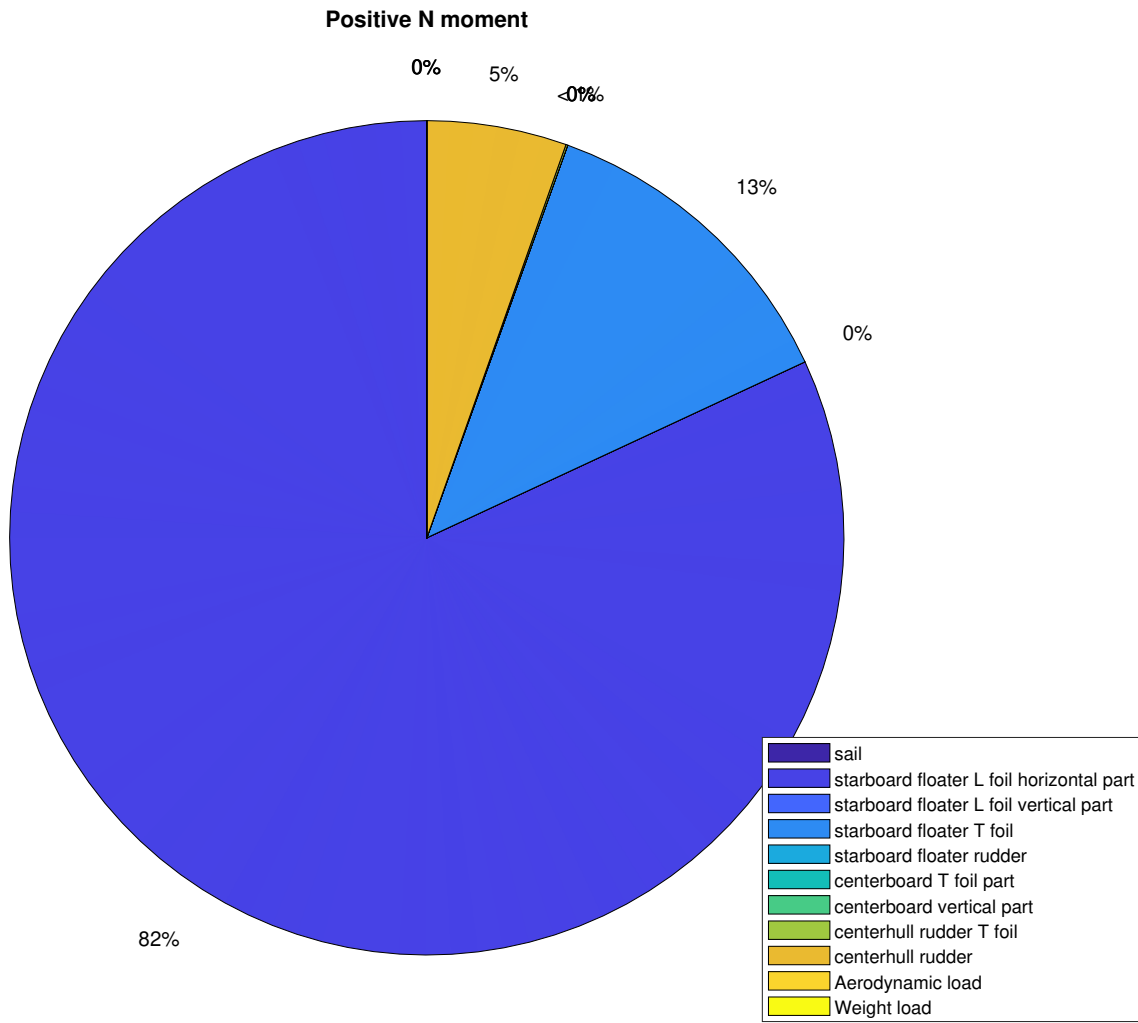


Figure A.11: Positive moment in yaw

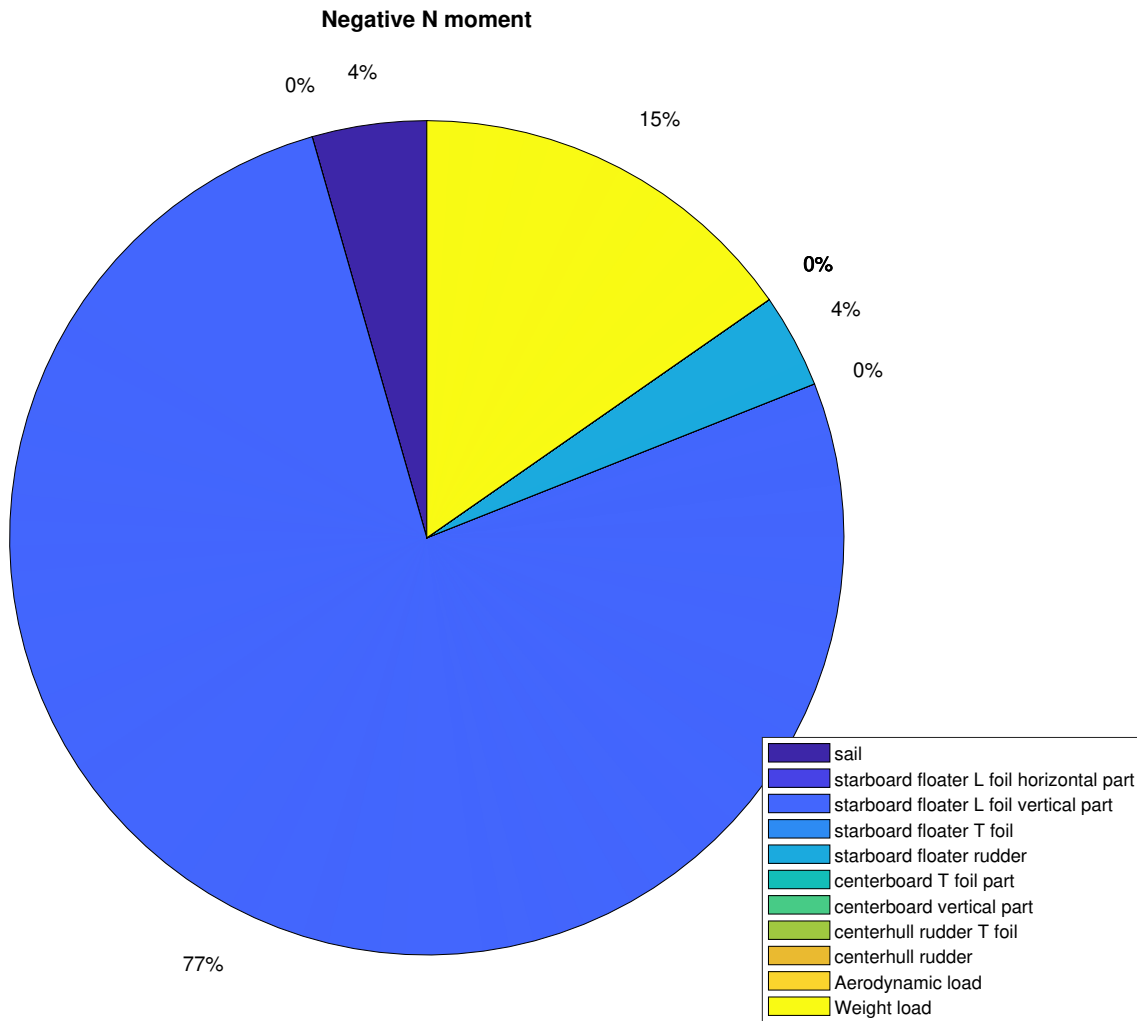


Figure A.12: Negative moment in yaw

Appendix B

Explanation of the code

The code is made in MATLAB and Simulink. To keep track of the different versions of the code, GitHub has been used as version control. The code for the model with and without waves are on two separate branches of the project. The main difference between the branches are the addition of calculating the wave effect, and adding this to Simulink.

A brief explanation of the different files follows.

B.1 initialize.m

This file is the main file, where the program is initialized, the constants are defined and the initial values are set. The simulations are also run from this file. The gains for all three controllers are defined here.

To start the program, run this file.

B.2 staticEquilibrium.m

The static equilibrium file is where the static equilibrium is found, and where the sensitivity of the forces and moments are found.

Initial values for the boat is defined in the start of the file. For the branch with waves, they are defined here. Then the foil loads, weight loads and the aerodynamic load on the superstructure is calculated and summed in a total load.

To find the equilibrium, an optimization is run on the attitude of the foils, apart from the sail and vertical centerboard.

This file prints the loads in the command window, before and after optimizing.

B.2.1 computeResidual.m

This file is a part of the optimization to find the static equilibrium. The function adjust the attitude of the optimized foils, and return the residual.

B.2.2 configurationMatrix.m

Calculates the configuration matrix of the Jacobian for the loads on the foils.

B.3 Functions for calculating loads

B.3.1 foilLoad.m

In this file, the loads for each foil is calculated. It takes in η , ν , the foil struct, wind and wave in addition to a boolean "verbose" to print details or not. The theory presented in Section 2.5 is applied here.

The file foilLoads.m is a modified version that is used in Simulink, due to Simulink not accepting structs from workspace.

loadFoilDescription.m

This is where all the foils are defined. The foils are saved in a struct, for type, position in {b}, attitude in {b}, chord length and span length.

B.3.2 aerodynamicLoadSuperstructure.m

This file calculates the aerodynamic load on the superstructures of the trimaran, such as the hulls, beams and mast. Input to the function is η , ν , wind and a boolean "verbose" to print details or not. The load is saved in a vector for the loads in {b}.

The file aeroLoadSuperstructure is a modified version used in Simulink model.slx.

B.3.3 weightLoad.m

The weight load is calculated in this file. Input to the function is η and a boolean. The function returns the load expressed in {b}.

B.3.4 coriolisCentripetal.m

This file includes a function to calculate the coriolis centripetal matrix using the mass matrix and ν .

B.3.5 massDistribTrimaran.m

Using the mass distribution for the Trimaran, this function calculated the mass matrix. All the inertia properties are defined here.

B.4 Simulation

B.4.1 tests.m

This is a script to define and run tests from. There are 8 tests defined, where test 1-4 is test 1-4 in this thesis, and test 7 corresponds to test 5 in this thesis.

For each of the tests 1-4 and 7, the script can either run through simulations for all three controllers, or run for one of them. This is defined in initialize.m. When a test simulation is done using model.slx, figures are plotted and saved to the matlab folder. The figures are defined in the test script for when more than one controller is used, and in figure.m for one controller. Figures can be plotted for each simulation run, as long as the run is saved as result. The runs are automatically saved as testnb for tests with one controller, and testnb_controllernb for all controllers.

If an error occurs in the simulation, it terminates and the script receives an error and stops.

B.4.2 figures.m

Prints and saves figures for a simulation.

B.4.3 model.slx

The simulink model is divided into several areas. First consists of the reference positions and velocities as well as the reference model, then the controller candidates are defined. Next, the foils are defined. There is a separate area for wind and wave. Lastly, the trimaran is defined, and the new positions and velocities are found.

To keep the look clean, GoTo and From blocks are used for the signals that are going into several of the blocks.

Controllers

The controllers are implemented parallel to each other, with a switch deciding which signal to send. A constant, defined in the matlab script, decides the switch.

B.4.4 Trimaran/ODETrimaran

Solves the EoM for the trimaran, and finds $\dot{\nu}$

B.4.5 referenceModel.m

Defines the matrices for the reference model in model.slx.

B.5 Supporting functions

B.5.1 Jbn.m, Rbn.m, Tbn.m

The files calculates the transformation matrix $J_\theta(\eta) = \begin{bmatrix} R(\Theta_{nb}) & 0 \\ 0 & T(\Theta_{nb}) \end{bmatrix}$, the Euler rotation matrix $R(\Theta_{nb})$ and the angular velocity rotation matrix $T(\Theta_{nb})$, as described in Section 2.2 and (2.1) and (2.2).

B.5.2 skewSym.m

This function calculates the Skew-Symmetric matrix, used in the Coriolis-Centripental matrix.

